

N70-31828

NOLTR 69-183

NASA CR-72652

PROPERTIES OF GRAPHITE FIBER COMPOSITES
AT CRYOGENIC TEMPERATURES

By
Robert A. Simon
Richard Alfring

NOL

13 MAY 1970

UNITED STATES NAVAL ORDNANCE LABORATORY, WHITE OAK, MARYLAND

NOLTR 69-183
NASA CR-72652

CASE FILE
COPY

NOTICE

This report was prepared as an account of Government-sponsored work. Neither the United States, nor the National Aeronautics and Space Administration (NASA), nor any person acting on behalf of NASA:

- A.) Makes any warranty or representation, expressed or implied, with respect to the accuracy, completeness, or usefulness of the information contained in this report, or that the use of any information, apparatus, method, or process disclosed in this report may not infringe privately-owned rights; or
- B.) Assumes any liabilities with respect to the use of, or for damages resulting from the use of, any information, apparatus, method or process disclosed in this report.

As used above, "person acting on behalf of NASA" includes any employee or contractor of NASA, or employee of such contractor, to the extent that such employee or contractor of NASA or employee of such contractor prepares, disseminates, or provides access to any information pursuant to his employment or contract with NASA, or his employment with such contractor.

Requests for copies of this report should be referred to

National Aeronautics and Space Administration
Scientific and Technical Information Facility
P. O. Box 33
College Park, Md. 20740

PROPERTIES OF GRAPHITE FIBER COMPOSITES
AT CRYOGENIC TEMPERATURES

Prepared by:
Robert A. Simon
Richard Alfring

ABSTRACT: Need for low-weight, cryogenic pressure vessels for spacecraft resulted in NASA-Lewis funding an investigation at NOL to measure graphite fiber composite properties at cryogenic temperatures. The investigation was divided into six tasks; only Tasks I and II are reported herein. Task I was an investigation of mechanical properties of several fibers and resins as composite strands, bars, and NOL rings and showed that composite moduli increased by 0 to 20% at -195°C , and composite tensile strengths decreased by 0 to 30%. Bending fatigue at 50% breaking stress and 1000 cycles deteriorated rings less when cold than when at room temperature. Thermal contraction tests of composites showed the graphite fibers to have a slight negative coefficient. Combined with resins in composites, the resin matrix would experience up to 1.5% strain when cold due to its thermal contraction.

Task II was the design, fabrication, and testing of graphite filament wound pressure vessels and was contracted to the Aerojet-General Corporation, Azusa, California. Vessel ultimate strains of 0.2 to 0.5% were found, which are generally compatible with the stainless steel liners used or with other candidate liner materials. The pressure vessel performance factor of PV/W showed the graphite vessels to be competitive with boron and two-thirds as high as fiberglass.

PUBLISHED 13 MAY 1970

APPROVED BY:

F. Robert Barnet, Chief
Non-Metallic Materials Division
CHEMISTRY RESEARCH DEPARTMENT
U. S. NAVAL ORDNANCE LABORATORY
WHITE OAK, SILVER SPRING, MARYLAND

UNCLASSIFIED

NOLTR 69-183

13 May 1970

PROPERTIES OF GRAPHITE FIBER COMPOSITES AT CRYOGENIC TEMPERATURES

This report describes the results of tests of graphite fiber composites at cryogenic temperatures. The tests were to get preliminary data leading toward use of this material for cryogenic tankage for spacecraft.

This report summarizes the results of Tasks I and II, which covered the period June 1967 - August 1969. Work is continuing, with Tasks III - VI in progress. A report will be issued on Task III and another on Tasks IV - VI. The work was funded as NASA Defense Purchase Request C10360B by the National Aeronautics and Space Administration (NASA), Lewis Research Center, Cleveland, Ohio.

The NASA Project Manager was Mr. R. F. Lark.

GEORGE G. BALL
Captain, USN
Commander


ALBERT LIGHTBODY
By direction

CONTENTS

	Page
I. INTRODUCTION	1
II. EXPERIMENTAL WORK	1
A. TASK I	1
1. Materials	1
a. Fibers	1
b. Fiber Surface Finishes	2
c. Resins	2
2. Composites	2
a. Strands	2
b. Bars	3
c. NOL Rings	3
d. Coefficient of Thermal Expansion Specimen	3
3. Temperatures	3
4. Tests	3
B. TASK II	3
1. Structural Analysis and Design	4
2. Fabrication	5
3. Tests	5
III. RESULTS	6
A. TASK I	6
1. Tensile Strengths of As-Received Fibers	7
2. Tensile Strengths of Whiskered Fibers	7
3. Tensile Strengths of Nitric Acid Treated Fibers	7
4. Cycling Fatigue - Split D Tensile (Bending) Test	8
5. Tensile Moduli	8
6. Flexural Strengths	9
7. Flexural Moduli	9
8. Interlaminar Shear Strengths	9
9. Resins	10
10. Coefficient of Thermal Contraction	10
11. Testing at Liquid Hydrogen Temperature	11
12. Choice of Materials for Task II	12
B. TASK II	12
1. Vessel Fiber Tensile Strengths	12
2. Filament and Composite Thicknesses	13
3. Vessel Fiber Content	14
a. Thornel 50 Vessels	14
b. Morganite II Vessels	15
4. Pressure Vessel Strain	15
5. Pressure Vessel Performance Factor	16
IV. DISCUSSION	17
A. DISCUSSION OF THE PROCEDURE	17
B. FIBER TENSILE STRENGTHS	17
1. Room Temperature	17
2. Cryogenic Temperatures	17
3. Effect of Whiskering and Nitric Acid Fiber Surface Treatments	18
4. Effects of Cycling Fatigue	18
C. MODULI AND EFFECT OF TEMPERATURE	18

UNCLASSIFIED
NOLTR 69-183

CONTENTS

	Page
D. FLEXURAL MODULI AND STRENGTHS	19
E. INTERLAMINAR SHEAR STRENGTHS	19
F. COEFFICIENTS OF EXPANSION	20
G. GRAPHITE FIBER QUALITY	20
H. BRITTLE FRACTURE OF VESSELS	20
V. CONCLUSIONS	21
VI. RECOMMENDATIONS	22
VII. FOLLOW ON WORK	22
REFERENCES	23
APPENDIX A. RESIN CONTENT DETERMINATION	A-1
APPENDIX B. AEROJET-GENERAL STRAND TEST PROCEDURE	B-1
APPENDIX C. PRESSURE VESSEL DESIGN	C-1
APPENDIX D. FABRICATION OF VESSEL LINERS	D-1
APPENDIX E. VESSEL WINDING PROCEDURE	E-1
APPENDIX F. VESSEL CRYOGENIC TEST PROCEDURE AND INSTRUMENTATION	F-1

ILLUSTRATIONS

Figure	Title
1	Graphite Roving and Yarn on Spools
2(A)	Strand Ready for Test
2(B)	Tensile Bars for Modulus and Strength
3(A)	NOL Ring
3(B)	NOL Ring in Split Pin Modulus Test Fixture
3(C)	NOL Ring in Split D Strength Test Fixture
3(D)	Cryogenic Shear and Flexural Strength Test Fixtures
4(A)	Metal-Lined Graphite Filament Wound Pressure Vessel - 8.00 Dia.
4(B)	Boss Detail for 8-In. Dia. Pressure Vessel
5	Thornel 50 Filament Wound Pressure Vessel T-1
6	Thornel 50 Filament Wound Pressure Vessel T-3
7	Thornel 50 Filament Wound Pressure Vessel T-3
8	Morganite II Filament Wound Pressure Vessel M-1
9	Fiber Tensile Strengths
10	Fiber and Composite Tensile Strengths
11	Fiber and Composite Tensile (Bending) Strengths
12	Fiber Tensile Strengths - Whiskered Fiber
13	Filament Tensile Strengths - Whiskered Fiber
14	Fiber Tensile Strengths - Nitric Acid Treated Fiber
15	Fiber and Composite Tensile Strengths - Nitric Acid Treated Fiber
16	Fiber Tensile Strengths and Composite Interlaminar Shear Strengths - Nitric Acid Treated Fiber - Thornel 50
17	Fiber and Composite Tensile Moduli
18	Fiber and Composite Tensile (Bending) Moduli
19	Fiber and Composite Tensile Moduli - Nitric Acid Treated Fiber
20	Fiber and Composite Flexural Strengths
21	Fiber and Composite Flexural Moduli
22	Composite Interlaminar Shear Strengths

UNCLASSIFIED
NOLTR 69-183

CONTENTS

Figure	Title
23a	Composite Interlaminar Shear Strengths
23b	Composite Interlaminar Shear Strengths
24	Viscosity of Resin/Hardener Systems Measured at 22°C
25	Ultimate Graphite Filament Strengths at Vessel Burst Pressures
26	Post Test Photograph Tank T-1
27	Post Test Photograph Tank T-4
28	Post Test Photograph Tank M-5
29	Pressure vs. Strain for Burst Test at 22°C (75°F) Tank T-1
30	Pressure vs. Strain for Burst Test at 22°C (75°F) Tank T-2
31	Pressure vs. Strain for Burst Test at 22°C (75°F) Tank T-3
32	Pressure vs. Strain for Burst Test at -195°C (-320°F) Tank T-4
33	Pressure vs. Strain for Burst Test at -253°C (-423°F) Tank T-5
34	Pressure vs. Strain for Burst Test at -253°C (-423°F) Tank T-6
35	Pressure vs. Strain for Burst Test at 22°C (75°F) Tank M-1
36	Pressure vs. Strain for Burst Test at -195°C (-320°F) Tank M-2
37	Pressure vs. Strain for Burst Test at -253°C (-423°F) Tank M-3
38	Pressure vs. Strain for Burst Test at -195°C (-320°F) Tank M-4
39	Pressure vs. Strain for Burst Test at -253°C (-423°F) Tank M-5
40	Pressure vs. Strain for Burst Test at 22°C (75°F) Tank M-6
C-1	Thornel 50 Pressure Vessel Stress-Strain Relationships Hoop Direction of Cylinder, 22°C (75°F)
C-2	Morganite (Type II) Pressure Vessel Stress-Strain Relationships, Hoop Direction of Cylinder, 22°C (75°F)
C-3	Thornel 50 Vessel Pressure-Strain Relationships
C-4	Morganite (Type II) Vessel Pressure-Strain Relationships
F-1	Location of Instrumentation on Test Vessel
F-2	Pressure vs. Temperature - Liquid Nitrogen Test
F-3	Pressure vs. Temperature - Liquid Nitrogen Test

TABLES

Table	Title	Page
1-A	Mechanical Properties of Thornel 50 Yarn	24
1-B	Mechanical Properties of Morganite Tow	24
2	Fabrication Data Summary - Twelve Graphite Filament-Wound Vessels	25
3	Pressure Vessel Performance Summary	26
C-1	Design Parameters for Graphite Filament-Wound Pressure Vessels	C-7
C-2	Dimensional and Material Parameters - Graphite Filament-Wound Pressure Vessels	C-10

I. INTRODUCTION

The graphite (or graphitic) fibers are candidate materials for making containers for pressurized cryogenic liquids. Filament wound containers made from these fibers should give wall strains of 1% or less. Use of glass fibers has given strains of 2 - 4%, too high for the strain capability of the materials used as the internal liners to prevent gas leakage (refs. (a) and (b)). But little is known of the mechanical properties of graphite fibers at cryogenic temperatures.

This program was done to obtain data on the strengths and moduli of graphite fiber composites at temperatures down to liquid hydrogen temperature. Work was divided by NASA into Tasks I - VI; only Tasks I and II are reported herein. Task I was a preliminary investigation of several fibers, resins and fiber finishes in various combinations as unidirectional composites.¹ Task II was the design, construction, and testing of filament wound pressure vessels using the best materials from Task I.² Follow-on work, involving Tasks III, IV, V, and VI, is now under way at this Laboratory and will be reported subsequently. Investigations of both graphite and boron in this application at other laboratories are being pursued (refs. (c) and (d)). Data from all of these tasks are expected to find eventual use in the design of filament wound cryogenic containers for NASA spacecraft.

II. EXPERIMENTAL WORK

A. TASK I

Task I was an exploratory investigation of candidate materials. Five fibers, two resins, and three fiber surface finishes were combined in various combinations into unidirectional composites and tested for mechanical properties at room and cryogenic temperatures. Not all combinations of materials were exposed to all tests; some unpromising combinations were eliminated early.

1. Materials

a. Fibers. The following table shows the fibers used in this study:

<u>Fiber</u>	<u>Form</u>	<u>Length</u>	Surface Treated by <u>Manufacturer</u>	<u>Sized</u>
RAE (Morganite) I	Tow	6 inches	No	No
Morganite II	Tow	1 meter & continuous	Some untreated, some treated	No
Thornel 50	2-Ply Yarn	Continuous	No	Yes - PVA
Hitco HMG	2-Ply Yarn	Continuous	No	No
Samco 320	Tow	6 inches	No	No

1 Task I was done by the Naval Ordnance Laboratory, Silver Spring, Maryland

2 Task II was contracted to and done by Aerojet-General Corp., Azusa, Calif.;
Project Manager Richard Alfring.

Fibers, as received, were experimental or early production lots from manufacturers and, in some cases, exhibited faults which would not be expected in volume production. Included were breaks, stiff spots, and small fuzz accumulations. Poor packing, resulting in fiber damage during shipment, was sometimes evident. These faults made handling the fibers and getting good composites more difficult. Figure 1 shows fiber yarn and tow on spools; no special fiber damage is evident in this photograph.

b. Fiber Surface Finishes. Fiber surface finishes were applied to increase the resin-to-fiber bond and to determine the effect on composite tensile strengths. The following table shows the finishes tried:

<u>Finish</u>	<u>Applied to Fiber</u>
None - fiber as received	All
Whiskering	All
Nitric Acid Boil	Thornel 50, HMG 25, RAE Type 1, and SAMCO 320

"Whiskering" is a process of depositing B-silicon carbide whiskers in the amount of 2 to 8% by weight on the surface of graphite fibers by exposure in a furnace to specific gases. Whiskering has produced shear strengths of up to 140×10^6 n/m² (20,000 psi) in graphite fiber composites. It is described more fully in reference (e). The nitric acid treatment was reported by Herrick (ref. (f)) and consists of refluxing the fibers in 70% nitric acid for 24 hours and then water washing. Both treatments reduce the tensile strength of the fibers. The inclusion of such treatments in this program was to determine if increased resin-fiber bond would yield unexpected composite results.

c. Resins. Two epoxy resin systems were chosen, as follows:

Resin 1.	ERLA 2256 Resin	
	ZZL 0820 hardener	27 phr
Resin 2.	Epon 828 resin	
	Duodecenyl succinic anhydride	117 phr
	Empol 1040	20 phr
	BDMA	1 phr

All ingredients were standard or commercial grade. Resin 1 was chosen as a standard for comparison. Resin 2 was developed by Aerojet-General for cryogenic use with glass (ref. (g)).

2. Composites

The composites made were the following:

a. Strands. A strand is a single fiber yarn or tow dip-impregnated with resin, hung straight, and cured. After curing, tabs are bonded to the ends for gripping in a tensile strength test fixture. The general procedure used was essentially what is now a tentative ASTM specification, reference (h).

Figure 2a shows a typical strand ready for test. Strands were used to measure the tensile strength of the graphite fibers.

b. Bars. The bar design used in this study is shown in Figure 2b. This has unidirectional fiber, cut to length, impregnated with resin, then hand laid in a mold and cured. After curing, electric strain gages suitable for cryogenic liquid immersion were bonded to each bar specimen. The bars were used to measure tensile moduli of the graphite fibers.

c. NOL Rings. The NOL ring, described in reference (i)) was used as a supplementary specimen to obtain additional tensile modulus and strength data, and it also was used to obtain tensile fatigue data at 75% of ultimate stress for 1000 cycles. Other tests run using ring segments were short beam interlaminar shear strengths and 3- or 4-point flexural strengths and moduli. Figure 3 shows an NOL ring and certain fixtures used in testing NOL rings.

d. Coefficient of Thermal Expansion Specimen. The coefficient of thermal expansion specimen consisted of a unidirectional molded laminate 10 cm (4 in.) long, with a thickness and width of 0.318 cm (0.125 in.) and 0.635 cm (0.250 in.), respectively. After thermal expansion measurements, the bars were cut into shear specimens of 5:1 span/depth ratio.

3. Temperatures

Test temperatures were 22°C (72°F), -195°C (-320°F) (liquid nitrogen), and -253°C (-423°F) (liquid hydrogen). NASA, Lewis Research Center performed the liquid hydrogen testing. Not all specimens were tested at all temperatures.

4. Tests

The following table summarizes the specimens and tests.

<u>Composite</u>	<u>Test</u>	<u>Method</u>
Strand	Tensile Strength	Ref. (h)
Bar	Tensile Modulus	Electric Strain Gage
Ring	Tensile (Bending) Modulus	Ref. (i)
	Tensile (Bending) Strength	Ref. (i)
	3- or 4-Point Flexural Modulus	Ref. (i)
	3- or 4-Point Flexural Str.	Ref. (i)
	Short Beam Shear Strength	Ref. (i)
	Tensile (Bending) Fatigue	
	Strength, 1000 Cycles, 75% of Ultimate Stress	Ref. (i)
All	Resin Content	Burn-off, Appendix A

B. TASK II

Task II was the design, fabrication, and testing of 12 closed-end graphite filament wound pressure vessels, approximately 20 cm (8 in.) in diameter and

33 cm (13 in.) in length. The purpose of testing the vessels was to determine the effect of test temperatures on the burst strengths of the vessels. Materials used were Thornel 50 and Morganite II* graphite fibers and resin 2 (828/DSA/E1040/BDMA), as shown to be best from Task I (Section III.A.12).

1. Structural Analysis and Design

The metal-lined, filament-wound test vessel was a closed-end cylinder designed to achieve a longitudinal-to-circumferential strain ratio of approximately 1:1 and a burst pressure of 17 to 19 x 10⁶ n/m² (2500 to 2750 psi) at 22°C (75°F). This vessel, fabricated from in-plane longitudinal windings and circumferential windings wound over a 0.015 cm (0.006 in.) thick Type 304 SS foil liner, was selected from experience acquired in previous development efforts (refs. (c) and (d)).

It was assumed that the ultimate filament stress for the longitudinal windings was 8.97 x 10⁸ n/m² (130,000 psi) and 10% higher, or 9.85 x 10⁸ n/m² (143,000 psi), for the hoop filaments. This design strength was selected from the results of Task I. Although different strengths were expected for Thornel 50 and Morganite (Type II) in the vessels, a single set of design stresses was used to facilitate a comparative evaluation of the two graphite filaments.

Two vessel designs were prepared and analyzed in detail, one for winding from Thornel 50 yarn and one for winding from Morganite II tow. However, midway through the program it was evident that two types of Morganite II vessels should be fabricated and tested. This was because the Morganite II tow received from NOL had a larger cross-sectional area than anticipated, produced a heavier vessel than desired, and gave a design burst pressure 40 to 50% higher than that of the Thornel 50 vessels. To allow fabrication of six vessels with the available Morganite II material, three vessels were made to the initial Morganite II requirements (called a "three-thirds wall vessel") and three vessels were made to a modified design (called a "two-thirds wall vessel"). The "two-thirds wall vessel" was wound with four layers (two revolutions) of longitudinal and nine layers of hoop winding. The balance of the discussion relates to the design of the Thornel 50 and Morganite II (three-thirds wall) vessels.

Dimensions of the head contours and other vessel characteristics were defined with the aid of a computer program that analyzed and provided design parameters. This program defined the optimum head contours, the filament and liner stresses and strains at various internal pressure levels, the required longitudinal composite thickness for the heads and cylinder, the hoop-wrap thickness for the cylinder section, the filament path length, and the weight and volume of the components and complete vessel.

* Morganite II fiber is also available from the manufacturer in a surface treated version, designated Morganite II S. It was the Morganite II S which was supplied and used throughout Task II. But in the Task II text and figures, the fiber is referred to simply as Morganite II.

The design of the vessel, resulting from the computer program, is shown in Figures 4a and 4b. The design includes a metal foil liner, an adhesive fiberglass scrim cloth layer to promote better bonding of the liner to the graphite vessel wall, and alternating longitudinal and hoop windings of graphite fiber impregnated with epoxy resin. Design parameters, winding pattern calculations, and an analysis of the stresses, strains, and weights are shown in Appendix C.

2. Fabrication

Graphite filament-wound, metal-lined tanks were fabricated in accordance with the design shown in Appendix B. The liners were made from AISI Type 304 stainless steel by pressure-forming the end domes, machining the polar bosses, rolling a cylindrical section, and roll-resistance seam welding the segments. The liners, covered with scrim cloth, then were overwound using in-process epoxy resin impregnated graphite fibers. Twelve tanks were fabricated and tested: six of Thornel 50 graphite yarn and six of Morganite II graphite tow. In addition to the twelve vessels, 137 graphite strand test specimens were fabricated and tested.

Liner fabrication was in accord with previous work done by Aerojet and is described more fully in Appendix D. The graphite filament used in the winding was 12 pounds of Thornel 50 and 12 pounds of Morganite II S supplied by NOL. Data, supplied by the manufacturers, for the fiber tensile moduli and strengths of these fibers are shown in Table 1. Many of the rolls were tested by Aerojet for the same properties. Extensometers for measuring elongation were mounted directly on impregnated and cured fiber strands. These procedures are described in Appendix B. (These measured properties are also shown in Table 1.)

An extensive description of the winding of the vessels is given in Appendix E.

A number of problems were encountered during the fabrication of filament-wound vessels. Such problems included yarn and tow received from the manufacturers in poor condition, many fiber breaks encountered during collation and winding, high resin pickup, fiber slippage on the domes during winding, and fiber "wash" and wrinkling when vacuum bag cures were used (Figure 5). Some of the problems were reduced or solved early, and others were not resolved prior to completion of the winding program. All were typical of first use of a new or experimental material. In all, 11 of the 12 vessels were considered to be adequate in construction and suitable for test. Only vessel M-2 was considered substandard in construction, and results of this test were partially discounted. Figures 6 - 8 show typical completed vessels. Table 2 gives a fabrication data summary for the vessels.

3. Tests

The 20 cm (8 in.) diameter by 33 cm (13 in.) long graphite filament-wound, metal-lined tanks were tested to determine their burst strengths and strain vs. pressure characteristics.

UNCLASSIFIED
NOLTR 69-183

The 12 vessels were subjected to single-cycle burst tests at a rate of pressurization that produced a strain of approximately 0.25% per minute in the longitudinal and circumferential directions. Five were tested at 22°C (75 °F), 3 at -195°C (-320°F), and 4 at -253°C (-423°F), as shown in the following table:

<u>Fiber</u>	<u>No. of Vessels</u>	<u>Test, °C</u>	<u>Temp., °F</u>
Thornel 50	3	22	75
	1	-195	-320
	2	-253	-423
Morganite II	2*	22	75
	2*	-195	-320
	2*	-253	-423

* Includes one "three-thirds" vessel and one "two-thirds" vessel.

Data recorded continuously were the internal pressure, exterior-surface temperature (cryogenic tests only), and deflection vs. pressure relationships at three points to provide hoop and longitudinal strains. One set of hoop-strain measurements was made at the center of the cylindrical section, and two sets of axial-strain measurements were made at different points along the cylindrical section. In addition to the strain measurement instrumentation usually used by Aerojet for testing, long-wire strain gages were evaluated by installation on all six Morganite II vessels.

Water was used for pressurization for the 22°C (75°F) tests, liquid nitrogen for the -195°C (-320°F) tests, and liquid hydrogen for the -253°C (-423°F) tests. The test fixture consisted of a vacuum chamber with provisions for instrument leads and vacuum-jacketed gas pressurization lines and cryogenic feed and vent lines. Remote instruments recorded pressure, temperature, time, and vessel strains. A television camera and audio system provided for viewing and listening. The tests ended at vessel rupture, as indicated by noise and sudden pressure dropoff. More details of the test procedure and instrumentation are given in Appendix F.

III. RESULTS

A. TASK I (Investigation of Fibers, Resins, and Finishes)

In general, compared to ambient temperature fiber properties, values of fiber tensile strength tended to decrease while tensile moduli tended to increase when tested at cryogenic temperatures.

Tensile strengths were measured using four different specimens, as follows: resin-impregnated strands, individual (dry) filaments, molded laminated bars, and NOL rings. These specimens were made from as-received fiber, whiskered fiber, and nitric acid treated fiber. Two different epoxy resins were used, and specimens were tested at both room temperature and liquid nitrogen temperature. Because of the large number of variables and specimens involved, this work constituted a major part of the whole effort on Task I. The results are shown

in Figures 9 - 16 and will be discussed in more detail in the following paragraphs. The determinations of tensile moduli, flexural strengths and moduli, and interlaminar shear strengths constituted the remainder of the work. These results are shown in Figures 16 to 23 and are discussed in the following paragraphs:

1. Tensile Strengths of As-Received Fibers

Tests of six resin-impregnated strands gave room temperature strengths ranging from 13×10^8 n/m² (189,000 psi) to 21×10^8 n/m² (305,000 psi) with Morganite II being highest. Figure 9 shows all values. Molded unidirectional laminate bars gave somewhat lower values. Of the four fibers tested, fiber strengths ranged from 7.5×10^8 n/m² (115,000 psi) to 15.2×10^8 n/m² (220,000 psi). Figure 10 shows these values. Filament wound NOL rings gave fiber strengths about the same as the molded bars, ranging from 7.9×10^8 n/m² (118,000 psi) to 16.8×10^8 n/m² (244,000 psi) for three fibers tested. Figure 11 shows these values.

At liquid nitrogen temperature, the three types of tests gave reasonably consistent results. Morganite II showed an average 30% strength drop, while all the other fibers gave much less change. Thornel 50 was particularly immune to temperature changes, varying in strength no more than a few per cent in any of the three types of tests. The result was that at liquid nitrogen temperature Thornel 50 has about 90% of the strength of Morganite II. Figures 9 - 11 show the strengths of strands, bars, and rings at liquid nitrogen temperature.

2. Tensile Strengths of Whiskered Fibers

Both resin impregnated strands and individual (dry) filaments (1440 filaments in Thornel 2-ply yarn; 10,000 filaments in Morganite tow) were used to measure tensile strengths of fibers whiskered by Thermokinetic Fibers, Inc. Both methods of measurement showed whiskering to lower the tensile strengths by 5 to 70%, with heaviest whiskering giving greatest reductions. The rayon precursor fibers showed least reduction, with Thornel 50 having 5% reduction with "medium-heavy" whiskering. The polyacrylonitrile (PAN) precursor fibers (Morganite and Courtaulds) showed 25 to 40% reduction resulting from "light to medium" treatments and 70% reduction from "heavy" treatments. Whiskered Morganite I was tested in liquid nitrogen as a strand, and again the strength reduction due to temperature was encountered--in this case, 10%. Figure 12 gives complete data on these whiskered strand tensile strengths, and Figure 13 shows individual whiskered filament tensile strengths.

3. Tensile Strengths of Nitric Acid Treated Fibers

Nitric acid treated fibers were tested as strands, individual filaments, and molded bars. Tests of two fibers in strands gave room temperature strengths from 10.2×10^8 n/m² (148,000 psi) to 13.9×10^8 n/m² (202,000 psi). These represent 2 to 13% strength decreases over the corresponding untreated fiber. Data are shown in Figure 14. Individual (dry) filament tests of Thornel 50 showed a 19% drop in strength of treated fiber, shown also in Figure 14. Tests of four fibers in molded bars gave strengths of 7.5×10^8 n/m² (110,000 psi) to 14.9×10^8 n/m² (206,000 psi). These are nearly identical to the values for

as-received fiber, and are shown in Figure 15. A short-term investigation was done on the effect of varying nitric acid treatment times on the tensile strength of treated fiber. Some scatter in the data was encountered, but the general indication is an initial tensile strength drop of 15 per cent from the first four hours of treatment, with no additional drop up to 48 hours of treatment. These results are shown in Figure 16.

At liquid nitrogen temperature, nitric acid treated fiber showed more tensile strength drop than did as-received fiber. Morganite II was not among the nitric acid treated fibers, but the others, which showed little change in the as-received fiber tests, dropped 6 to 30% after nitric acid treated. Both strand tests and bar tests gave essentially the same results. This appreciable drop when cold, coupled with the drop resulting from the nitric acid treatment, reduces these fiber strengths to rather low values. The best value in strands, when cold, was 12.2×10^8 n/m² (177,000 psi) for Thornel 50, and the best value in molded bars was 13.0×10^8 n/m² (188,000 psi) for Morganite I. Figures 14 and 15 give complete results.

4. Cycling Fatigue - Split D Tensile (Bending) Test

NOL rings were made using Thornel 50 and HMG 25 graphite fibers. These were tested using the Split D test fixture at 75% ultimate stress (then back to no stress) for 1000 cycles. Cycling rate was seven cycles/minute. When subsequently stressed to failure, a comparison of strength with the strength of uncycled controls gave the extent of degradation due to cycling. These tests showed that rings made from Thornel 50 were weakened by room temperature cycling by 10%, but cold cycling resulted in stronger rings which gave higher break strengths than the cold controls. HMG 25 gave a more expected result, with room temperature cycling causing a 17% strength reduction and cold cycling resulting in a 9% reduction. Figure 11 shows these results.

5. Tensile Moduli

Tensile moduli values were determined from molded bars and from NOL ring test specimens. The ring test is more of a bending modulus, and so ring test results will also be compared later with flexural moduli results. First, the fiber moduli generally translated at 100% effectiveness into composite moduli. When fiber moduli were known, either by manufacturer's data or by NOL measurements, the composite moduli could be predicted quite accurately by knowing the fiber content and applying the rule of mixtures. This was expected, since it is typical of unidirectional fiber reinforced composites.

Second, the fiber (and composite) moduli nearly always increased when measured at cold temperature as compared to room temperature. Of four fibers tested as bars, three of them showed 5 to 20% moduli increases when cold, and one was unchanged. Tests with NOL rings gave the same absolute values and the same percentage increases when cold. Results of moduli tests of bars and rings are shown in Figures 17 and 18. Rings made from Thornel 50 and tested after fatiguing for 1000 cycles at 75% stress showed no change in moduli due to cycling. No other fibers were cycle tested. These results are shown on Figure 18.

Four nitric acid treated fibers were molded into bars, and tests showed the nitric acid treatment to have no significant effect on moduli when the bars were tested at room temperature or when tested cold. These results are shown in Figure 19. To summarize the results, moduli increases can be expected when tested cold, averaging 10% and ranging from 0 to 20%.

6. Flexural Strengths

NOL rings made from as-received fiber were cut into 3-inch length segments and tested in 3-point bending at 16:1 span-to-depth ratio for flexural strengths (and moduli). Five fibers were used. Two of them, Morganite II and Morganite II S gave such high fiber strengths as to be in a class by themselves. These strengths, 20.6×10^8 n/m² (300,000 psi) and 24.7×10^8 n/m² (358,000 psi), were three times as high as the next closest, HMG 25, which gave 6.6×10^8 n/m² (96,000 psi). All strengths were relatively unaffected by cold. Results are shown in Figure 20.

7. Flexural Moduli

The same ring segments tested for strengths generally were also tested for moduli. Fiber moduli at room temperature for four fibers tested gave reasonable agreement with moduli obtained from the NOL ring bending test and from the tensile bar test. However, the moduli of Thornel 50 and HMG 25 flexural specimens increased from 32 to 62% when tested cold, as compared to an average 10% increase for the ring and bar specimens when tested cold. Some of these flexural tests were repeated, with essentially the same results. Figure 21 gives these results.

8. Interlaminar Shear Strengths

A considerable amount of interlaminar shear strength data were generated both from NOL rings and molded bars. Of five as-received fibers tested in rings at room temperature, Morganite II S gave by far the highest interlaminar shear value, 91×10^6 n/m² (13,200 psi). Values for other fibers in composites ranged from 20×10^6 to 54×10^6 n/m² (2900 to 7800 psi). Testing at liquid nitrogen temperatures invariably increased the shear strengths, Morganite II S increasing by 4% and the others increasing by 2 to 54%. The values are shown in Figure 22.

Four fibers were molded into bars. Morganite II and Morganite II S were not among them; the fibers used gave shear strengths of 16×10^6 to 35×10^6 n/m² (2300 to 5100 psi) at room temperature. At liquid nitrogen temperature, higher shear strengths again were obtained. Increases ranged to over 100%, to 68×10^6 n/m² (9800 psi) for HMG 25. Figures 23a and 23b show the results.

Some of the fibers were nitric acid treated and then molded into bars. When compared to as-received fiber, the treated fiber gave significant interlaminar shear increases at room temperature. HMG 25 was least affected, giving 12% increase for the treated fiber. Morganite I had spectacular response to the treatment; shear values going to 67×10^6 n/m² (9700 psi) or four times higher than as-received fiber. When tested cold, the nitric acid treated fiber gave the expected strength increases, up to 25%. Treated Morganite I, when cold,

UNCLASSIFIED
NOLTR 69-183

gave a value of 85×10^6 n/m² (12,300 psi). Values are shown in Figures 23a and 23b.

9. Resins

For the two resins used in this study, no significant difference was found in any composite mechanical property which would indicate superiority of one resin over the other. Measurement of just resin properties (not in composites) gave some differences, as shown in the following table:

Resins - Tested at Room Temperature

Resin	Initial Modulus		Yield			Ultimate		
	10 ⁸ n/m ²	psi	Elon-	Strength		Elon-	Strength	
			gation %	10 ⁶ n/m ²	psi	gation %	10 ⁶ n/m ²	psi
1) 2256/0820	29.5	414,000	1.7	55	8,000	5.0	99	14,300
2) 828/DSA/ E1040/BDMA	20.5	297,000	1.5	31	4,500	4.2	50	7,300

Although resin 1 is stronger at room temperature, its use in composites did not result in stronger composites, at least for those properties measured in this work. Use of resin 2 was easier because of its longer working time, as shown in Figure 24. Also, resin 2 was lighter in weight, having a specific gravity of 1.09 compared to 1.23 for resin 1. For these reasons, resin 2 was chosen for Task II work, as will be noted in a later paragraph.

10. Coefficient of Thermal Contraction

Molded bar composites made from four fibers, along with one of the resins and three other materials for calibration, were tested for coefficient of thermal contraction over the temperature range of +22°C to -195°C (295°K to 78°K). Contraction for all of the graphite composite specimens was extremely low, being about 0.5×10^{-4} cm/cm, or 0.5×10^{-2} %, or 50 micro-cm/cm. The following table gives more complete results:

Thermal Contraction Between 22°C and -195°C

Material	Reduction in Length Due to Temperature	Linear Coeff. of Thermal Expansion	Handbook Value
	Microcentimeter/cm.	10 ⁶ per °C	
Morganite I Composite*	50 ±50	0.2 ± 0.2	-
Thornel 50 Composite*	50 ±50	0.2 ±0.2	-
HMG 25 Composite*	50 ±50	0.2 ±0.2	-
SAMCO 320 Composite*	50 ±50	0.2 ±0.2	-
(All composites measured in the fiber direction)			
Fused Quartz	75 ±25	0.3 ±0.1	0.256
Steel	2400 ±125	9.5 ±0.5	9.0

Thermal Contraction Between 22°C and -195°C (continued)

<u>Material</u>	<u>Reduction in Length Due to Temperature Microcentimeter/cm.</u>	<u>Linear Coeff. of Thermal Expansion 10⁶ per °C</u>	<u>Handbook Value</u>
Aluminum	4200 ±125	16.9 ±0.5	17.0
Resin 1 in this study	11,100 ±125	44.4 ±0.5	
Resin 2 in this study	14,500	58	Aerojet Value

* All with Resin 1

Calculations of the thermal contraction coefficient of the bare graphite fibers show them to be slightly negative. That is, as the temperature gets colder, the graphite fibers get slightly longer. Combining the fibers with resin gives composites which get slightly shorter when colder, as shown in the table. This is presented more fully in section IV, "Discussion."

Other composites made with resin 2 (828/DSA/E1040/BDMA) and also composites made with nitric acid treated fiber were tested. No differences from the value shown in the table were found. Note that values in the table have apparently wide tolerances. This is because the accuracy of the measurements was limited by the standard ASTM apparatus used. Total linear contraction for the four-inch long graphite composite specimens was only two ten-thousandths of an inch. The quartz tubes and rods of which the apparatus itself is made have a greater contraction. However, the apparatus and results were completely adequate to show that the graphite composites have little thermal contraction, while the epoxy resin used with them has over 200 times as much contraction. Thermal stresses are indicated, as will be pointed out in the Discussion.

11. Testing at Liquid Hydrogen Temperature

The scope of this work in Task I included testing at liquid hydrogen temperature. This testing was done by NASA, Lewis on samples fabricated and supplied by NOL. Scheduling problems at NASA and certain inconsistencies in the results prevented these data from being as useful and consistent as originally anticipated. The results generally were as follows:

a. Thornel 50 rings increased in tensile strength by 10% over results obtained at -195°C (-320°F). This result also was confirmed by vessel tests in Task II, noted elsewhere in this report.

b. Morganite II rings increased in tensile strength compared to room temperature strength. This result is interpreted as being unexpected and unlikely and may be the result of a fabrication or testing error. It is inconsistent with the Task I test results at -195°C (-320°F) and also inconsistent with the Task II vessel results.

c. Flexural strengths of both Thornel and Morganite composites were 30 to 70% higher than previously obtained at either room temperature or liquid

UNCLASSIFIED
NOLTR 69-183

nitrogen temperature. These results were unexpected, and we have no confirmation through other experiments.

d. Interlaminar shear results were varied, with Morganite II giving a much higher value than its room temperature control and Thornel 50 giving a much lower value than its room temperature control. We have no explanation for these results.

e. Tensile moduli generally were within 10% of the values obtained by NOL in -195°C (-320°F) tests.

In all, these results of tests in liquid hydrogen gave some useful data, but additional tests would be required to confirm or disprove certain results which now appear anomalous.

12. Choice of Materials for Task II

The final responsibility in Task I work was choosing two fibers and one resin for the Task II work. The following were chosen:

<u>Material</u>	<u>Remarks</u>
Morganite II S Fiber	Highest room temperature and liquid nitrogen strength. Highest interlaminar shear strength. Available in long (one-pound) lengths.
Thornel 50 Fiber	Second highest strength at liquid nitrogen temperature. Lowest fiber density.
Resin 2 (828/DSA/ E1040/BDMA)	Longer working life than resin 1. Lower resin density than resin 1.

Additional reasons for choosing the above two fibers were to evaluate the difference between a PAN precursor and rayon precursor fiber and the handling differences between a tow and a yarn.

B. TASK II (Burst Testing of Closed-End Graphite Filament-Wound Pressure Vessels)

Task II tensile strength test data from closed-end pressure vessels, in general, confirmed NOL ring tensile strength test data from Task I. That is, Thornel 50 tensile strength was not reduced (even increased in Task II) at cryogenic temperatures, but Morganite II tensile strength was reduced considerably at cryogenic temperatures. Therefore, in both Tasks I and II, at cryogenic temperatures, there was slight difference in the tensile strengths of the two fibers.

All vessels shattered in a brittle fracture mode when they failed. Photographs of typical tested vessels are shown in Figures 26 - 28.

1. Vessel Fiber Tensile Strengths

The comparison of fiber tensile strengths of Morganite II and Thornel 50 graphite fibers obtained by burst testing closed-end filament-wound vessels is shown below:

Morganite II was 46% stronger than Thornel 50 at ambient temperature, having an average filament tensile strength value of 12.3×10^8 n/m² (178,000 psi) vs. 8.3×10^8 n/m² (121,000 psi).

At liquid nitrogen temperature, -195°C (-320°F), excluding vessel M-2 data, Thornel 50 was 6% stronger than Morganite II, having an average value of 10.2×10^8 n/m² (148,000 psi) vs. 9.65×10^8 n/m² (140,000 psi).

At liquid hydrogen temperature, -253°C (-423°F), Thornel 50 was 14% stronger than Morganite II, having an average value of 11×10^8 n/m² (159,000 psi) vs. 9.65×10^8 n/m² (140,000 psi).

Thornel 50 gained 21% in strength at liquid nitrogen temperature and 31% in strength at liquid hydrogen temperature over its strength at ambient temperature.

Morganite II showed reductions of 17% in strength at liquid nitrogen and 22% at liquid hydrogen temperatures compared to ambient tensile strength. The Morganite II vessels were wound with two different wall thicknesses. Failure stress was found to be influenced by wall thickness. The stress at burst in the thicker wall was 20% less than in the thinner wall. This compares to a 3% lower stress in fiberglass vessels with a similar change in wall thickness.

Average hoop strengths and average longitudinal strengths for the three configurations of vessels at the three temperatures are plotted for comparison in Figure 25.

2. Filament and Composite Thicknesses

The filament thicknesses in the longitudinal and hoop wraps were calculated as shown in Appendix G, and, using the fiber content (vol. %) determined by burnout, the composite thicknesses were calculated. They compare with design requirements as follows:

<u>Vessel Type</u>	<u>Filament Thickness*</u>			<u>Composite Thickness*</u>		
	<u>Longi- tudinal</u>	<u>Hoop</u>	<u>Total</u>	<u>Longi- tudinal</u>	<u>Hoop</u>	<u>Total</u>
Thornel 50	0.092	0.157	0.249	0.178	0.300	0.477
Morganite II ("Three-Thirds" wall)	0.114	0.178	0.292	0.302	0.472	0.774
Morganite II ("Two-Thirds" wall)	0.076	0.119	0.196	0.203	0.315	0.518
Design Requirement	0.097	0.165	0.262	0.147	0.254	0.401

* All data in centimeters.

The filament thicknesses shown for the first two configurations differ from the design requirement as a result of variation of the yarn weight from

that anticipated during the design phase. The variation of the ratio of longitudinal-to-hoop filament thicknesses for the Morganite II was caused by the decision to delete the last hoop layer in order to develop more hoop failures and, consequently, higher hoop stresses. A review of the failure modes shown in Table 3 indicates that the attempt was successful. The high composite thicknesses shown are a result of higher than anticipated resin content in the composite. The fiber content for the Thornel 50 vessels was 52 vol. %, and for Morganite II vessels the fiber content was 37.5 vol. % as compared with 65 vol. % anticipated during the design phase. The buildup of composite thickness in the Morganite II vessels was no doubt responsible for the 20% strength difference between the thin and the thick wall vessels. All vessels were wound by using in-process resin impregnated fibers. It is very probable that filament winding with a lower resin content preimpregnated yarn would allow attainment of higher filament strengths as well as composite strengths.

3. Vessel Fiber Content

The graphite fiber content (wt. %) for the Thornel 50 and Morganite II vessels is shown in Table 2, together with the standard deviation for the six individual determinations for each vessel. Also shown in Table 2 are the determined vs. known graphite fiber contents of the control specimens of Morganite II fiber furnished by NOL.

a. Thornel 50 Vessels. The graphite fiber content of the 36 Thornel 50 fiber strand specimens varied from 58.9 to 67.3 wt. %. The average graphite fiber content for each of the six Thornel 50 vessels ranged from 59.7 to 66.0 wt. %. The standard deviation between the six specimens from a given vessel ranged from 0.6 to 3.0 wt. %.

Vessel No. T-1 (Thornel 50 fiber) had the resin applied with a brush and was cured with vacuum bag compaction. If the high value for the specimen taken from the knuckle area is discarded, an average graphite content of 59.4 wt. % is obtained, the lowest for the six vessels. With the discard, the standard deviation of the remaining five specimens also becomes the least of that shown for the six vessels, rather than the highest, indicating a more consistent resin content.

Vessel No. T-2 was also compacted with vacuum bag pressure during cure. The resin was applied, however, by pulling the fiber through a resin bath and between "squeegee" rollers. This vessel had the highest graphite content of the six Thornel 50 vessels. The balance of the vessels received no compaction during cure, since it was observed that vacuum bagging was seriously degrading the composite structure (as explained in Appendix E). The remaining four vessels showed fairly consistent graphite contents. The lack of vacuum-bagging accounts for the higher resin content. Vessel No. T-5 had the least and most consistent graphite content and the highest performance factor, based on actual composite weight (Table 3). But this is probably the result of the increased strength at cryogenic temperatures previously discussed rather than the lower graphite content.

The average graphite content for the six Thornel 50 vessels was 62.1 wt. %. Using densities of 1.63 gm/cm³ (0.0588 lb/in.³) for the graphite

and 1.08 gm/cm^3 (0.039 lb/in.^3) for resin 2, the average graphite content by volume for the Thornel 50 vessels was 52 vol. %.

b. Morganite II Vessels. The values of fiber content for the vessels ranged from 45.9 to 54.2 wt. %. The standard deviation of specimens from a given vessel ranged from 0.39 to 2.18 wt. %. As a check of the procedure, Morganite II S fiber composites with known amounts of fiber and resin were fabricated by NOL and sent to the contractor for fiber content tests. The values obtained by the contractor for the specimens agreed closely with the known values. The inaccuracies ranged from 0.02 to 2.94% with an average inaccuracy over the eight lots of 0.78%.

All Morganite II vessels were cured without vacuum bag compaction, and all but vessel M-6 had the resin applied by pulling the fiber through a resin bath. On vessel M-6, the resin was applied by brush in an attempt to reduce damage observed in passing the tow through the resin bath and squeegee roller. This vessel showed the lowest graphite content but also the most consistent content of the three vessels of this thickness. (Vessel T-1, which also had the resin brush-applied, had the most consistent graphite content of its group.) The average graphite fiber content for the three thicker vessels was 51.1 wt. % as compared with 49.3 wt. % for the thinner vessels. This is probably due to a greater squeeze-out of resin caused by the additional layers of windings.

Vessel M-5 showed about 8% less graphite fiber content than the other two vessels of the thick-wall construction. The reason for this is not known. If its burst pressure of $19.2 \times 10^6 \text{ n/m}^2$ (2789 psi) is compared with the 12.6 n/m^2 (1820 psi) burst pressure of vessel M-3 (tested at the same temperature, -253°C , but of a thinner wall), vessel M-5 had better performance. This was unexpected, since in the discussion of filament stresses, a reduction of ultimate stress of about 20% was observed in the thicker walled vessels as compared with the thinner walls.

The average filament content for the six Morganite II vessels was 50.17 wt. %. Using densities of 1.75 gm/cm^3 (0.063 lb/in.^3) for the graphite fiber and 1.08 gm/cm^3 (0.039 lb/in.^3) for the resin system (resin 2), the average graphite fiber content by volume for the Morganite II vessels was 37.5 vol. %. This very low graphite content must be improved in order to achieve any significant weight saving with vessels fabricated of this material.

4. Pressure Vessel Strain

All of the vessels tested strained 0.17 to 0.5%, suitably low to function properly with a thin metal liner. The strains compared as follows:

Thornel 50 vessels were strained at burst (with one exception) from 0.20 to 0.30%. The hoop and longitudinal strains were approximately equal but increased with increasing strength as a result of cryogenic testing. The filament modulus held between 35 and $38 \times 10^{10} \text{ n/m}^2$ (51 and 55 million psi) through the three temperatures.* The average strain was 0.26%.

* Based on calculated vessel stress and measured strains.

The Morganite II vessels failed at strains ranging from 0.17 to 0.5%. The average strain for all six vessels was 0.33%. If vessel M-2 is excluded as being non-representative, the strains range from 0.29 to 0.50% with an average of 0.39%. The filament modulus for these five vessels ranged from 23 to 29×10^{10} n/m² (33 to 42 million psi), a rather high scatter of values, with an average modulus of 27×10^{10} n/m² (39 million psi)*. The strain and modulus differences between Thornel 50 and Morganite II stem from the differences in filament modulus as advertised by the supplier, namely, 34×10^{10} n/m² (50 million psi) for Thornel 50 vs. 21 to 28×10^{10} n/m² (30 to 40 million psi) for Morganite II.

Vessel M-2 had some defective hoop windings, and more windings were added to bring the defective area to proper strength. The repair was only partially successful, the vessel failing at about 86% of the interpolated value for its temperature. The low hoop strain of 0.17% was attributed to the extra hoop reinforcement.

Graphs of strains for all 12 vessels are shown in Figures 29 - 40.

5. Pressure Vessel Performance Factor

The pressure vessel performance factors (pV/W) shown in Table 3 were computed from burst pressure, volume, and composite weight actually measured for the cured vessels and range from 0.81 to 1.2×10^6 cm (0.32 to 0.46×10^6 inches). They reflect the weight of the resin-rich structure and additional windings added, as well as lowered strengths resulting from other material and processing difficulties encountered during winding. In addition to the actual performance factors noted in Table 3, performance factors for hypothetical vessels were calculated.

Using the filament weights used in calculating filament stresses (based on a uniform minimum wall thickness), together with a reduction in resin content to obtain a 65 vol. % fiber content, a performance factor for a hypothetical vessel was calculated using the actual burst pressures achieved on the test program. This performance factor is believed to be achievable for the three vessel configurations on future programs and is probably conservative, since it includes only a reduction in weight which appears feasible and does not take into account the increased burst pressures which may result from such improvements.

The performance factors for the "improved" or hypothetical vessels and also for S glass and boron filament vessels are shown in the following table:

Vessel Type	Performance Factor x 10 ⁻⁶					
	22°C		-195°C		-253°C	
	cm	in.	cm	in.	cm	in.
Thornel 50	1.22	0.48	1.50	0.59	1.60	0.63
Morganite II (Thick Wall)	1.62	0.64	-	-	1.42	0.56

* Based on calculated vessel stress and measured strains.

Performance Factor $\times 10^{-6}$ (continued)

Vessel Type	22°C		-195°C		-253°C	
	cm	in.	cm	in.	cm	in.
Morganite II (Thin Wall)	1.98	0.78	1.45	0.57	1.40	0.55
S Glass	2.3	0.90				
Boron Filament	1.3 - 1.8	0.50 - 0.70				

IV. DISCUSSION

A. DISCUSSION OF THE PROCEDURE

The dividing of the work into a preliminary investigation of materials (Task I) and the winding of vessels using the best materials (Task II) was devised by personnel of NASA and NOL. This procedure proved entirely suitable and showed the best materials, as well as giving an indication of problems. Some changes might be recommended for similar future programs. These are presented in Section VI. Recommendations.

B. FIBER TENSILE STRENGTHS

1. Room Temperature

Fiber tensile strengths at room temperature ranged from 13.8×10^8 n/m² (189,000 psi) to 21×10^8 n/m² (305,000 psi) when measured by strands in Task I. Values were consistently below the manufacturer's specification values. Molded bars or filament wound rings gave 61 to 80% of the fiber strength of strands. This is typical; more massive specimens give lower values. Also, the Split-D test for rings imposes a bending load which is not corrected in the stress calculations.

Task II strand tests of Thornel 50 at room temperature gave 14.9×10^8 n/m² (216,000 psi) or 83% of the manufacturer's value, and tests of Morganite II gave 20.2×10^8 n/m² (293,000 psi), or 79% of the manufacturer's value. Again, a disparity is shown between manufacturer's values and test values. In filament wound vessels, fiber hoop strengths of 59% and 67% of the respective strand strengths were attained for Thornel 50 and Morganite II. These relatively low values are attributed to low winding tension and resin rich composites, as discussed more fully in section G which follows.

2. Cryogenic Temperatures

Fiber tensile strengths of Morganite II composites decreased significantly at cryogenic temperatures as compared to room temperature. Task I work using strands, bars, and rings gave 30% strength drops. Task II work using vessels gave 17% strength drop at -195°C and 22% drop at -253°C. This is

undesirable for purposes of this study. No single-filament tests were run at cryogenic temperature to see if the strength drop is an intrinsic feature of the fiber.

Tensile strengths of Thornel 50 composites remained essentially constant with temperature in the Task I work and increased with lower temperatures in the Task II work by 16 to 30%. Part of the increase is attributed by Aerojet to their learning curve, the later vessels made being tested at lower temperatures. This constant or increasing strength at lower temperatures results in the Thornel 50 being at least as strong as the Morganite II at cryogenic temperatures, while at room temperature the Thornel 50 has only two-thirds the strength of Morganite II.

3. Effect of Whiskering and Nitric Acid Fiber Surface Treatments

Both the whiskering and the nitric acid fiber surface treatments reduced the fiber tensile strengths. From a strength standpoint, therefore, these treatments were not in accord with the objectives of this program. Strength reductions from 5 to 50% were observed with Thornel 50; Morganites I and II gave 25 to 75% reductions. Nitric acid treatment gave 2 to 13% strength reductions in strands but also made the strands more vulnerable to larger-than-usual values of tensile strength reduction at cryogenic temperatures. Both surface treatments were for the purpose of improving the resin to fiber bond, but in the case of predominately tensile stresses (as encountered in an internal pressure vessel), stronger resin bonds have not been shown to necessarily improve the composite tensile strength in the fiber direction. Because the treatments reduced the composite strengths, they were eliminated from use in the Task II vessel winding work.

4. Effects of Cycling Fatigue

Cycling fatigue of rings in the Split-D fixture to 1000 cycles gave relatively good results. Room temperature cycling reduced strengths by 10 to 17%, but cycling while cold gave from 9% reduction to an actual slight increase in strengths. The test imposes a bending load on the ring, and the higher inter-laminar shear strength at cold temperature is theorized to help the ring withstand this type of load. It seems that cryogenic temperatures pose no extra problem in the fatigue cycling of unidirectional laminates, at least for the fibers and resins tested. The excellence of graphite fiber composites in tensile fatigue has been reported, references (j) and (l).

C. MODULI AND EFFECT OF TEMPERATURE

Composite tensile moduli increased for all composites at cold temperatures by 0 to 20% compared to room temperature values. This is both an expected and a desirable condition. The moduli values at room temperature for Thornel 50 and Morganite II fibers averaged 10 to 20% lower than the manufacturers' values. These values are sensitive to the sampling procedure used, since there is considerable variation in properties along the fiber within a single roll. Thornel 50 fiber, for instance, consists of 5 to 15 lengths of yarn adhesively bonded together to make a one-pound roll. Manufacturers' sampling procedures are not known, and they do not list a range of values on each roll nor do they assign a coefficient of variation to the mean value for each roll.

The ultimate strain values of 0.2% to 0.5% found for the graphite fiber composites in this work were consistent with the objective of the overall NASA program--that is, the development of a filament wound structure which is strain compatible with thin metallic liner materials at cryogenic temperatures. These strain values for graphite filament are one-fifth the strain values obtained for glass filament wound structures.

D. FLEXURAL MODULI AND STRENGTHS

Although flexural testing is not directly applicable to the problem of designing internal pressure vessels, it was decided that some flexural data would help to give a broader basic knowledge of these materials. The tests showed that the Morganite II was in a class by itself for high flexural strength, giving up to $24.7 \times 10^8 \text{ n/m}^2$ (358,000 psi) fiber strength. High flexural strengths require both a strong fiber and a good interlaminar bond of resin to the fiber, and the Morganite II was unexcelled in these two features. Strengths were almost unaffected by cold temperature, which for Morganite II may reflect the interaction of decreasing fiber strength and increasing shear strength when cold. Flexural moduli at room temperature were about the same as the tensile moduli, but when cold the flexural moduli increased from 32 to 62%, as compared to 10% for the other modulus tests. The large increase in flexural modulus probably is due to errors introduced by the assumptions commonly made in these modulus calculations. One of these assumptions--that the effect of resin shear modulus is negligible--probably is the main culprit in this case. One could expect the shear modulus to increase severalfold when going from warm to cold and, therefore, make the composite somewhat stiffer due to less resin deflection. Resin shear moduli at cryogenic temperatures were not determined.

E. INTERLAMINAR SHEAR STRENGTHS

The significance of the composite interlaminar shear strength of the composite in the wall of an internal pressure vessel has many ramifications. Higher shear strengths are desired as the fiber strengths are higher, as the fiber diameter is larger, or as the lengths of fibers are decreased. Also, as transverse loads are introduced (as in "in-plane" winding in which the strand does not take the shortest path), higher shear strengths are desired. Lower shear strengths are better as the fiber strengths are lower and generally in the reverse of the above conditions. The objective is to get the strongest composite but to avoid a brittle, glassy composite which shatters on impact loading or becomes very vulnerable to scratches or winding flaws. But it is difficult to calculate the optimum shear strength necessary for a given set of conditions. Shear strengths for as-received fiber in composites at room temperature were from 20×10^6 to $91 \times 10^6 \text{ n/m}^2$ (2900 to 13,200 psi), with Morganite II S giving highest values. These values are typical of values obtained with these fibers since the inception of commercial graphite fibers in 1965 and, compared to glass or boron fiber composites (ref. (k)), are generally quite low. Hence, the fiber surface treatments of whiskering and nitric acid boil were developed to increase this shear strength. Whiskering has been shown in other work (ref. (e)) to increase shear strengths to as high as $138 \times 10^6 \text{ n/m}^2$ (20,000 psi). Nitric acid boil is less effective and gave strengths in this study to $67 \times 10^6 \text{ n/m}^2$ (9700 psi). But the drawbacks to both treatments include their weakening effect on the fibers, as noted in section B of this discussion. For these reasons, they were dropped from the Task II vessel program.

The effect of cryogenic temperatures on shear strengths was to increase the strengths by 2% to over 100%. This increase is an expected result, as indicated by past studies with glass fiber composites (ref. (b)), and comes probably from the increased strength of the resin at cold temperatures.

F. COEFFICIENTS OF EXPANSION

There is a considerable mismatch in the coefficients of expansion (or contraction) of the materials used in this program. The composite contraction was very low, 0.2×10^{-6} cm/m/°C. The resin was 200 to 300 times higher, 44 to 58×10^{-6} cm/cm/°C. Calculating from the strengths and moduli of fibers and resins, the coefficient of the bare fiber is negative, -0.2×10^{-6} cm/cm/°C. The coefficient of the stainless steel liner is intermediate, 9.5×10^{-6} cm/cm/°C. The resin has a heat cure and may be at 100°C when it gels. Cooling to room temperature after the cure introduces an 80°C thermal differential to cause stresses. Further cooling to -195 or -253°C results in up to 1.5% tensile strain in the resin, sufficient to cause microcracking and 0.3% tensile strain in the stainless steel liner. When the vessel is pressurized, an additional tensile strain averaging 0.3% is imposed. Total strains are the sum of the thermal and mechanical strains and can be 1.8% for the resin and 0.6% for the liner. These are rather high strains for both materials at cold temperatures and could indicate possible vessel problems if both mechanical pressure cycling and temperature cycling tests are imposed.

G. GRAPHITE FIBER QUALITY

Graphite fiber, as received from the manufacturers, was not of good quality. It was often inadequately packed and damaged by shipping. Some contained many splices and some snarls or tangles. Changes in weight and cross-sectional area along the length was evident. In use, some of it had weak spots and broke during filament winding to the detriment of the part being fabricated. The measured tensile strength and modulus values generally were appreciably below the values claimed by the manufacturers. The rather low fiber quality caused particular problems during the pressure vessel fabrication phase when using in-process resin impregnation. The necessary low winding tension to avoid an excessive number of breaks left too much resin in the composite, which in turn caused fiber buckling and fiber wash when the resin was squeezed out on vacuum bagging. The bagging thereby had to be discontinued, leaving a composite both resin rich and with excessive voids. Heat was not used during winding to reduce resin viscosity, because in-plane winding places the strand in an unstable path, and problems of strand slippage would be increased by lower resin viscosity. Some of the problems could have been avoided by the use of pre-impregnated fiber, which is recommended for any future winding of vessels. In all, the material was time consuming to use, and part quality in some cases was lower than it should have been. We look forward to an improvement in the quality of future fibers.

H. BRITTLE FRACTURE OF VESSELS

All of the tested vessels exhibited a brittle fracture mode of failure, with the vessel shattering into several large pieces. This is an undesirable failure mode, since the vessel is vulnerable to catastrophic failure from scratches or

impacts (micrometeoroids). This failure mode is not the result of improper fabrication but rather is inherent to stiff, non-ductile fiber materials which are well bonded. Some possible ways of reducing this brittleness and increasing the impact strength include winding in a small amount of a ductile fiber and optimizing the resin-fiber bond at a value neither too high nor too low.

V. CONCLUSIONS

1. The objective of obtaining mechanical property data on graphite filament epoxy resin composites at room and cryogenic temperatures was accomplished.

2. Cold temperatures generally decreased the fiber tensile strengths. Morganite II was most seriously affected, with 18 to 30% strength loss when cold. Thornel 50 in pressure vessels was an exception and increased up to 30% in strength when cold. This difference in response to cold temperatures resulted in Thornel vessels having a slightly higher performance factor (PV/W) than Morganite at cold temperatures. This performance factor, estimated at 1.5×10^6 cm for graphite vessels with optimum fiber content, is competitive with boron fiber (1.3 to 1.8×10^6 cm) and two-thirds that of glass fiber (23×10^6 cm). This is promising for the future of graphite fiber in this application.

Fatigue cycling of NOL rings to 1000 cycles at 75% ultimate stress gave 10 to 17% strength decreases at room temperature and less at cryogenic temperatures. Therefore, low temperatures favor an increase in fatigue life of these composites.

The fiber surface treatments of whiskering and nitric acid boil reduced the fiber and composite tensile strengths (in the fiber direction) by 5 to 70% and are concluded to be undesirable for the objectives of this program. Transverse composite properties were not measured.

3. Composites moduli increased by 0 to 20% when cold compared to room temperature. This is desirable for this program. Ultimate strain values of 0.2 to 0.5% in pressure vessels, resulting from the internal pressure applied, are generally compatible with thin metallic liner materials, i.e., stainless steel type 304. The concept of constructing lightweight filament-wound vessels by winding graphite fibers over a metallic liner appears promising.

4. Flexural and interlaminar shear properties were measured to give a broader basic knowledge of the materials. Flexural strengths were unaffected by cold, but flexural moduli increased up to 62% when cold. Interlaminar shear strengths increased by 2% to over 100% when cold.

5. The thermal contraction of the fiber over the temperature range +22 to -195°C was calculated to be slightly negative; that is, the fiber increased in length in going down through this 217°C range. The resin and the stainless steel liner material, on the other hand, shrink considerably. These materials combined into a vessel, cooled to liquid nitrogen temperature, and pressurized would give approximately 0.3% tensile strain for the fiber, but the liner strain would be 0.6% and the resin strain 1.8%. These are rather high strains for the liner and resin materials.

6. Graphite fibers as received from the manufacturers were not always of good quality. Strength and modulus measurement results were nearly always below the manufacturers stated values, and yarns and tows were sometimes fuzzy and broken. As a result, the fibers were often difficult to use and composite quality sometimes suffered.

7. All of the tested vessels exhibited a brittle fracture mode of failure at both room and cryogenic temperatures. This is undesirable but is inherent to these stiff, brittle fibers and composites thereof. Brittle structures are particularly vulnerable to fabrication and handling damage and require careful procedures and good inspection.

VI. RECOMMENDATIONS

From the results obtained as reported herein, certain problems were uncovered and certain questions left unanswered. Any further work could include the following:

1. Run single filament tests at cryogenic temperature to see if modulus and strength changes are intrinsic to the fiber.
2. Use prepreg in the vessel winding to allow closer control of the fiber-resin content.
3. Use learning, or proof, vessels and qualify these before the main test vessels are constructed.
4. Consider helical winding instead of in-plane winding for cylindrical shaped vessels. Helical winding places the strand in a stable path and should eliminate strand slippage on the mandrel. A discussion of the relative merits of in-plane vs. helical winding would be extensive, but at least strand slippage is easier to control with helical winding.

VII. FOLLOW ON WORK

This cryogenic work is continuing as Tasks III - VI. The objectives of this continued work include tests of additional resins, particularly rubber-epoxy polyblends, crack propagation and fracture studies, and testing of bidirectional filament-wound plates. Reports will be issued.

REFERENCES

- (a) Hanson, M. P., Richards, H. T. and Hickel, R. O., NASA TN D-2741, "Preliminary Investigation of Filament Wound Glass Reinforced Plastics and Liners for Cryogenic Pressure Vessels," March 1965.
- (b) Lewis, A. and Bush, G. E., Improved Cryogenic Resin/Glass-Filament-Wound Composites, NASA CR-72163 (Aerojet-General Report 3392 under Contract NAS 3-6297), April 1967.
- (c) Hanson, M. P., NASA TN D-4412, "Glass-Boron-, and Graphite-Filament-Wound Resin Composites and Liners for Cryogenic Pressure Vessels," Feb. 1968.
- (d) Molho, Ralph, Aerojet W.O. 8712-21-3xxx, "Boron, Graphite, and Glass Filament Wound Pressure Vessels with Load-Bearing, Non-Buckling Metal Liners," Nov. 1967.
- (e) Simon, R. A. and Prosen, S. P., NOLTR 68-132, "Carbon Fiber Composites," 25 Oct. 1968.
- (f) Herrick, V. W., Gruber, P. E., Jr., and Mansur, F. T., "Surface Treatments for Fibrous Carbon Reinforcements," AFML-TR-66-178, Part 1, July 1966.
- (g) Soffer, L. M. and Molho, R., Cryogenic Resins for Glass-Filament-Wound Composites, NASA CR-72114 (Aerojet-General Report 3392 under Contract NAS 3-6287), Jan. 1967.
- (h) ASTM D-20, Subcommittee XVIII, Sect. K and D-30, Subcommittees IV and V, "Proposed Method of Test for Tensile Properties of Strands, Yarns and Rovings," 24 Jan. 1969.
- (i) Kinna, M. A., NOLTR 64-156, "NOL Ring Test Methods," Sep. 1964.
- (j) Hanson, M. P., NASA TM X-52539, "Tensile and Cyclic Fatigue Properties of Graphite Filament-Wound Pressure Vessels at Ambient and Cryogenic Temperatures," presented at 15th SAMPE Natl. Symposium and Exhibit, Los Angeles, Calif., April 29 - May 1, 1969.
- (k) Gutfreund, K. and Broutman, L. J., "Interfacial Investigations of Boron Fiber Reinforced Plastics," presented at 10th Natl. SAMPE Meeting, San Diego, Calif., Nov. 9-11, 1966.

UNCLASSIFIED
NOLTR 69-183

TABLE 1

A. MECHANICAL PROPERTIES OF THORNEL 50 YARN

Manufacturer's Data (Total 12 Rolls):

	<u>n/m²</u>			<u>pfsi</u>			<u>C_v</u>
	<u>min.</u>	<u>avg.</u>	<u>max.</u>	<u>min.</u>	<u>avg.</u>	<u>max.</u>	
Tensile Modulus	31.0 x 10 ¹⁰	33.2	35.2	45.0 x 10 ⁶	48.2	51.0	0.05
Tensile Strength	15.9 x 10 ⁸	17.9	19.8	230 x 10 ³	259	287	0.06

Strand Test Data (Total 12 Rolls and 43 Individual Tests):

Tensile Modulus	26.1 x 10 ¹⁰	30.4	33.5	37.9 x 10 ⁶	44.1	48.6	0.07
Tensile Strength	9.65 x 10 ⁸	14.9	19.7	140 x 10 ³	216	285	0.23

B. MECHANICAL PROPERTIES OF MORGANITE TOW

	<u>n/m²</u>			<u>pfsi</u>			<u>C_v</u>
	<u>min.</u>	<u>avg.</u>	<u>max.</u>	<u>min.</u>	<u>avg.</u>	<u>max.</u>	
Manufacturer's Data (Total 16 Rolls):							
Tensile Modulus	22.8 x 10 ¹⁰	26.6	29.7	33.1 x 10 ⁶	38.6	43.1	0.09
Tensile Strength	23.0 x 10 ⁸	25.4	28.8	333 x 10 ³	369	418	0.08

Strand Test Data (Total 4 Rolls and 42 Individual Tests):

Tensile Modulus	20.2 x 10 ¹⁰	21.1	21.9	29.3 x 10 ⁶	30.6	31.8	0.03
Tensile Strength	18.2 x 10 ⁸	20.2	22.1	264 x 10 ³	293	320	0.08

TABLE 2
FABRICATION DATA SUMMARY - TWELVE GRAPHITE FILAMENT-WOUND VESSELS

Vessel S/N	Configu-ration	Order of Fab.	Liner Weight Grams a	Ancillary Weight Grams ^b	Deposited Filament Weight Grams			Vessel Cured Weight Grams		Composite Weight Grams		Average Graphite Content % (by wt) ^c
					Long.	Hoop	Total	Grams	Grams	Pounds		
										Grams	Grams	
T-1 ^d	1269214-1	1	1042	69	444	341	785	2230	1119	2.465	60.7	
T-2 ^e	1269214-1	2	1044	77	441	334	775	2250	1129	2.487	66.0	
T-3 ^f	1269214-1	3	1045	77	450	325	775	2412	1290	2.841	61.5	
T-4	1269214-1	4	1043	69	501	342	843	2495	1383	3.046	62.3	
T-5	1269214-1	5	1044	76	475	326	801	2441	1321	2.910	59.7	
T-6	1269214-1	6	1041	64	463	312	775	2445	1340	2.951	62.3	
M-1	1269228-1	7	1035	63	566	379	945	2668	1570	3.458	53.17	
M-2 ^g	1269228-1	8	1041	58	570	434	1004	2808	1709	3.764	54.18	
M-3	1269228-2	9	1040	64	364	261	625	2255	1151	2.535	49.20	
M-4	1269228-2	10	1036	65	397	263	660	2280	1179	2.597	51.43	
M-5	1269228-1	11	1041	58	598	381	979	2949	1850	4.075	45.86	
M-6	1269228-2	12	1035	62	398	274	672	2338	1241	2.733	47.14	

a Includes two bosses weighing 390g each.

b Scrim cloth, adhesive and wound-in instrumentation.

c Standard deviation ranged from 0.6 to 3.0% for Thornel 50 vessels and 0.39 to 2.18% for the Morganite II vessels.

d Vacuum bag cure and resin applied by brush.

e Vacuum bag cure and resin pot used.

f Standard cure and resin pot used from this point on.

g Severe hoop breakage. Additional filament added.

TABLE 3
PRESSURE VESSEL PERFORMANCE SUMMARY

S/N	Order of Fab.	Graph-ite Content (wt %)	Test Temp. (°C)	Burst Pressure (n/m ² x 10 ⁻⁶)	Burst Pressures		Strain at Burst (%)		Com-posite Weight (gms)	Per-formance Factor x 10 ⁻⁶	Apparent Failure Origin
					Hoop Fila-ments	Long. Fila-ments	Hoop Fila-ments	Long. Fila-ments			
T-1	1 ^b	60.7	23	14.60	907	809	0.22	0.20	1118	1.09	Hoop
T-2	2 ^c	66.0	23	112.80	795	709	0.16	0.22	1128	0.94	Hoop
T-3	3 ^d	61.5	23	15.37	955	852	0.27	0.23	1289	0.99	Knuckle
T-4	4	62.3	-196	17.34	1078	961	0.29	0.28	1382	1.04	Knuckle
T-5	5	59.7	-253	18.53	1151	1027	0.27	0.30	1320	1.17	Knuckle
T-6	6	62.3	-253	18.66	1160	1034	0.30	0.29	1339	1.14	Knuckle
M-1	7	53.2	23	21.89	1228	1066	0.37	0.50	1569	1.17	Hoop
M-2	8 ^e	54.2	-196	16.97	952	780	0.17	0.30	1707	0.81	Hoop & Long.
M-5	11	45.9	-253	19.23	1078	883	0.33	0.33	1848	0.86	Hoop & Long.
M-6	12 ^f	47.1	23	17.70	1472	1193	0.51	0.40	1240	1.19	Hoop
M-4	10	51.4	-196	12.82	1066	864	0.35	0.29	1178	0.91	Hoop & Long.
M-3	9	49.2	-253	12.55	1044	846	0.49	0.35	1150	0.91	Knuckle

^a n/m² x 10⁻⁶

^b Resin painted on; vacuum-bagged.

^c Resin pot used; vacuum-bagged.

^d Vacuum bag deleted from here on.

^e Severe hoop breakage during winding. Additional hoop filament added.

^f Resin painted on.

Morgantite II Tanks
"2/3 Wall" "3/3 Wall"
Thornel 50 Tanks

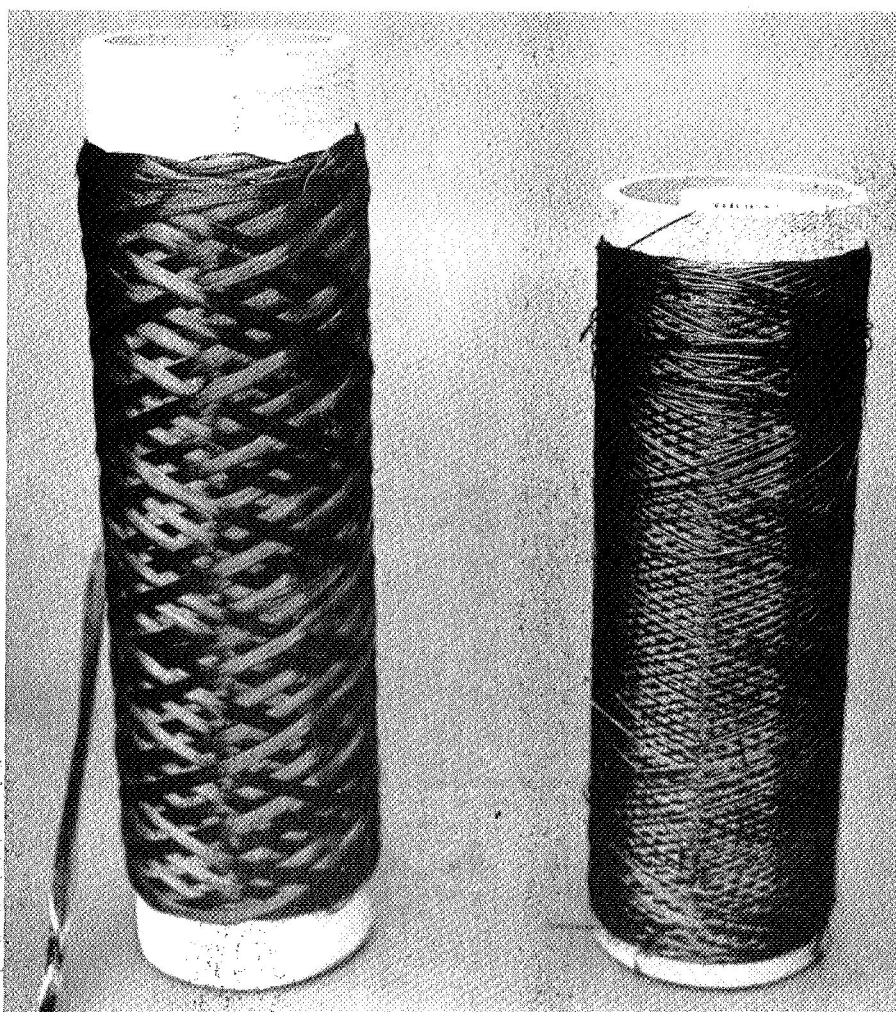
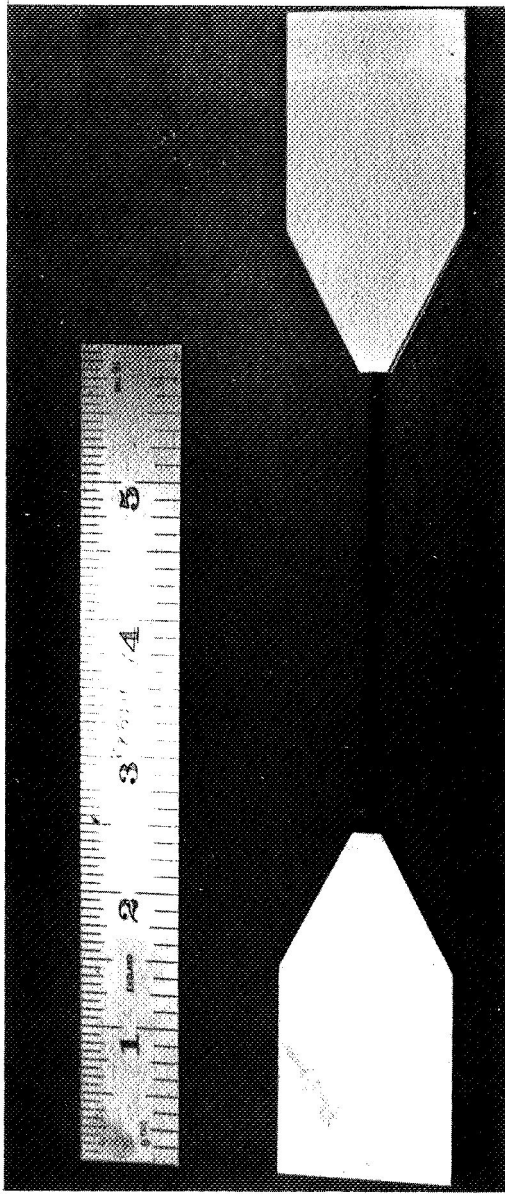
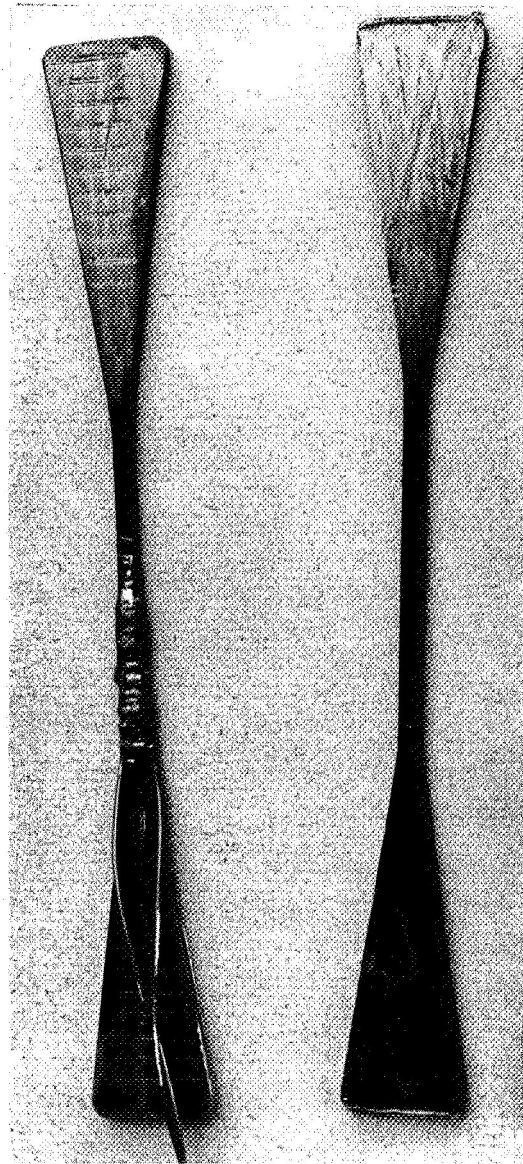


FIG. 1 GRAPHITE ROVING AND YARN ON SPOOLS

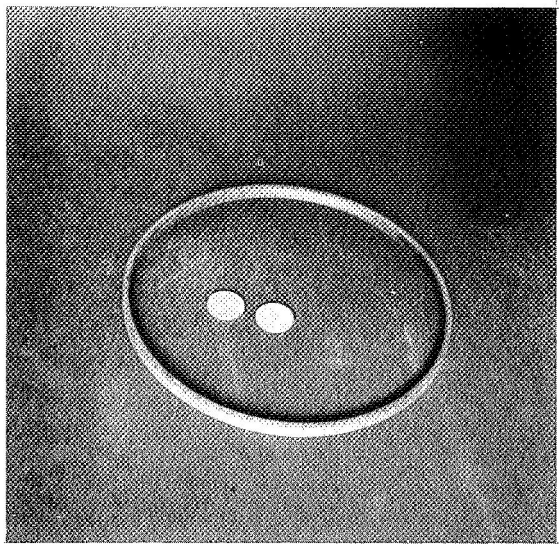


(A) STRAND READY FOR TEST

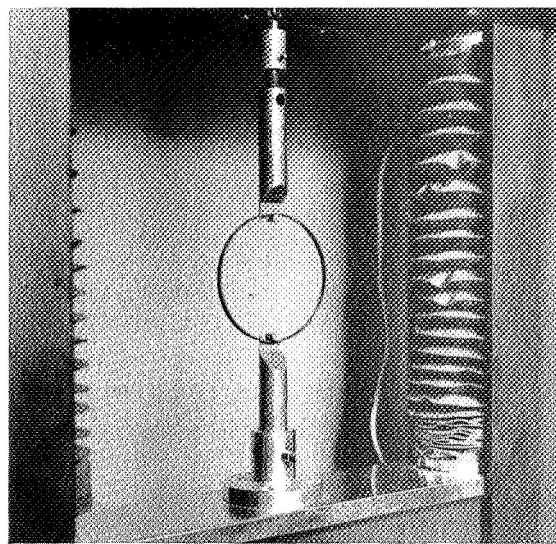


(B) TENSILE BARS FOR MODULUS AND STRENGTH. BAR ON LEFT HAS ELECTRIC STRAIN GAGE BONDED ON.

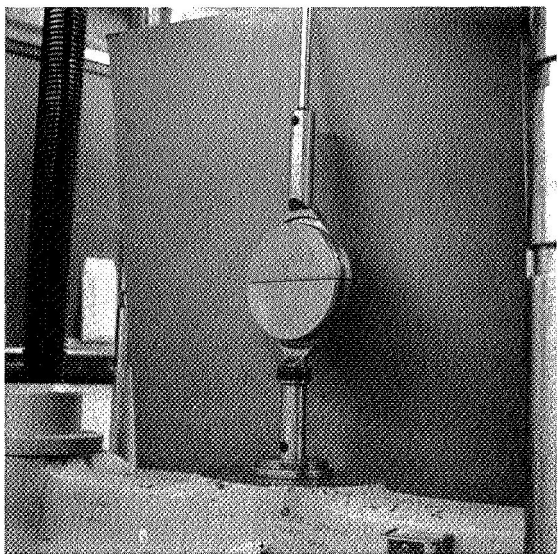
FIG. 2



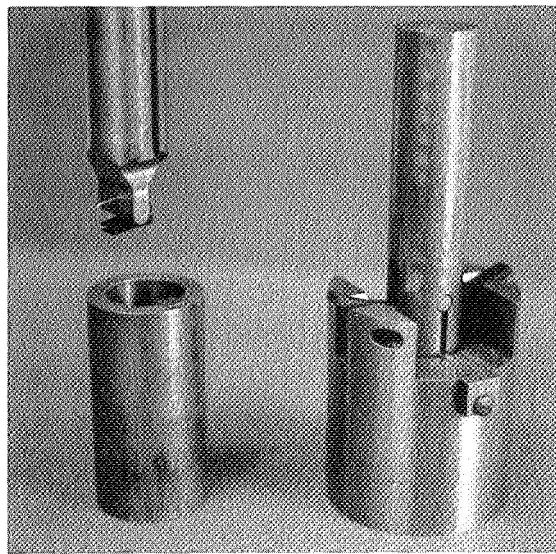
(A) NOL RING



(B) NOL RING IN SPLIT PIN
MODULUS TEST FIXTURE



(C) NOL RING IN SPLIT D
STRENGTH TEST FIXTURE



(D) CRYOGENIC SHEAR AND FLEXURAL
STRENGTH TEST FIXTURES

FIG. 3



FIG. 4a METAL-LINED GRAPHITE FILAMENT WOUND PRESSURE VESSEL - 8.00 DIA

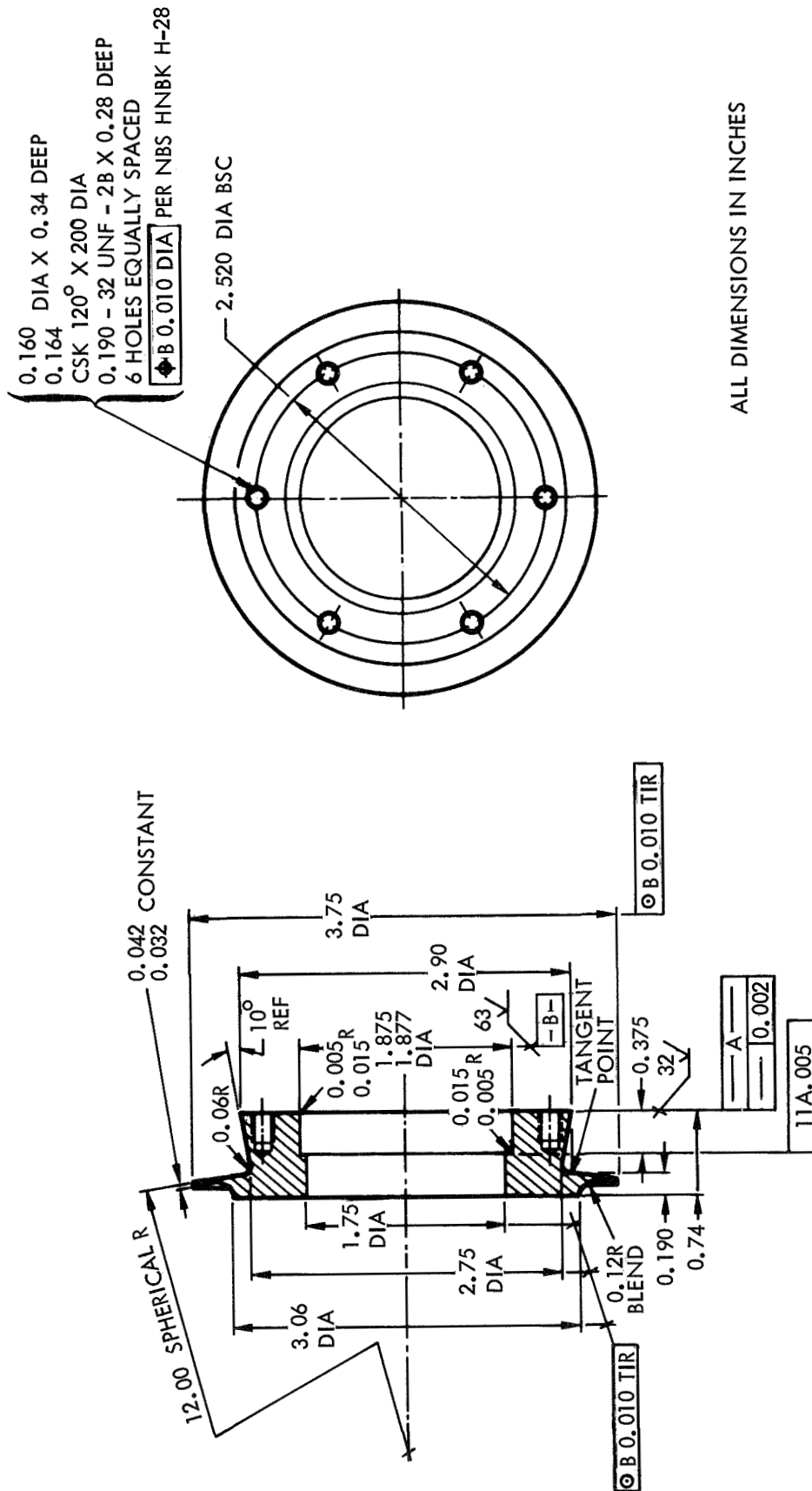


FIG. 4b BOSS DETAIL FOR 8-IN. DIA. PRESSURE VESSEL

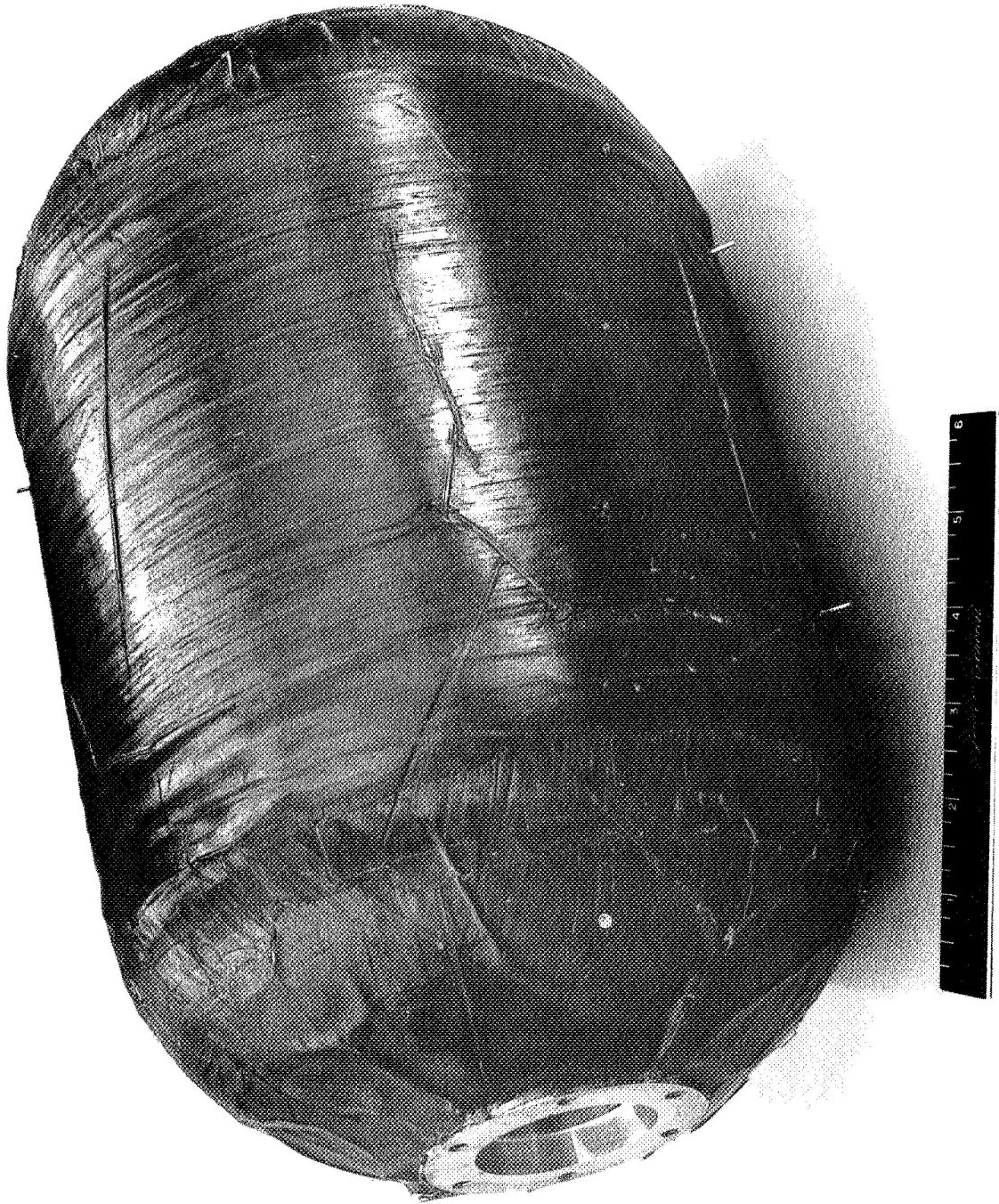


FIG. 5 THORNEL 50 FILAMENT WOUND PRESSURE VESSEL T-1



FIG . 6 THORNEL 50 FILAMENT WOUND PRESSURE VESSEL T-3

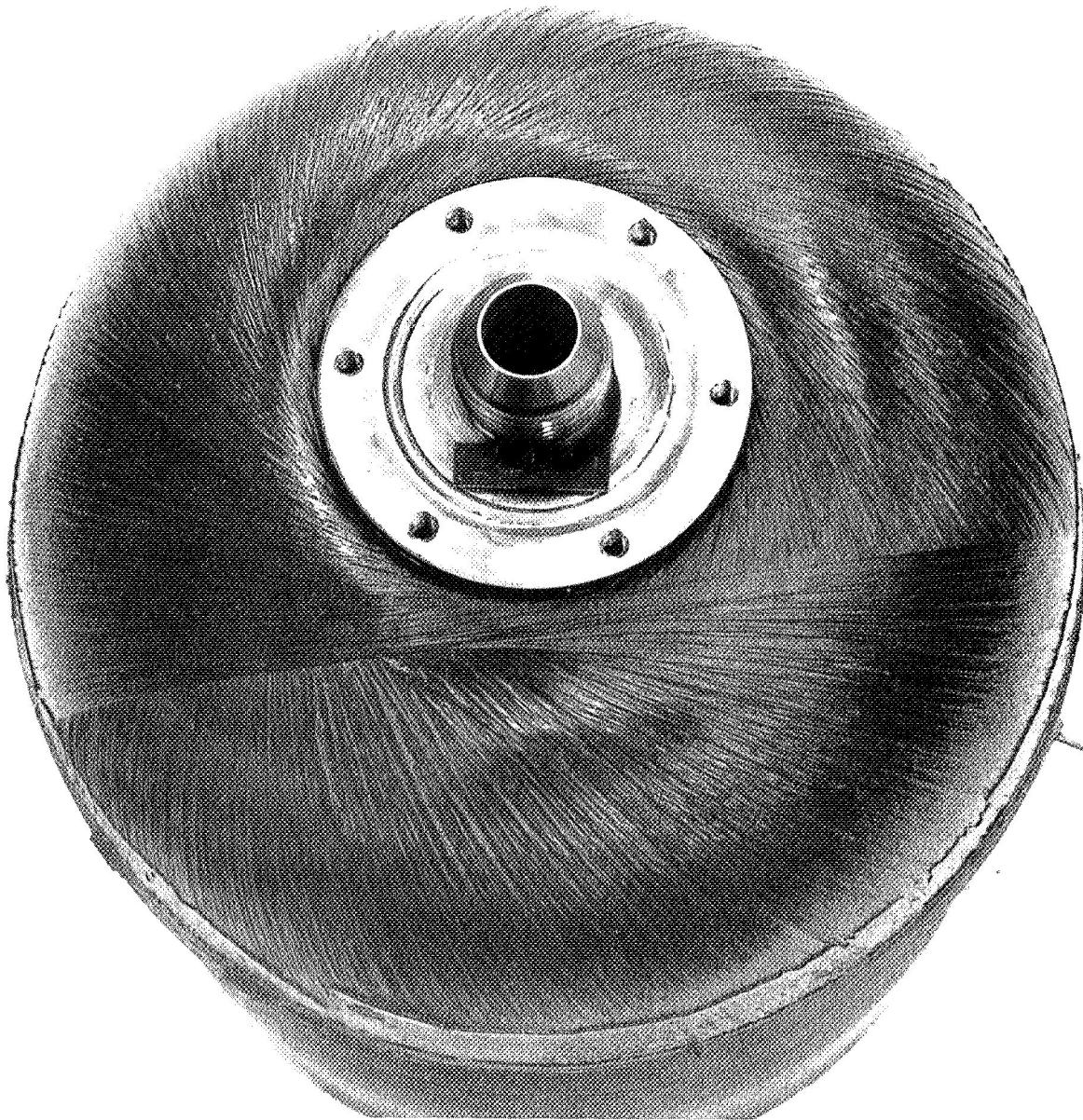


FIG. 7 THORNEL 50 FILAMENT WOUND PRESSURE VESSEL T-3



FIG. 8 MORGANITE II FILAMENT WOUND PRESSURE VESSEL M-1

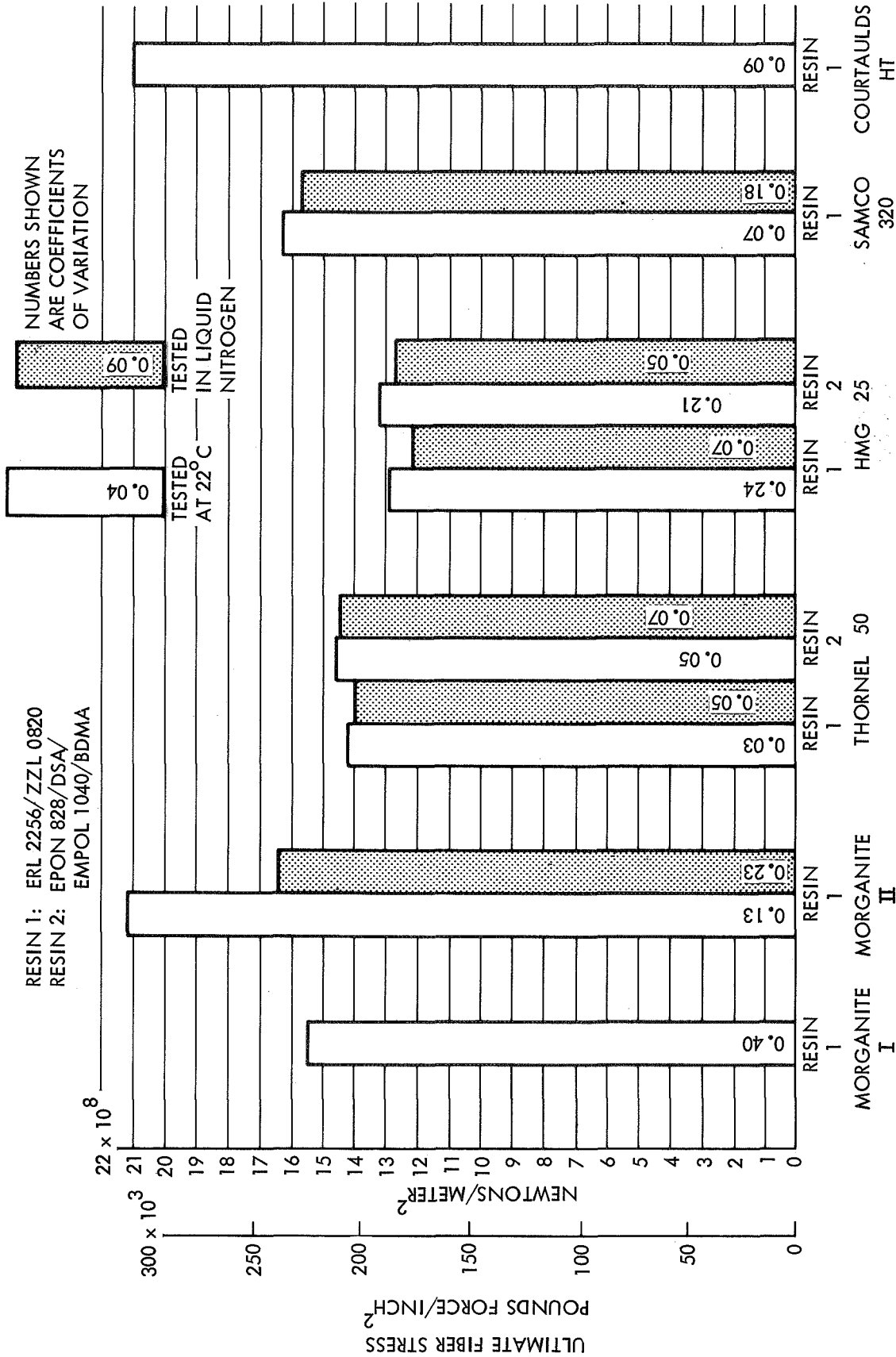


FIG. 9 FIBER TENSILE STRENGTHS
AVERAGE VALUES FROM RESIN - IMPREGNATED STRANDS
TESTED AT 22°C AND IN LIQUID NITROGEN

NUMBERS SHOWN
ARE COEFFICIENTS
OF VARIATION

DOTTED LINES SHOW
COMPOSITE VALUES

RESIN 1: ERL 2256/ ZYL 0820
RESIN 2: EPON 828/DSA/
EMPOL 1040/BDMA

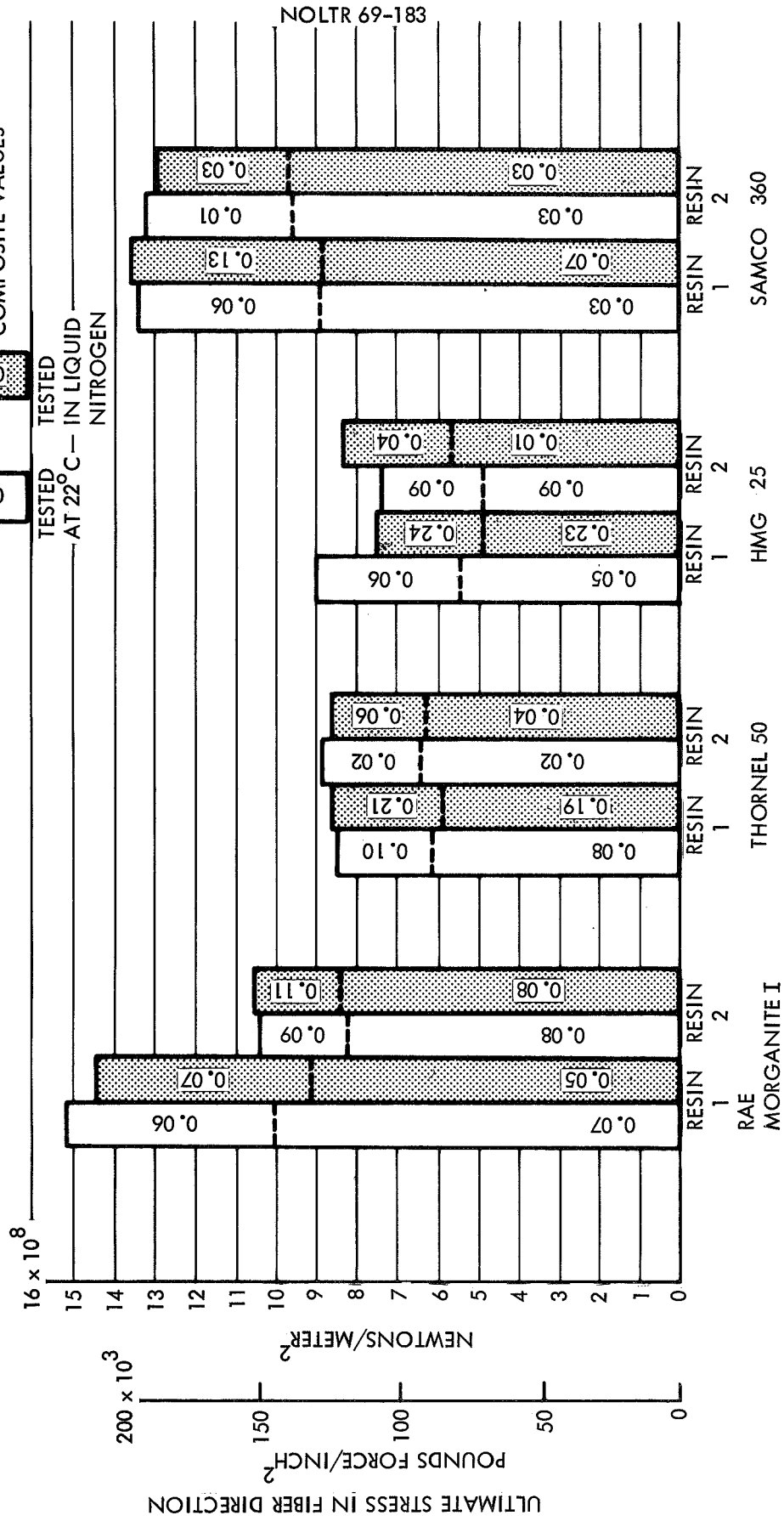


FIG. 10 FIBER AND COMPOSITE TENSILE STRENGTHS
AVERAGE VALUES FROM UNIDIRECTIONAL MOLDED BARS
TESTED AT 22°C AND IN LIQUID NITROGEN

RESIN 1: ERL 2256/ZZL 0820
RESIN 2: EPON 828/DSA/
EMPOL 1040/BDMA

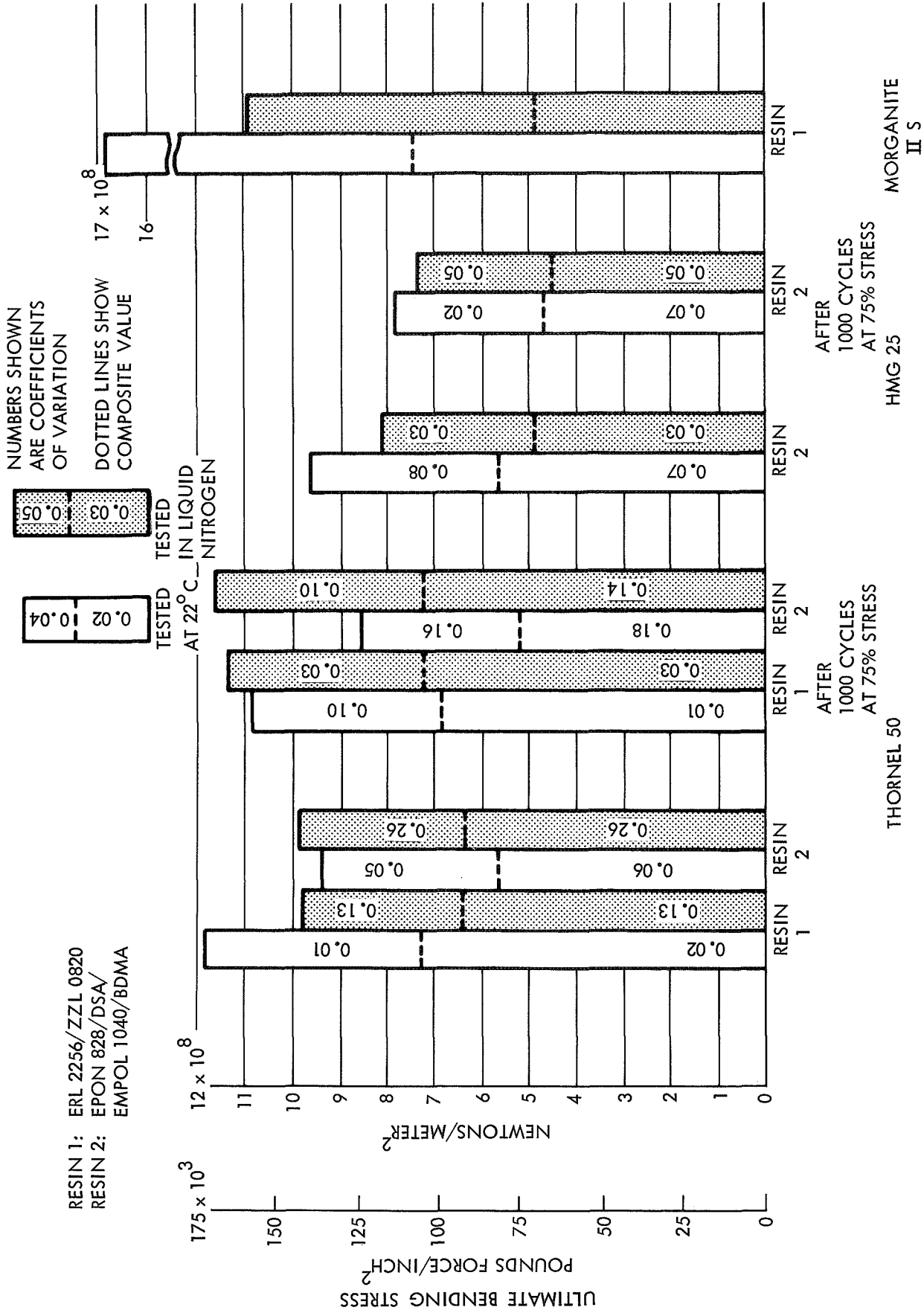


FIG. 11 FIBER AND COMPOSITE TENSILE (BENDING) STRENGTHS
AVERAGE VALUES FROM NOL RINGS - "SPLIT D" METHOD
TESTED AT 22°C AND IN LIQUID NITROGEN

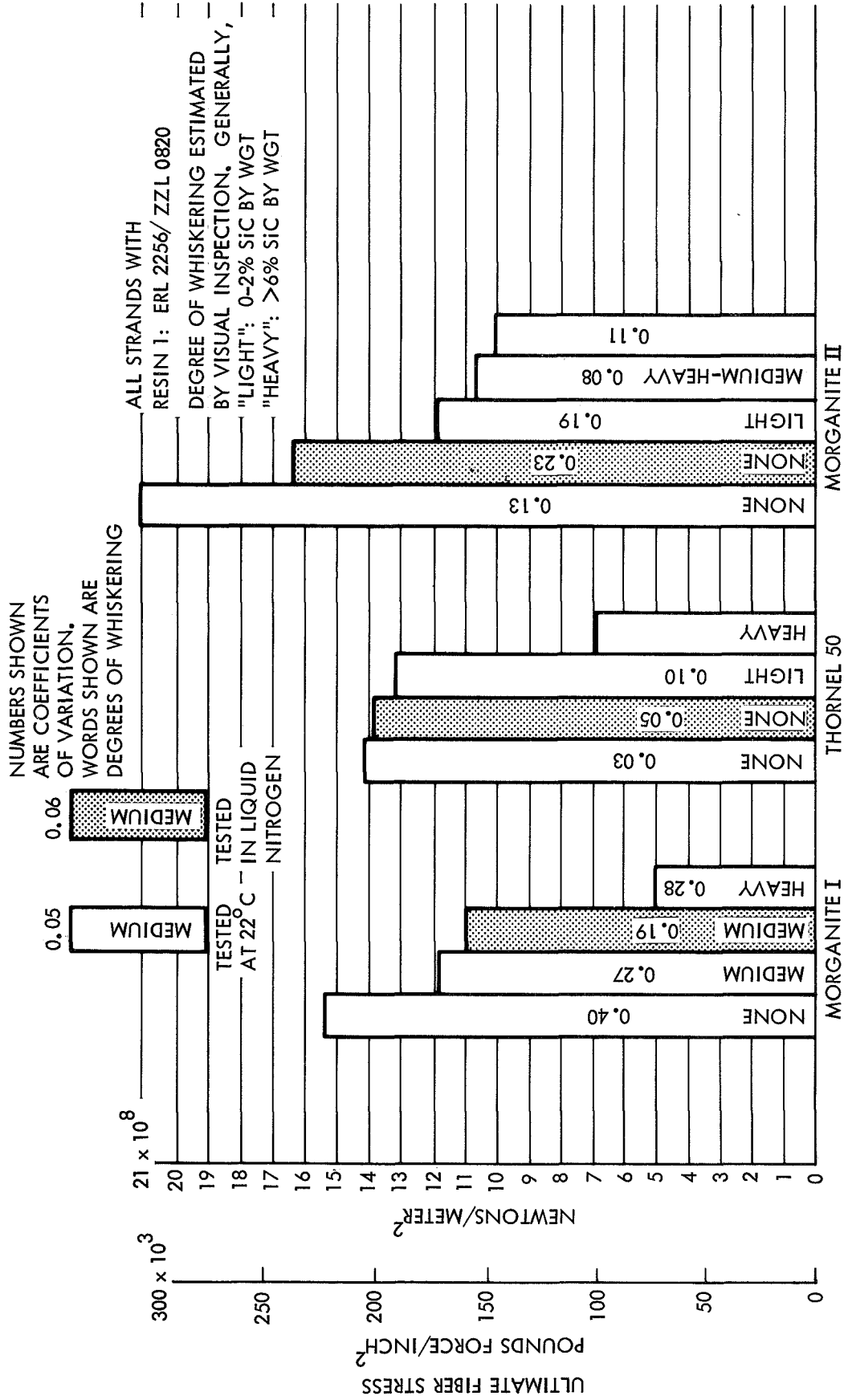


FIG. 12 FIBER TENSILE STRENGTHS - WHISKERED FIBER
AVERAGE VALUES FROM RESIN-IMPREGNATED STRANDS
TESTED AT 22°C AND IN LIQUID NITROGEN

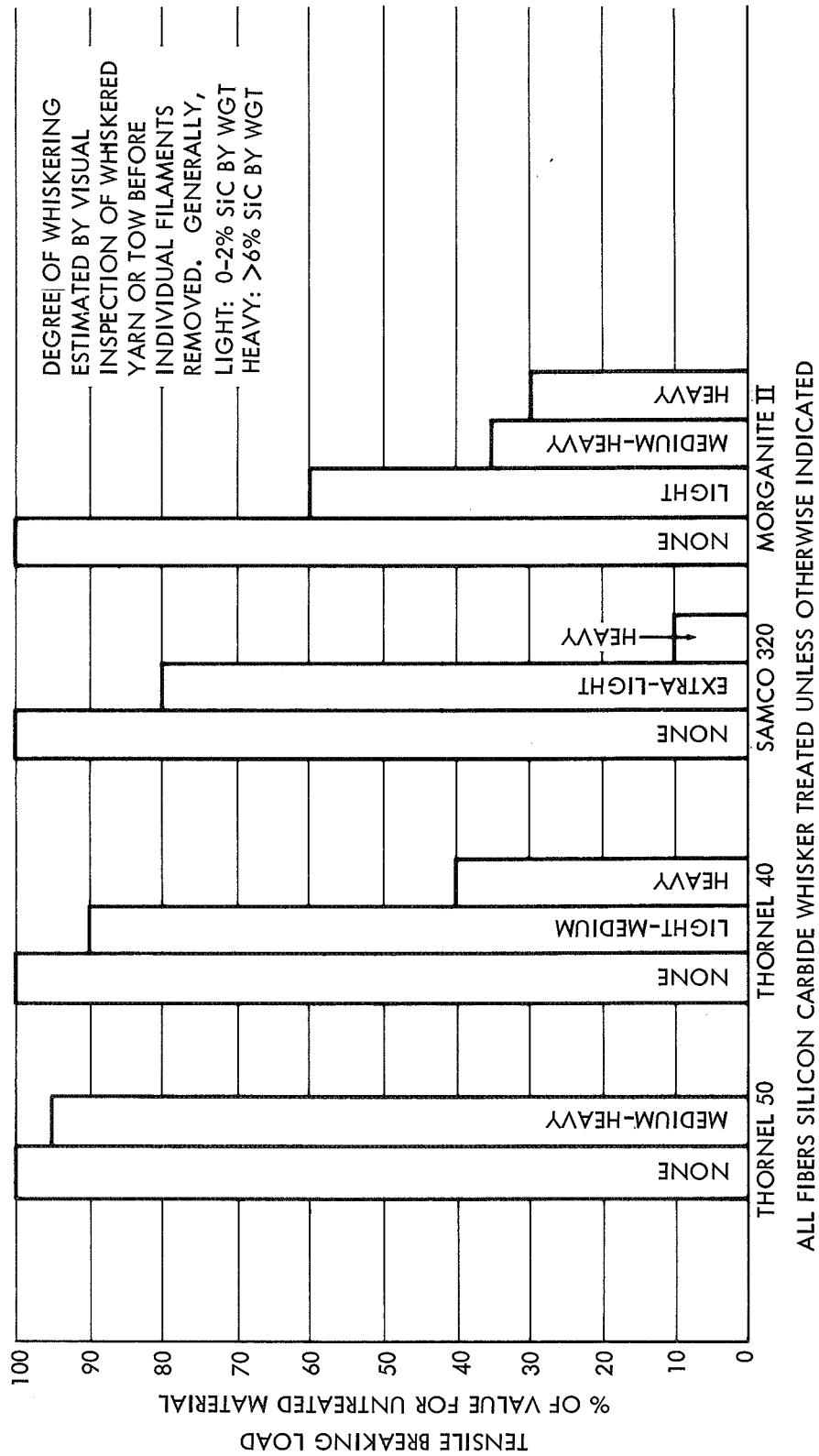
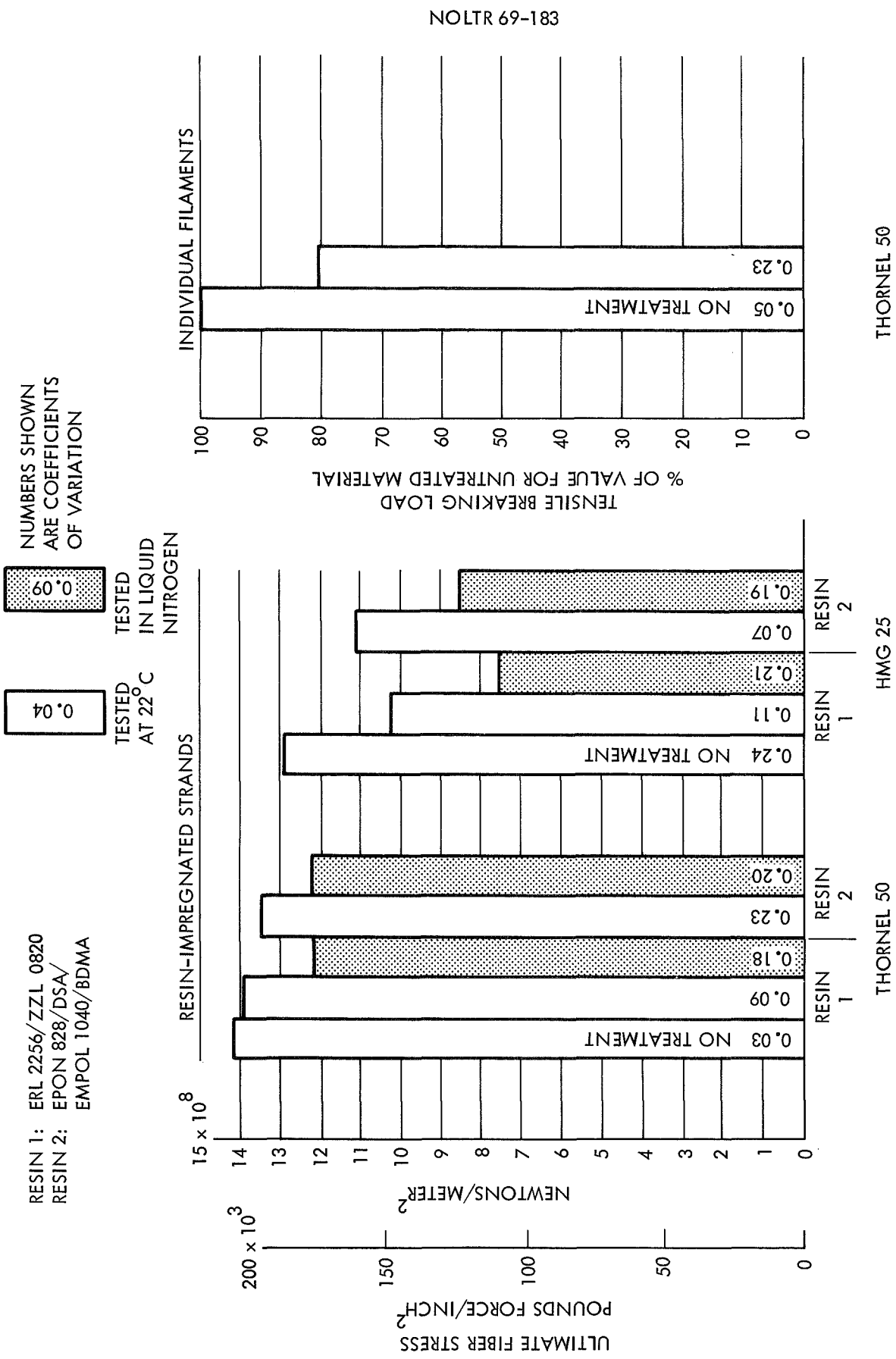


FIG. 13 FILAMENT TENSILE STRENGTHS - WHISKERED FIBER
AVERAGE VALUES FROM INDIVIDUAL FILAMENTS
TESTED AT 22°C



ALL FIBERS NITRIC ACID TREATED UNLESS OTHERWISE INDICATED

FIG. 14 FIBER TENSILE STRENGTHS - NITRIC ACID TREATED FIBER
AVERAGE VALUES FROM RESIN- IMPREGNATED STRANDS AND FROM INDIVIDUAL FILAMENTS

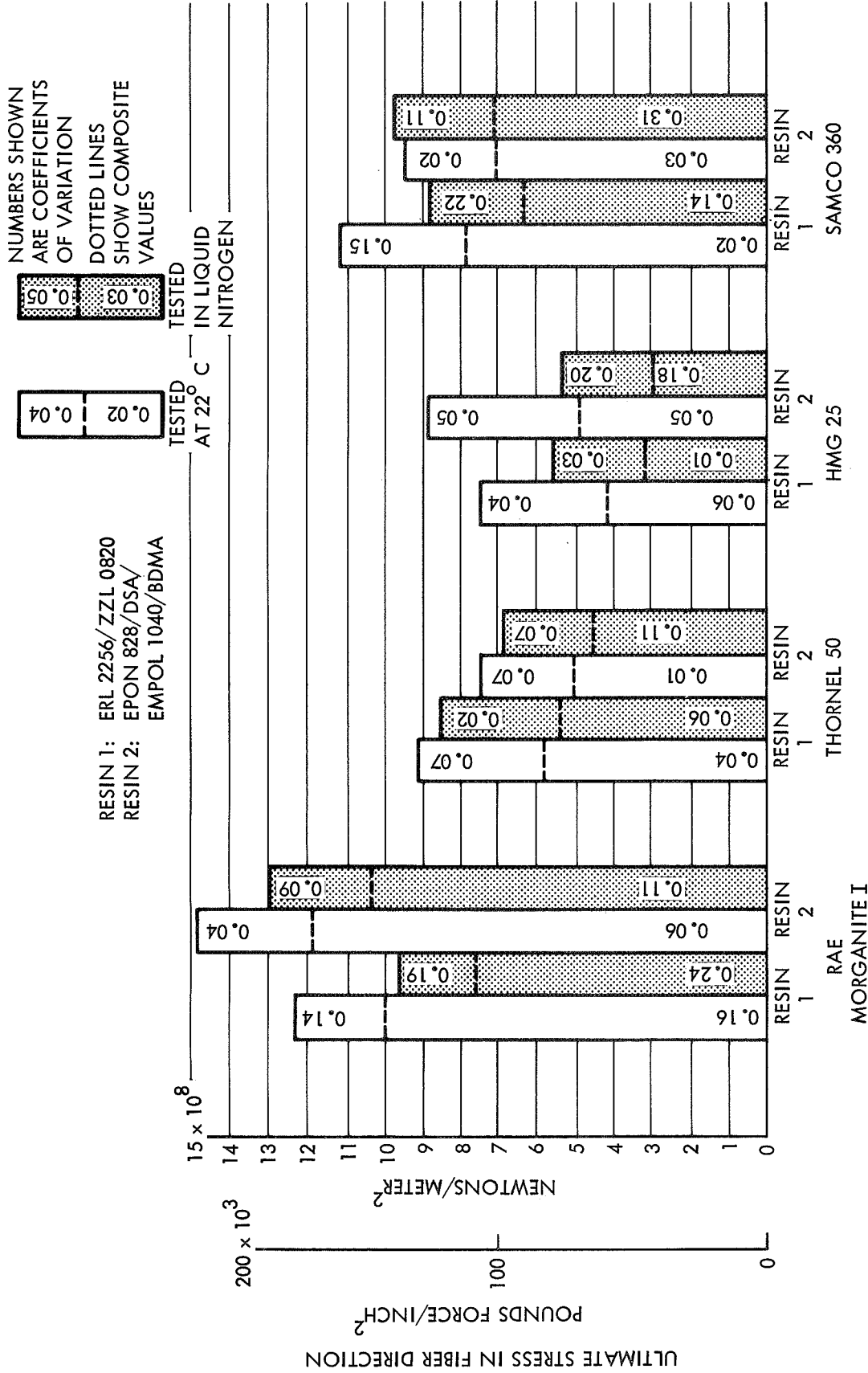


FIG. 15 FIBER AND COMPOSITE TENSILE STRENGTHS - NITRIC ACID TREATED FIBER
AVERAGE VALUES FROM UNIDIRECTIONAL MOLDED BARS
TESTED AT 22° C AND IN LIQUID NITROGEN

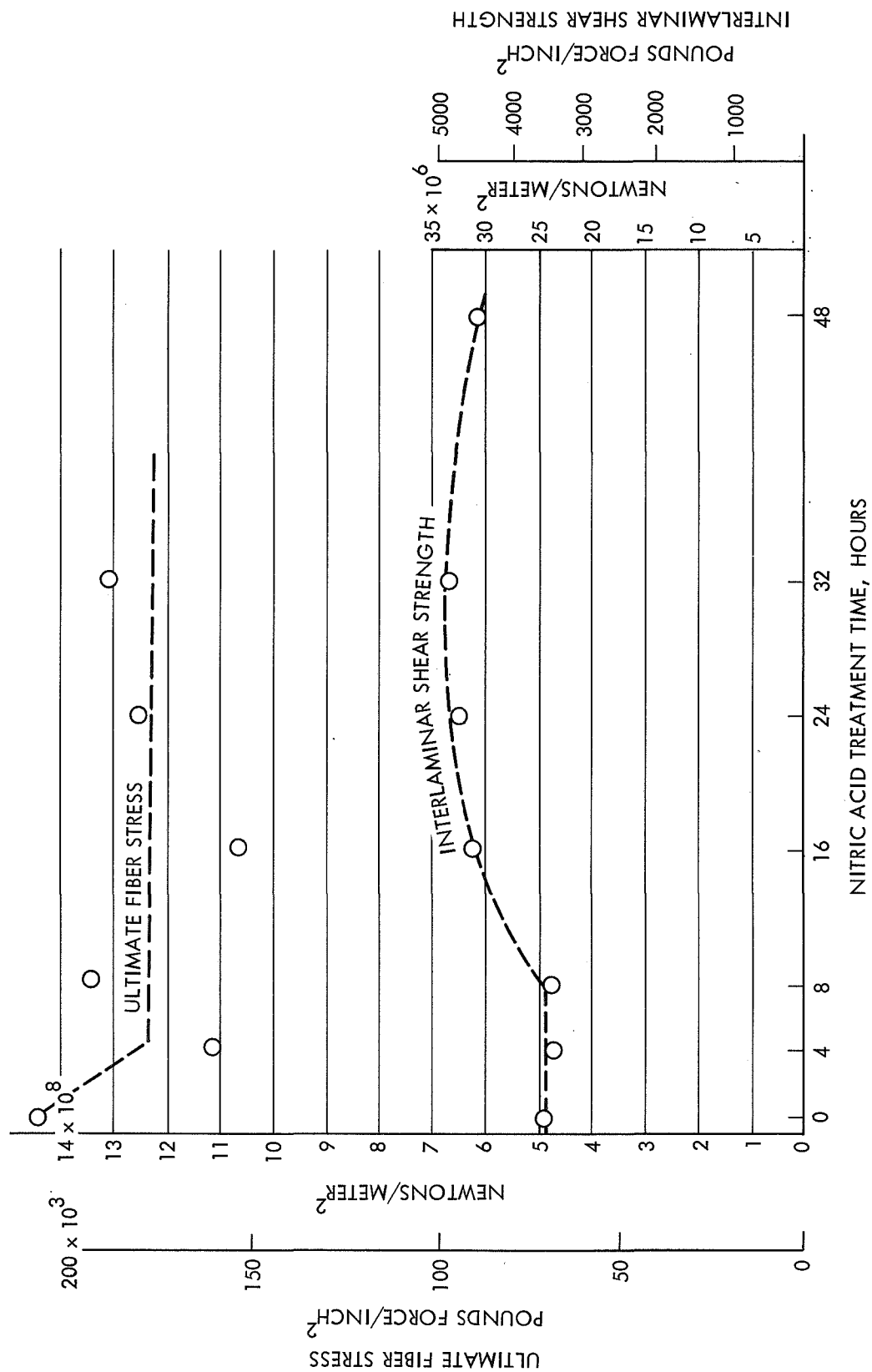


FIG. 16 FIBER TENSILE STRENGTHS AND COMPOSITE INTERLAMINAR SHEAR STRENGTHS
 NITRIC ACID TREATED FIBER - THORNEL 50
 TENSILE STRENGTHS FROM RESIN-IMPREGNATED STRANDS } RESIN 1:
 COMPOSITE INTERLAMINAR SHEAR STRENGTHS FROM MOLDED LAMINATE BARS } ERL 2256/ZZL 0820

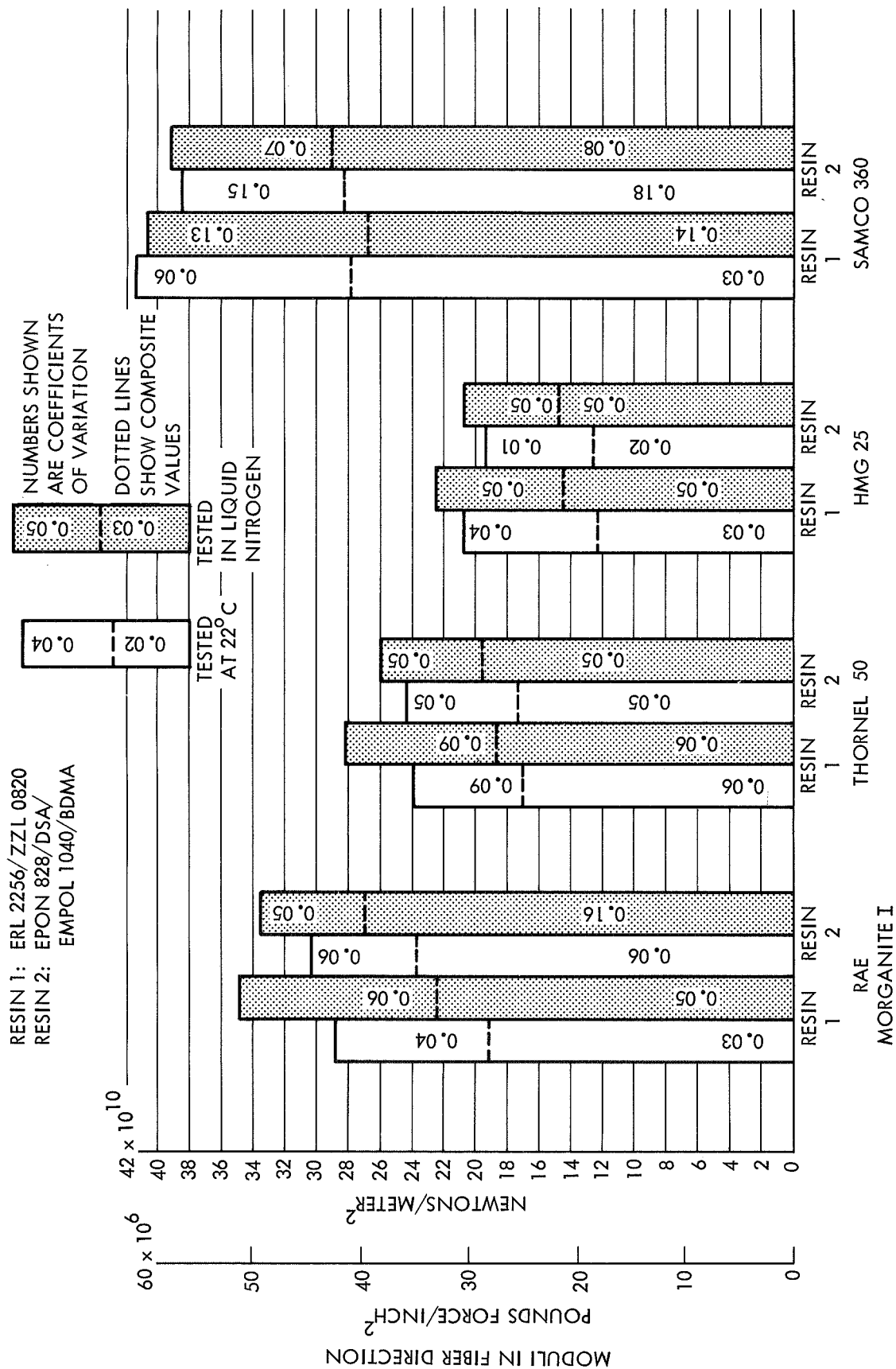


FIG. 17 FIBER AND COMPOSITE TENSILE MODULI
AVERAGE VALUES FROM UNIDIRECTIONAL MOLDED BARS
TESTED AT 22°C AND IN LIQUID NITROGEN

RESIN 1: ERL 2256/ZZL 0820

RESIN 2: EPON 828/DSA

EMPOL 1040/BDMA

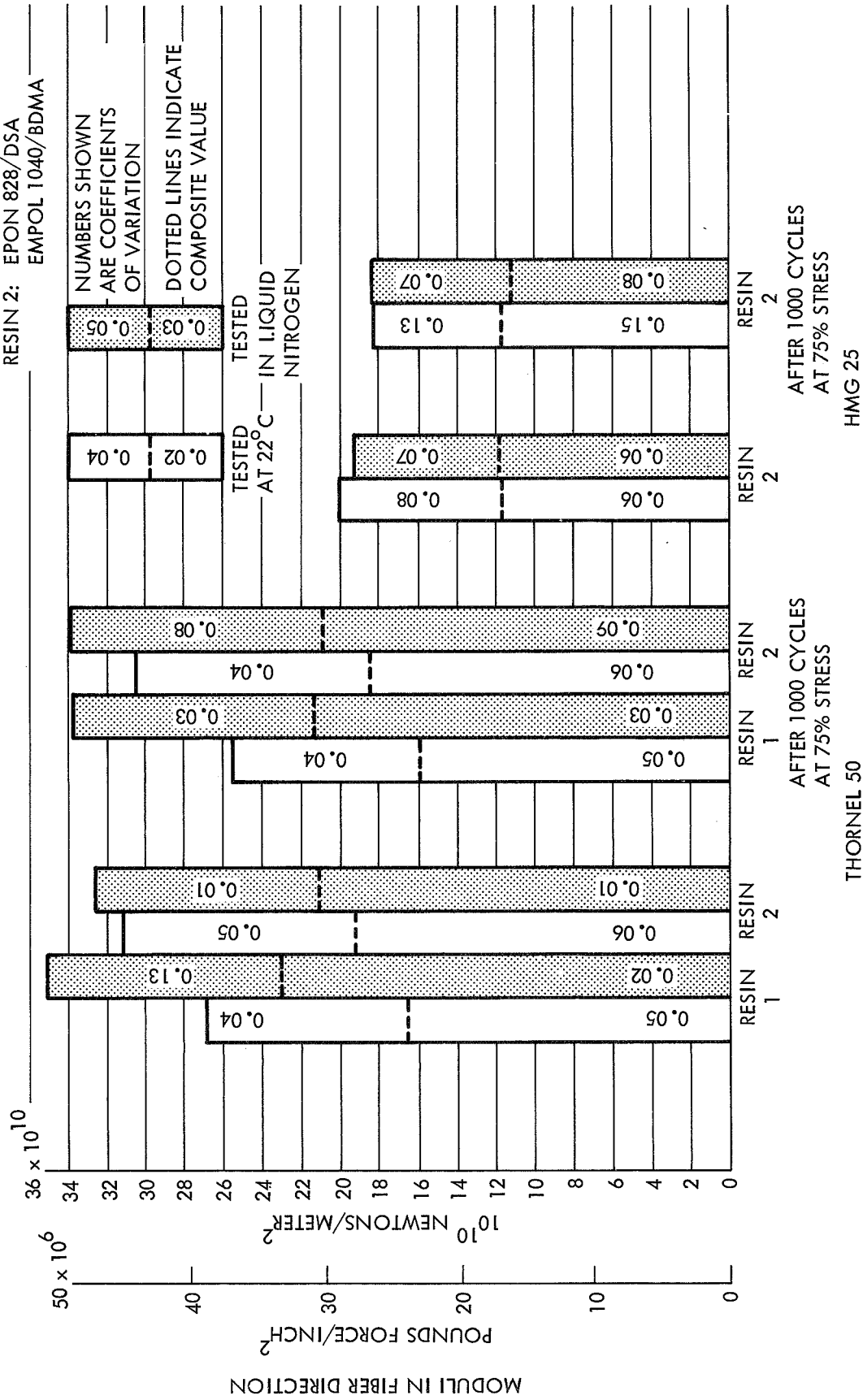


FIG. 18 FIBER AND COMPOSITE TENSILE (BENDING) MODULI
AVERAGE VALUES FROM NOL RINGS - "SPLIT PIN" METHOD
TESTED AT 22°C AND IN LIQUID NITROGEN

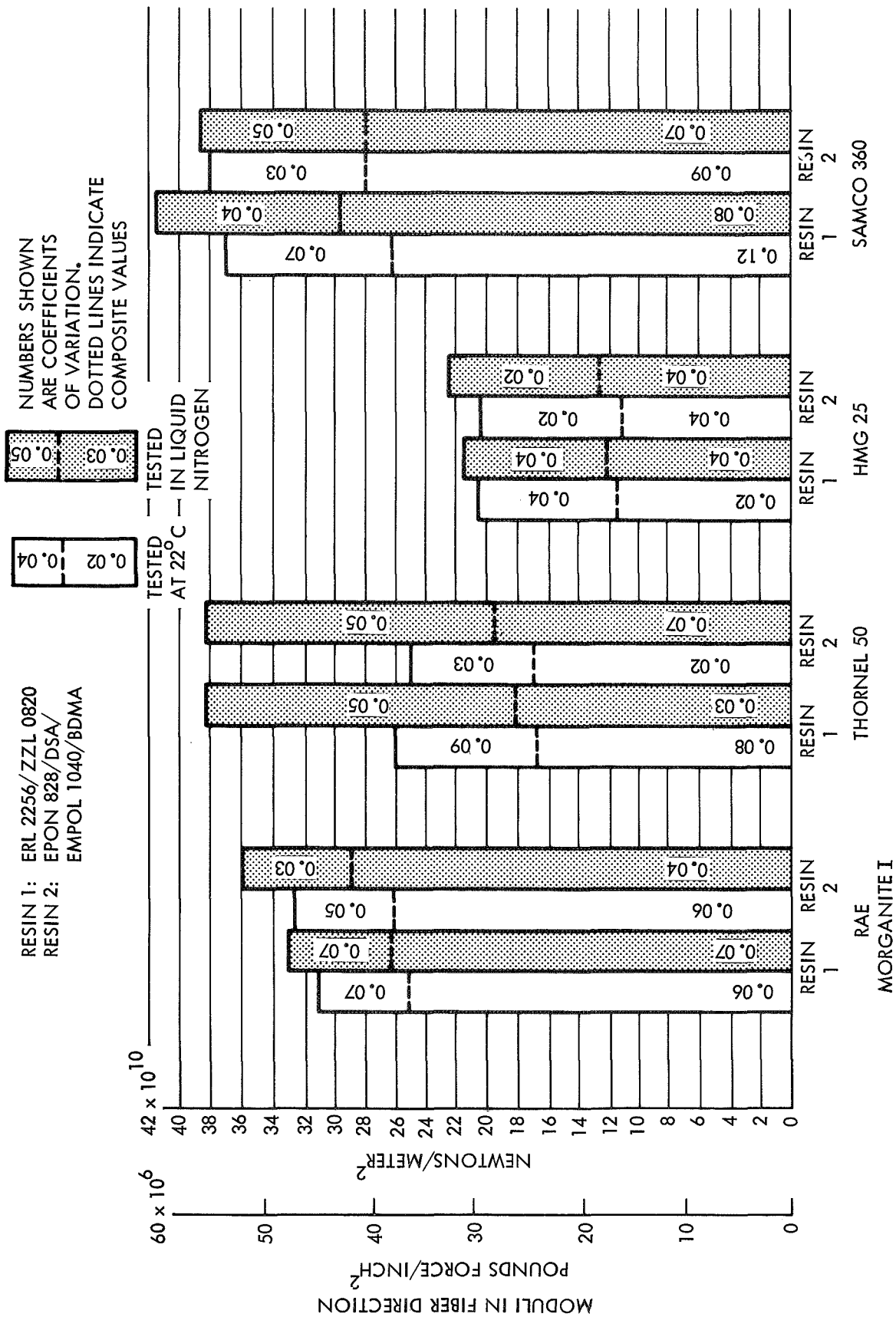


FIG. 19 FIBER AND COMPOSITE TENSILE MODULI - NITRIC ACID TREATED FIBER
AVERAGE VALUES FROM UNIDIRECTIONAL MOLDED BARS
TESTED AT 22°C AND IN LIQUID NITROGEN

ULTIMATE STRESS IN FIBER DIRECTION



FIG. 21 FIBER AND COMPOSITE FLEXURAL MODULI
AVERAGE VALUES FROM NOL RING SECTIONS - 3-POINT METHOD
TESTED AT 22°C AND IN LIQUID NITROGEN

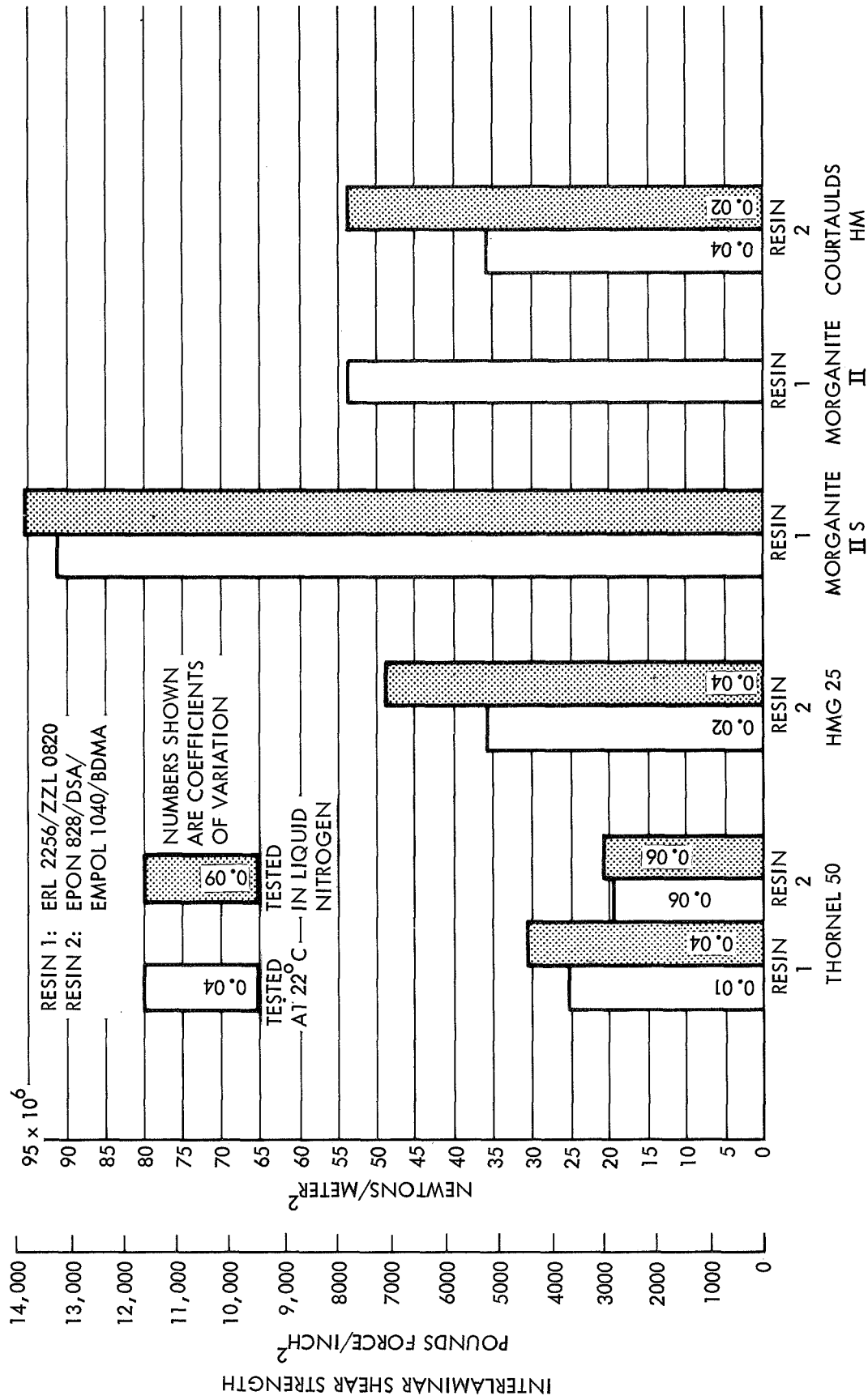


FIG. 22 COMPOSITE INTERLAMINAR SHEAR STRENGTHS
AVERAGE VALUES FROM NOL RING SECTIONS
TESTED AT 22°C AND IN LIQUID NITROGEN

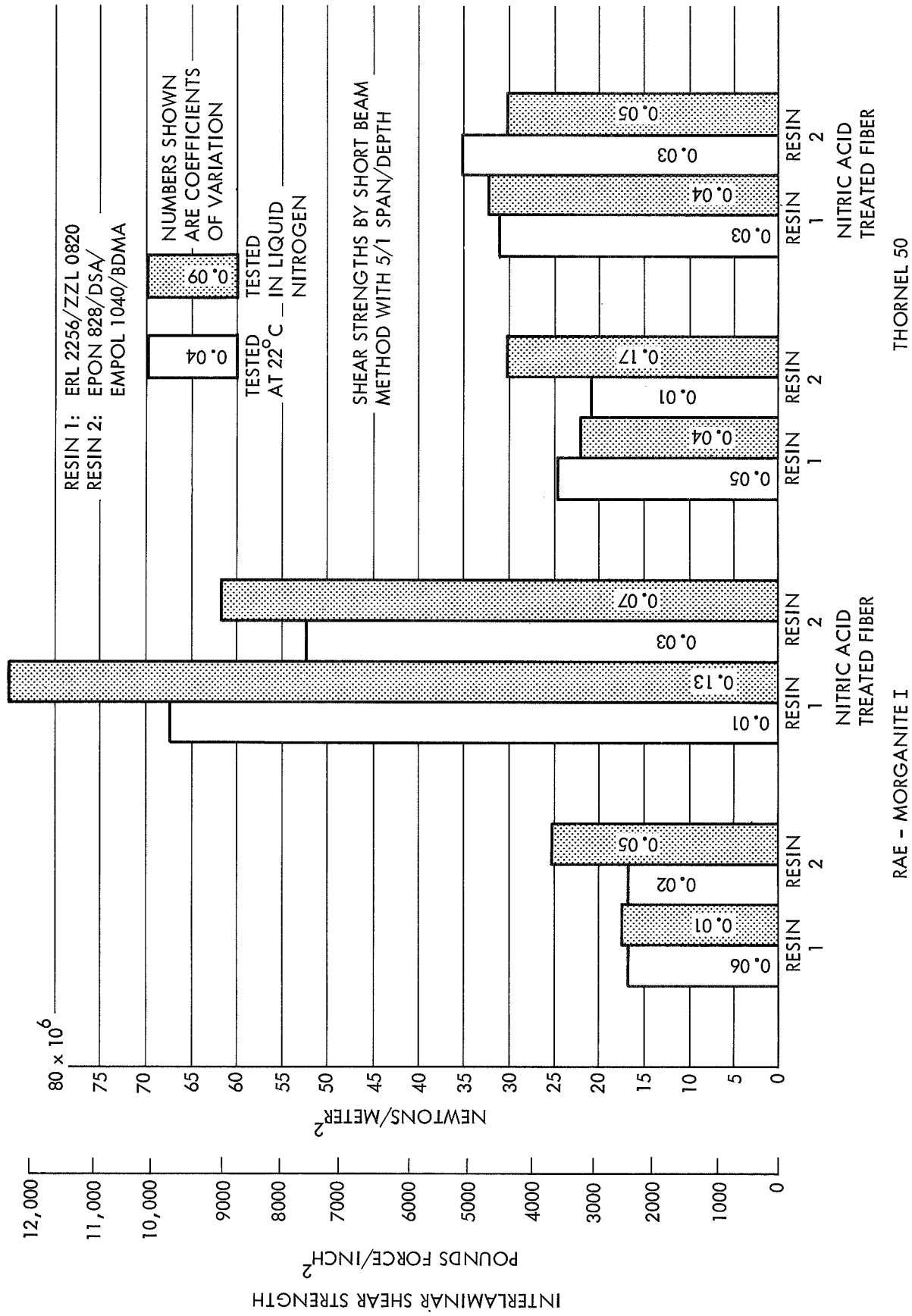


FIG. 23a COMPOSITE INTERLAMINAR SHEAR STRENGTHS
AVERAGE VALUES FROM UNIDIRECTIONAL MOLDED BARS
TESTED AT 22°C AND IN LIQUID NITROGEN

FIG. 23b COMPOSITE INTERLAMINAR SHEAR STRENGTHS
AVERAGE VALUES FROM UNIDIRECTIONAL MOLDED BARS
TESTED AT 22°C AND IN LIQUID NITROGEN

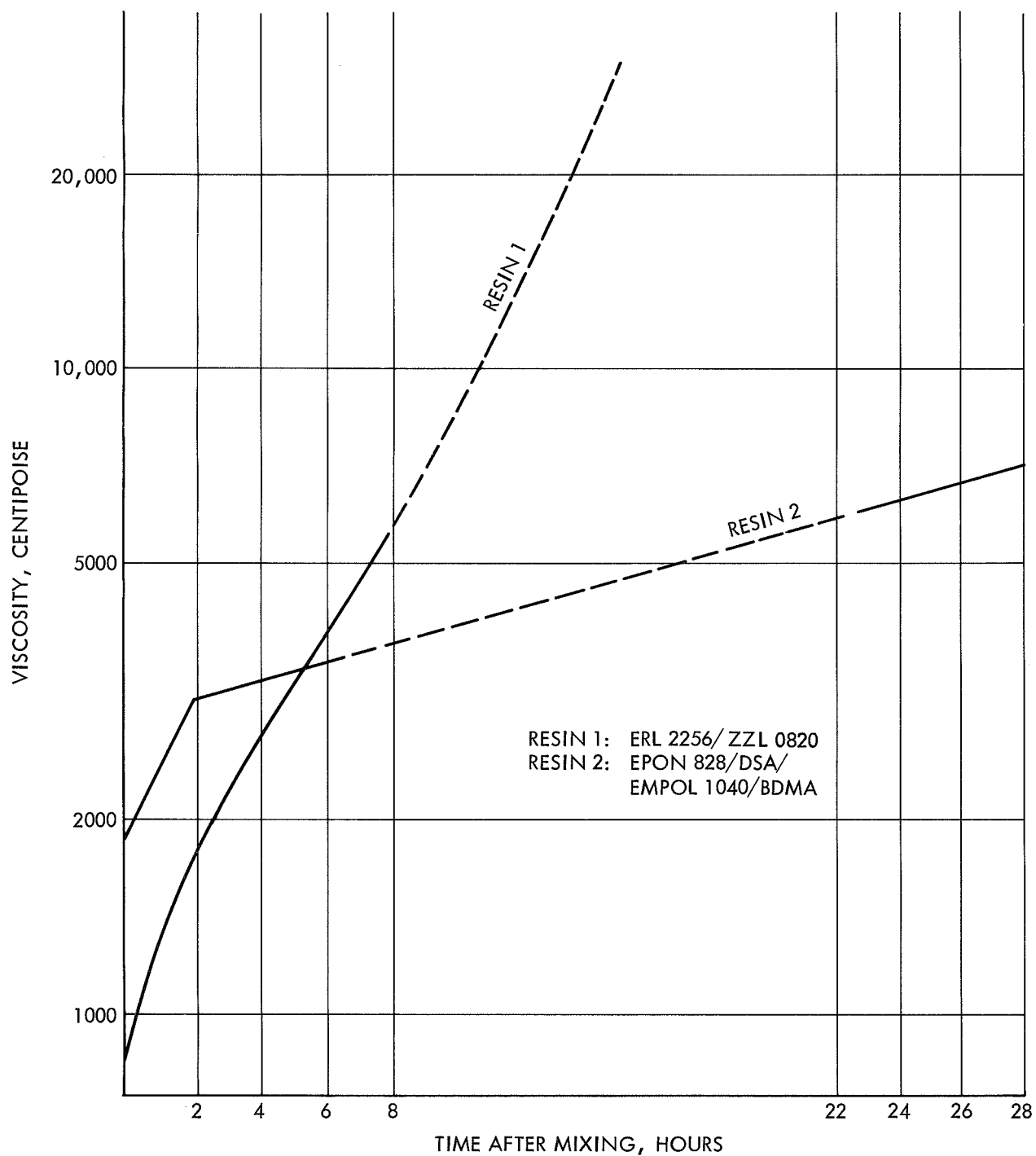


FIG. 24 VISCOSITY OF RESIN/HARDENER SYSTEMS MEASURED AT 22°C

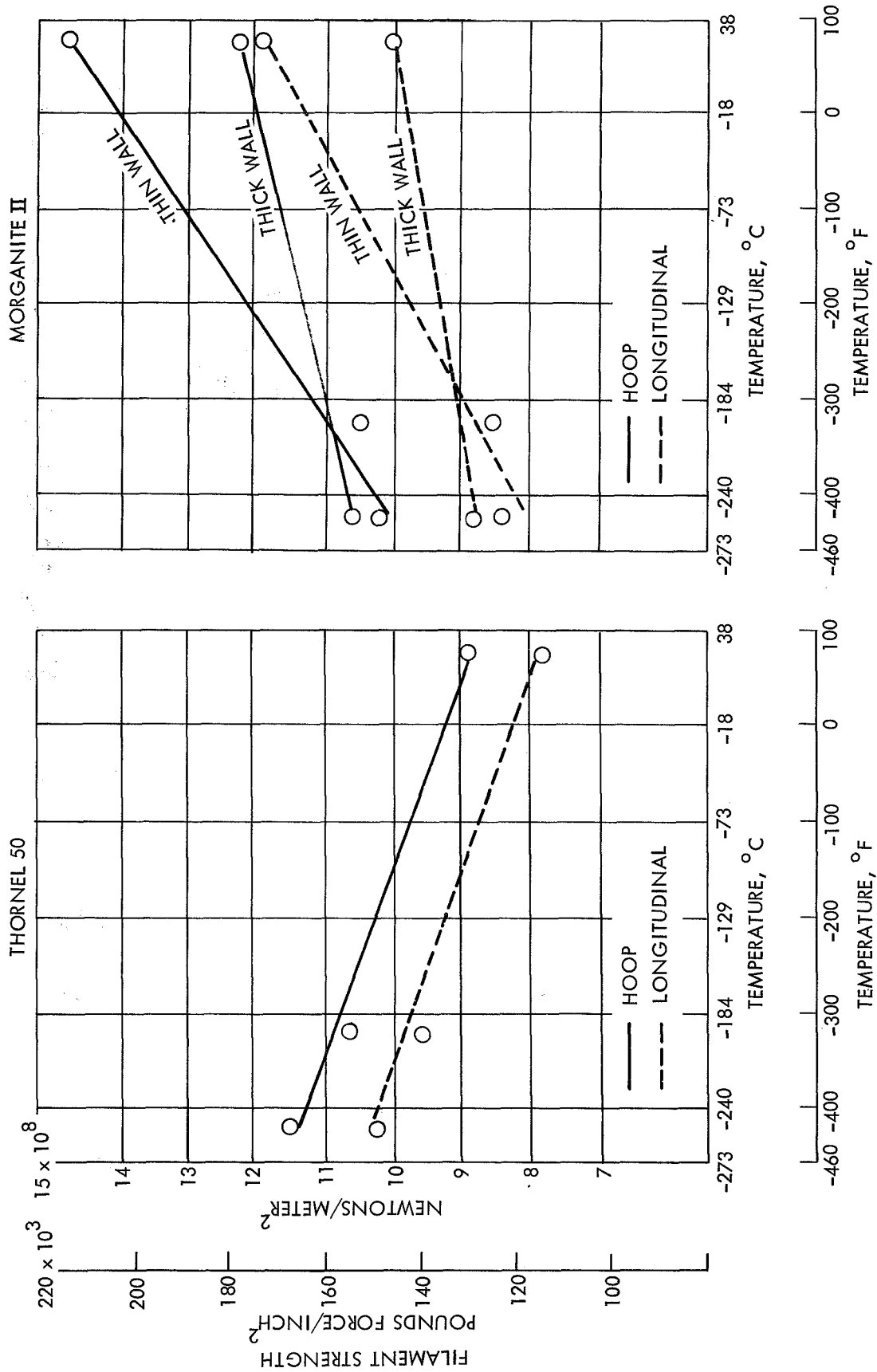


FIG. 25 ULTIMATE GRAPHITE FILAMENT STRENGTHS AT VESSEL BURST PRESSURES

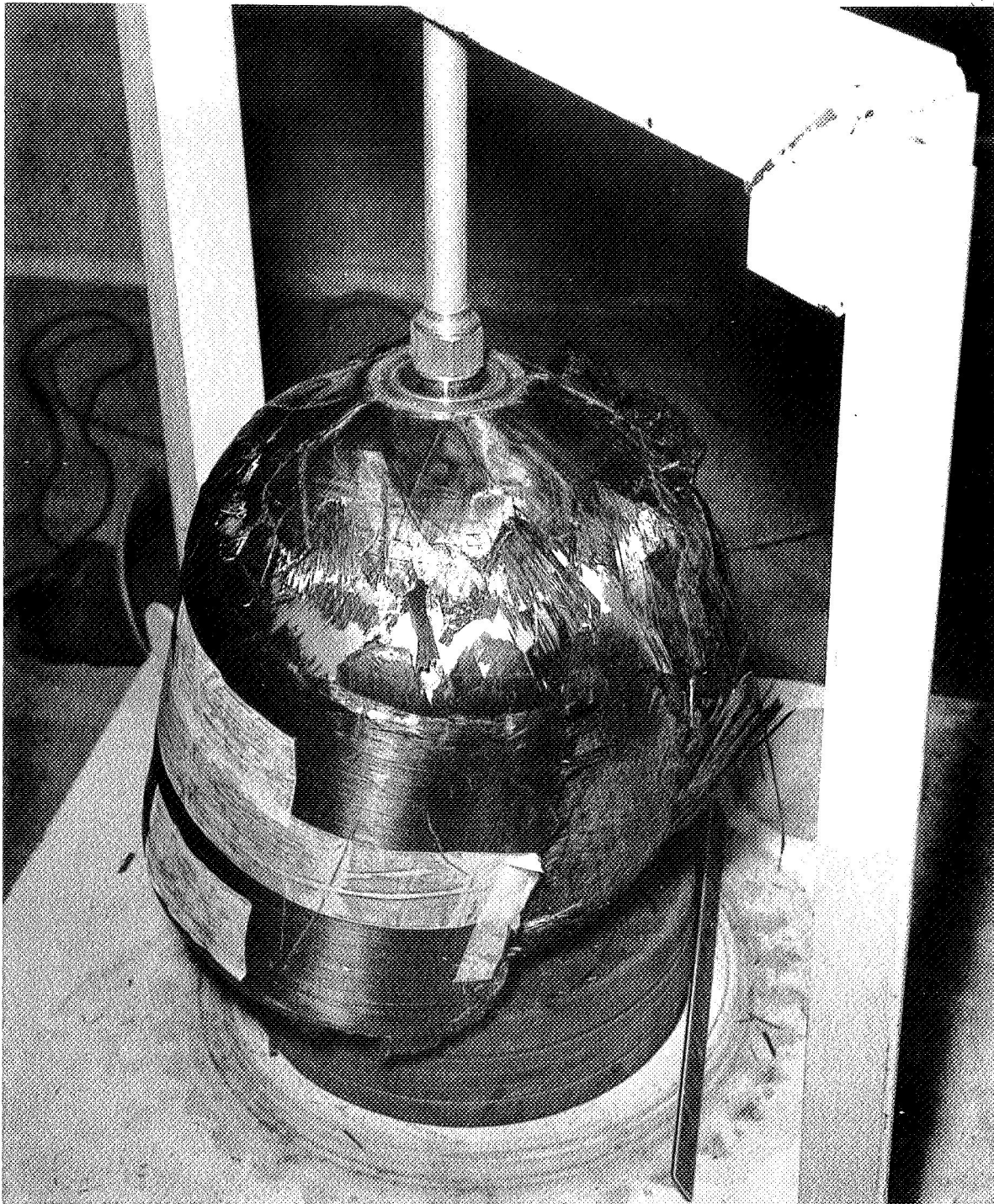


FIG. 26 POST TEST PHOTOGRAPH TANK T-1



FIG. 27 POST TEST PHOTOGRAPH TANK T-4



FIG. 28 POST TEST PHOTOGRAPH TANK M-5

NOTES:
 "HOOP" means strains in the hoop direction.
 "LONGO-1" means strains in the longitudinal direction as indicated by strain gage 1.
 "LONGO-2" means strains in the longitudinal direction as indicated by strain gage 2.

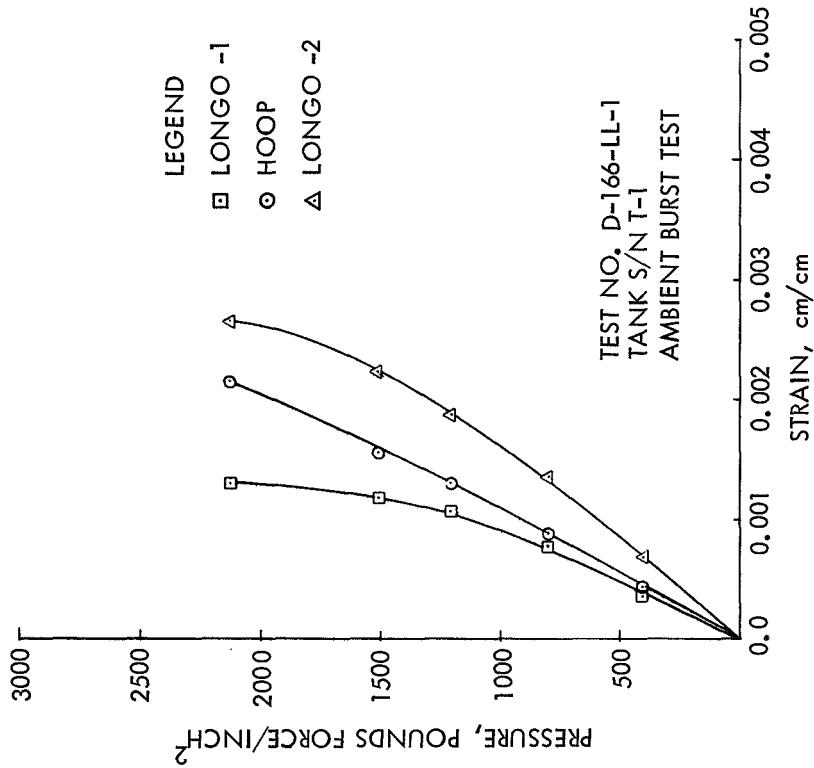


FIG. 29 PRESSURE VS STRAIN FOR BURST TEST AT 22°C (75°F) TANK T-1

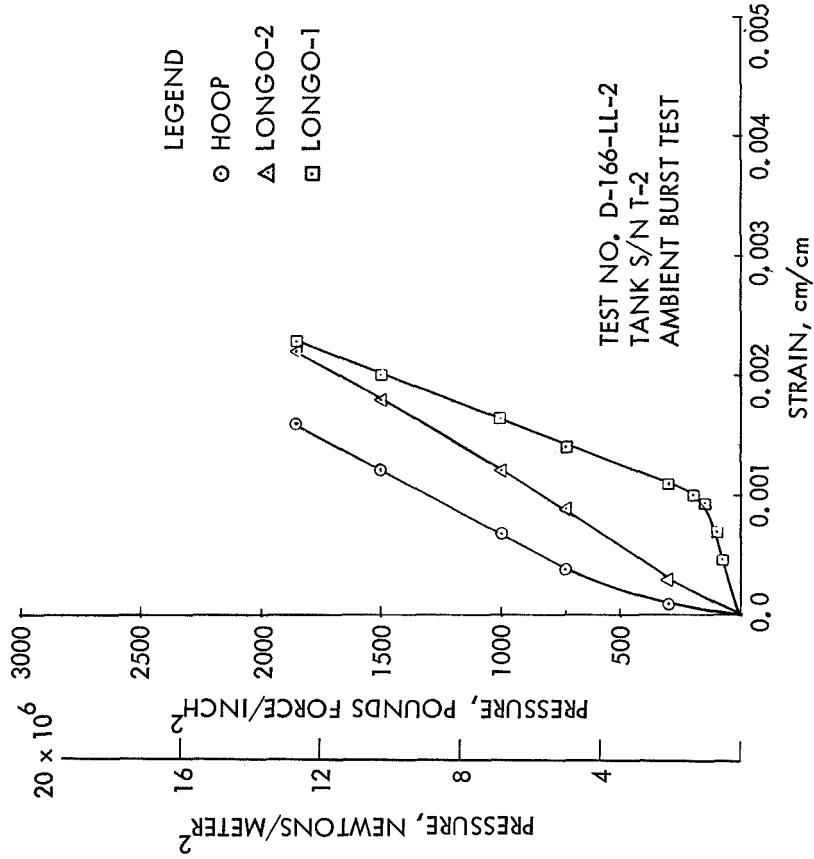


FIG. 30 PRESSURE VS STRAIN FOR BURST TEST AT 22°C (75°F) TANK T-2

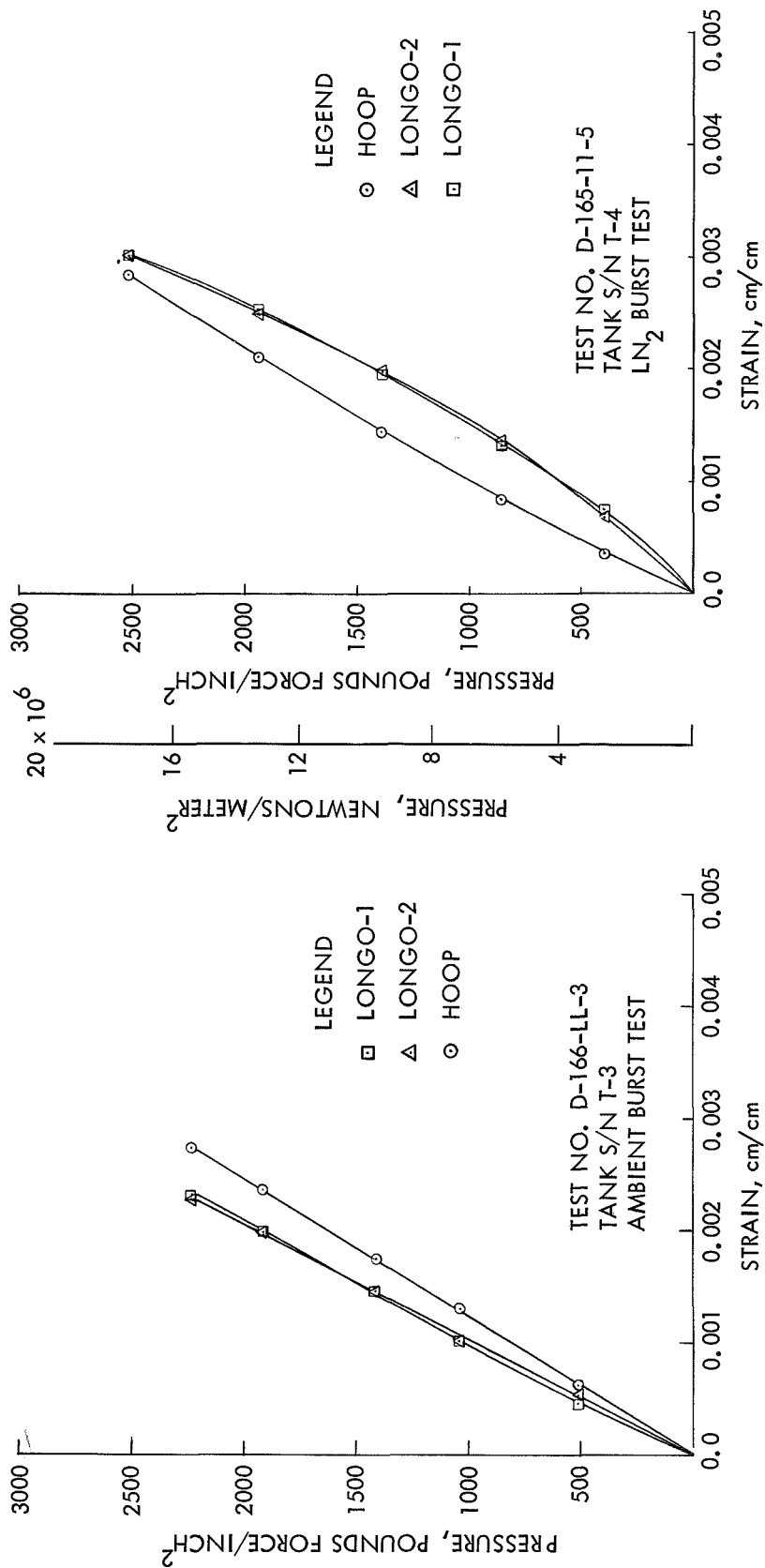


FIG. 31 PRESSURE VS STRAIN FOR BURST TEST AT 22°C (75°F) TANK T-3

FIG. 32 PRESSURE VS STRAIN FOR BURST TEST AT -195°C (-320°F) TANK T-4.

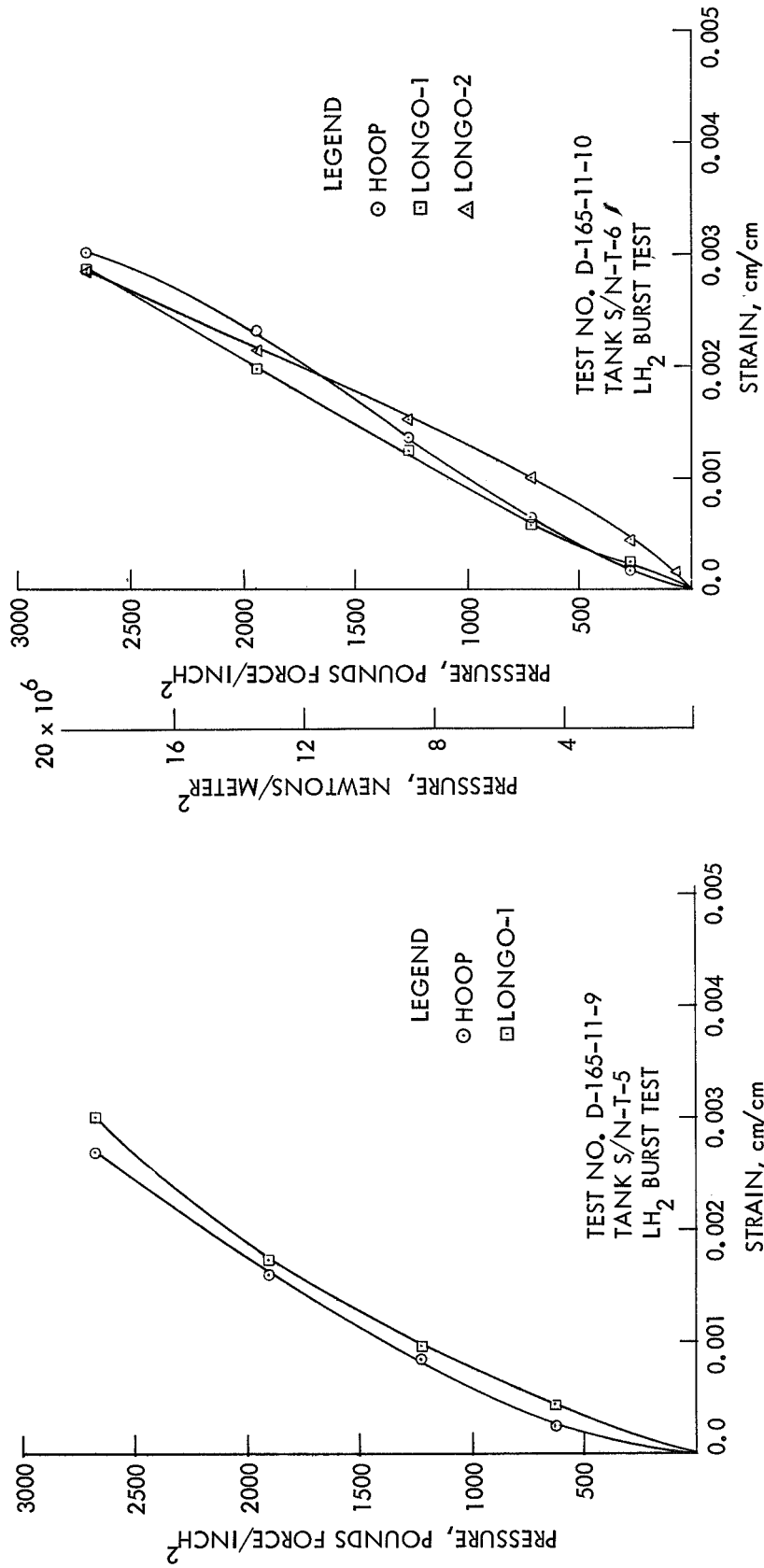


FIG. 34 PRESSURE VS STRAIN FOR BURST TEST AT -253°C (-423°F) TANK T-6

FIG. 33 PRESSURE VS STRAIN FOR BURST TEST AT -253°C (-423°F) TANK T-5

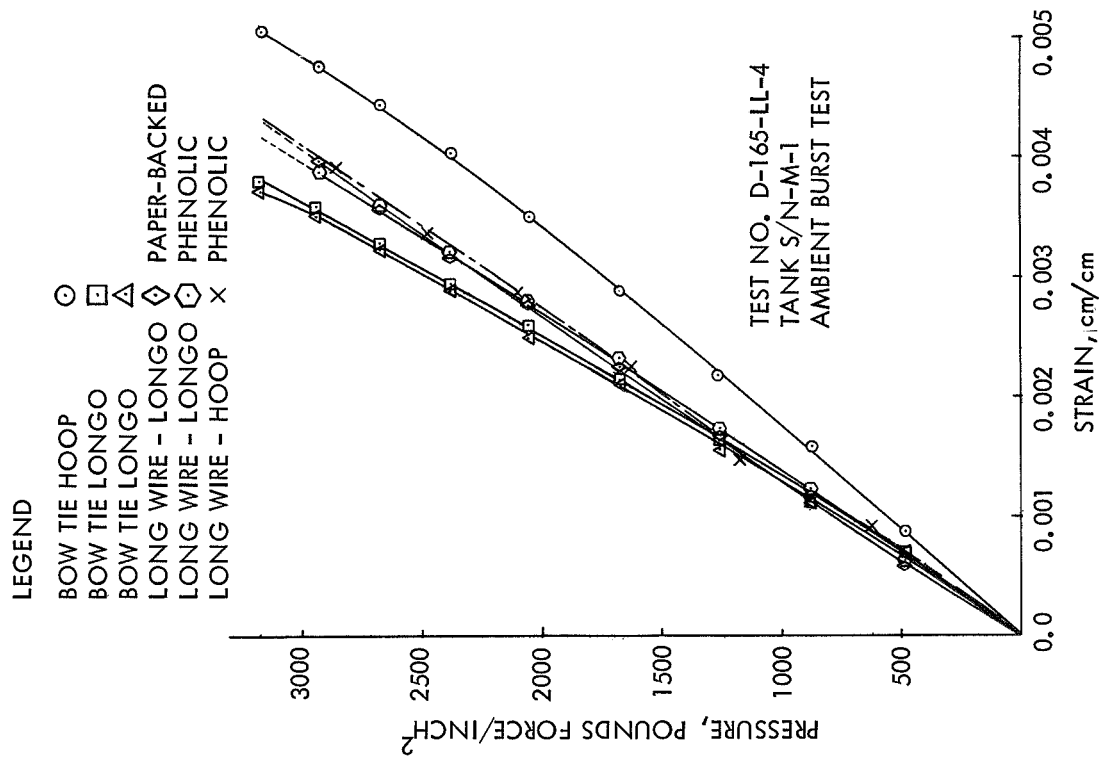


FIG. 35 PRESSURE VS STRAIN FOR BURST TEST AT 22°C
(75°F) TANK M-1

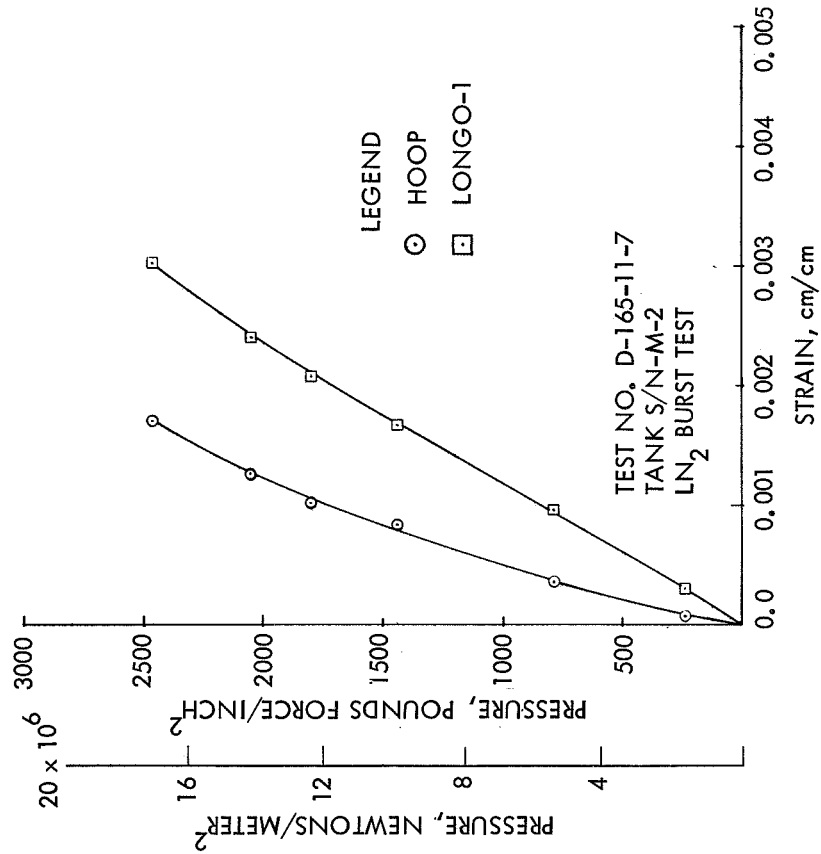


FIG. 36 PRESSURE VS STRAIN FOR BURST TEST AT -195°C
(-320°F) TANK M-2

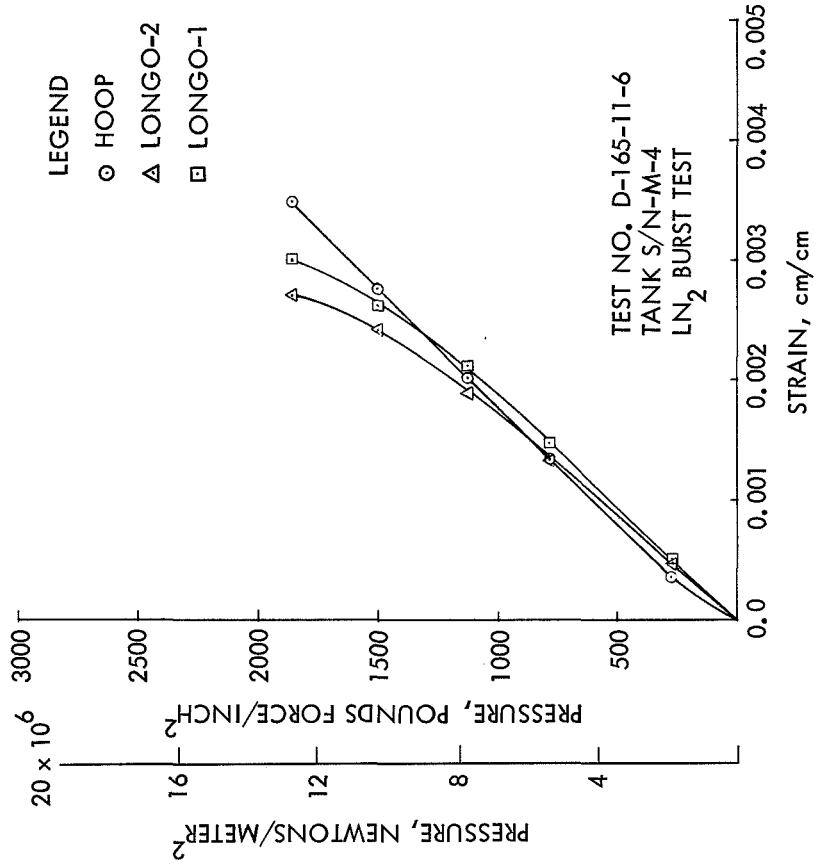


FIG. 38 PRESSURE VS STRAIN FOR BURST TEST AT -195°C
(-320°F) TANK M-4

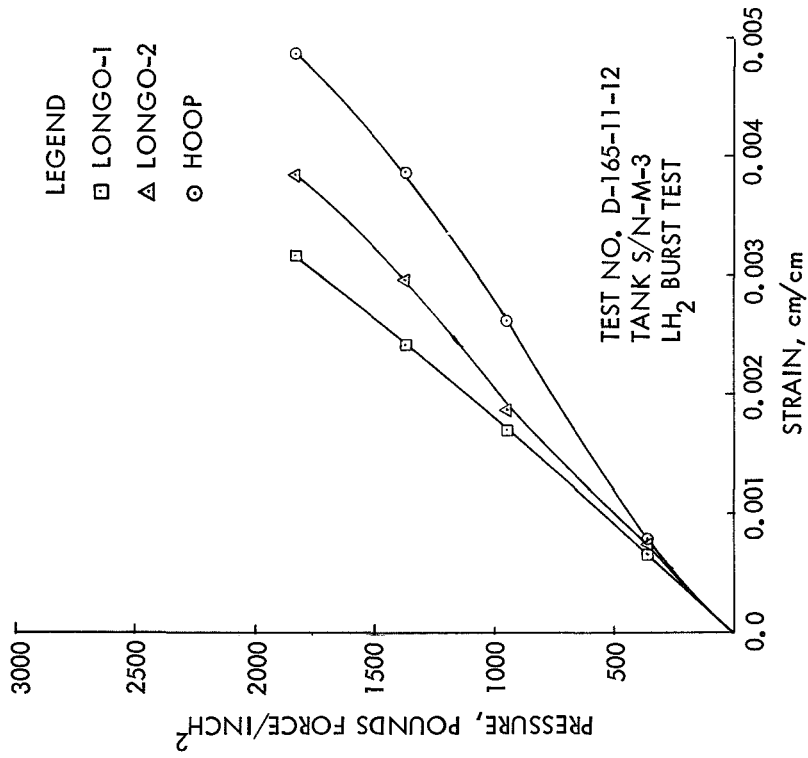


FIG. 37 PRESSURE VS STRAIN FOR BURST TEST AT -253°C
(-423°F) TANK M-3

- LEGEND
- BOW TIE HOOP
 - BOW TIE LONGO
 - △ BOW TIE LONGO
 - ◇ LONG WIRE - LONGO
 - ◊ LONG WIRE - LONGO
 - × LONG WIRE - HOOP
 - -1 PHENOLIC-BACKED STRAIN GAGE
 - -2 PAPER-BACKED STRAIN GAGE
 - △ -3 PAPER-BACKED STRAIN GAGE

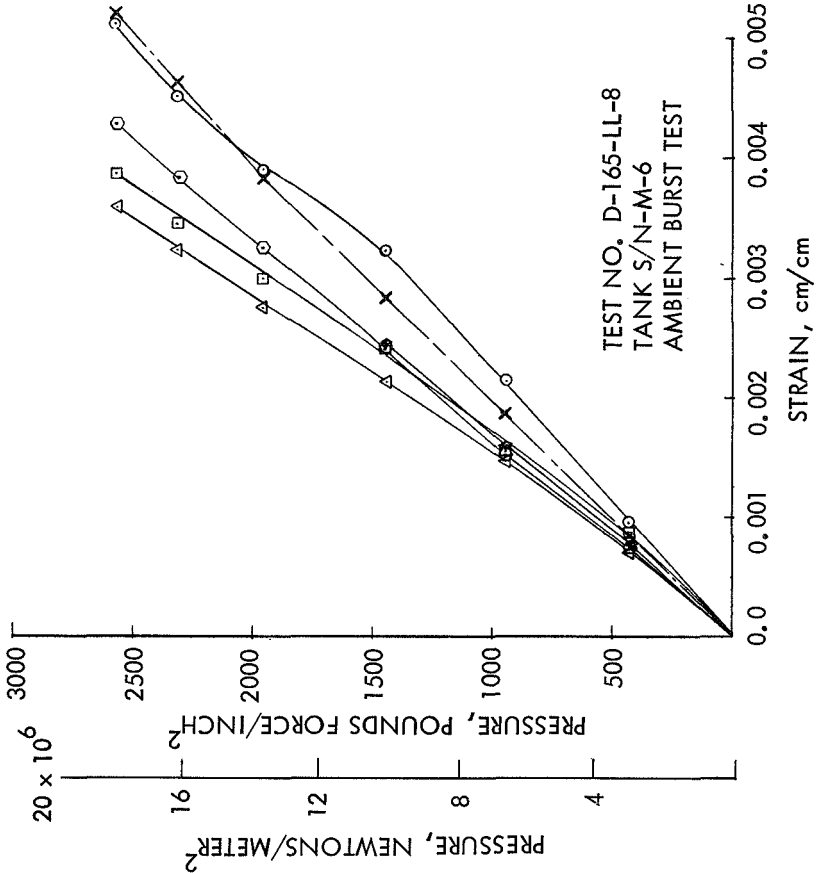


FIG. 40 PRESSURE VS STRAIN FOR BURST TEST AT 22°C (75°F) TANK M-6

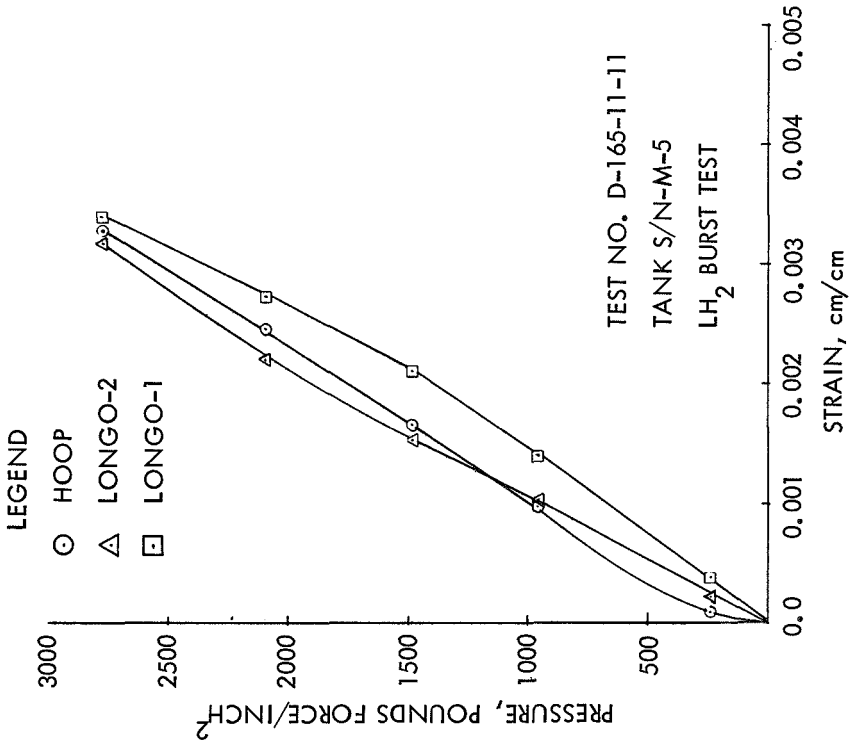


FIG. 39 PRESSURE VS STRAIN FOR BURST TEST AT -253°C (-423°F) TANK M-5

APPENDIX A

RESIN CONTENT DETERMINATION

The composite resin contents for both Tasks I and II were determined by burnoff in air or by thermal degradation of the resins in vacuum. Burnoff in air was done at 370°C for 16 hours but was not suitable for use with Morganite II fibers, since the fibers oxidized readily under these conditions. When Morganite II fibers were present, the analysis procedure was typically as described by Aerojet for their vessels in Task II.

Test Procedure

The resin and graphite content of the composite of each vessel was determined by a thermal degradation process using six specimens from each vessel. The specimens were placed in tared containers, then dried and weighed at 49°C (120°F) for 24 hours or so, or until a repetition of the drying and weighing showed no further weight loss. The Thornel 50 specimens were then placed in a vacuum chamber and heated at 427°C (800°F) for 60 hours. The Morganite II specimens were held in vacuum at 538°C (1000°F) for 16 hours. The pressure during burnoff was 2.7 n/m² (0.02 torr) or less. The chamber and samples were then cooled to 93°C (200°F) or lower under vacuum, after which the specimens were placed in desiccators for final cooling.

Each lot of Morganite II specimens included two additional control specimens furnished by NOL with known graphite content. Previously, several burnoff tests of specimens of resin 2 only were performed to establish the ash residue of the resin, which was determined to be 3.1%.

The specimens were cut with a hole-saw and were 3.43 cm (1.35 in.) in diameter by composite thickness (0.457 to 0.762 cm, or 0.180 to 0.300 in.). All of the specimens were taken from the cylindrical section of the vessel to obtain uniform values, except for vessel T-1 which also had specimens from the boss and knuckle areas. Care was taken to remove the innermost portion of each specimen to eliminate the scrim cloth and adhesive system used for bonding the composite to the stainless steel liner.

APPENDIX B

AEROJET-GENERAL STRAND TEST PROCEDURE

Test Requirement

The contract specified that a quantity of 120 to 360 strand tests to measure strengths and moduli would be performed. A suggested procedure for performing the tensile testing was provided by NOL.

Test Procedure

Aerojet prepared and tested 137 strand specimens, 52 during technique development midway through the program and 85 later in the program. A 4,540 Kg (10,000 lb) Instron testing machine was used for the tensile testing of the strands. The specimen grips were Instron Screw-Action Model G-61-1D with smooth-ground rubber faces. An Instron Strain-Gage Extensometer (with a 2.54 cm (1 in.) gage length and 500 magnification) was used for strain measurement.

Testing techniques for Thornel 50 yarn were developed first. In accordance with the suggested procedure of NOL, lengths of single 50.8 cm (20 in.) yarn were impregnated with resin 2 and cured. A tension of 35 grams was applied to the strand during the cure. At first, the ends of the strand were then bonded between cardboard tabs to facilitate mounting of the specimen in the test grips. Strain measurement was attempted through measurement of cross-head travel over 15.2-centimeter (six-inch) and 25.4-centimeter (ten-inch) gage lengths of the strand. Testing of the cardboard-mounted strands showed representative values for strength but low modulus values. This was attributed to minor slippage of the strand in the cardboard faces or the cardboard faces in the grips. Since slippage could be tolerated in the strength measurement but not in the strain measurement, the strain-gage extensometer was tried by mounting it directly on the strand, resulting in accurate modulus values but low strength values. The cardboard holders were then discarded, since they interfered with the extensometer and the strands were clamped directly in the rubber-faced grips. Mounting the extensometer on the strands bent them and probably caused the low strengths. A pretensioning of 10% was then tried before the extensometer was attached; this procedure proved successful and resulted in good values for both moduli and strengths.

The tensile testing of Morganite II strands was performed in the same way, with one exception. The Morganite II tow had approximately 13 times the cross-sectional area of the Thornel yarn. Consequently, the ends of the strand needed a greater surface area to prevent slippage in the rubber-faced grips during testing. The greater area was achieved by clamping the ends of the strand between flat aluminum plates during cure. A tension of 4.5 Kgms (ten pounds) per strand was used for the Morganite tow during the cure.

APPENDIX C

PRESSURE VESSEL DESIGN

1. Design Analysis

The pressure vessel design parameters are shown in Table C-1. The design was analyzed to determine stresses and strains in the filaments and liner under various loading conditions. The Thornel 50 vessel stress-strain relationship (at 24°C) for the hoop windings of the cylindrical portion of the vessel and the liner up to theoretical burst strength is shown on Figure C-1. Figure C-2 shows the same relationship for the Morganite II vessel.

The computer output was used to construct pressure-strain curves, for 24°C test temperature, to compare the measured pressure-strain characteristics with the predicted behavior. The predicted curves for 24°C are presented in Figure C-3 for the Thornel 50 vessels and in Figure C-4 for the Morganite vessels. The initial slightly steeper portion of the curve is due to the load-carrying capacity of the liner. As the liner undergoes plastic deformation above $6.89 \times 10^6 \text{ n/m}^2$ (1000 psi) for Thornel and $4.83 \times 10^6 \text{ n/m}^2$ (700 psi) for Morganite, the increasing load is taken up by the filament-wound composite. From these computer results, dimensional and material parameters for the vessels were calculated, as shown in Table C-2.

2. Weight Analysis

The weights of the various components of the tank, calculated from design details, are as follows:

	Estimated Weight					
	Thornel 50		Morganite II			
			-1 Vessel ^a		-2 Vessel ^b	
	<u>Pounds</u>	<u>Kg</u>	<u>Pounds</u>	<u>Kg</u>	<u>Pounds</u>	<u>Kg</u>
Graphite Filament-Wound Composite						
Graphite	1.63	0.74	1.71	0.78	1.14	0.52
Resin	0.67	0.30	0.67	0.30	0.45	0.20
<u>Subtotal</u>	2.30	1.04	2.38	1.08	1.59	0.72
Metal Liner						
Membrane	0.55	0.25	0.55	0.25	0.55	0.25
Bosses ^c	1.46	0.66	1.46	0.66	1.46	0.66
<u>Subtotal</u>	2.01	0.91	2.01	0.91	2.01	0.91
<u>Total</u>	4.31	1.96	4.39	1.99	3.60	1.63

a 3/3 wall vessel; b 2/3 wall; c redundant boss design & excessive wt.

3. Winding Pattern Calculations*

a. Features of Thornel 50 Yarn and Morganite (Type II) Tow

(1) Thornel 50. From Union Carbide Data Sheet, equivalent filament diameter of individual fibers of Thornel 50 is 6.6 microns, or 2.6×10^{-4} in.

In a single yarn there are 720 filaments per ply and two plies per yarn, or a total of 1440 filaments per yarn. The cross-sectional area of a single yarn, A_y , is then:

$$A_y = A_f N_f = \frac{\pi D_f^2}{4} N_f$$

where

A_f = area of single filament, in.²

N_f = number of filaments/yarn

D_f = diameter of single filament

$$A_y = \frac{\pi (2.6 \times 10^{-4})^2}{4} (1440) = 76.4 \times 10^{-6} \text{ in.}^2$$

Using another method, the yield of Thornel 50 yarn averages 19,600 ft/lb. The density of Thornel 50 is 0.0588 lb/in.³. The cross-sectional area of a single yarn, A_y , is then:

$$A_y = \frac{W}{L\rho}$$

where

W = weight, lb

L = length, in.

ρ = density, lb/in.³

$$A_y = \frac{1 \text{ lb}}{(19,600 \text{ ft/lb}) (12 \text{ in./ft}) (0.0588 \text{ lb/in.}^3)} = 72.3 \times 10^{-6} \text{ in.}^2$$

This compares with a cross-sectional area of 420×10^{-6} in.² for 20-end S glass roving:

$$\frac{420 \times 10^{-6}}{72.3 \times 10^{-6}} = 5.8$$

* Presentation of these calculations in both the S.I. and English systems would be cumbersome and difficult to follow. The English system only is used.

Thus, 5.8 Thornel yarns are equivalent to 20-end S glass roving in cross-sectional area.

(2) Morganite (Type II)

The yield of Morganite II tow average 1710 ft/lb. The density is 0.063 lb/in.³

$$A_y = \frac{1 \text{ lb}}{(1710 \text{ ft/lb}) (12 \text{ in./ft}) (0.063 \text{ lb/in.}^3)} = 774 \times 10^{-6} \text{ in.}^2$$

In comparison with 20-end S glass roving, the Morganite II tow is:

$$\frac{420 \times 10^{-6}}{774 \times 10^{-6}} = 0.543$$

By area, 1.8 glass rovings equal one Morganite II tow.

b. Thornel 50 Winding Pattern

(1) Longitudinal

(a) Number of Layers. From the design analysis, the required longitudinal filament-wound composite thickness at the equator, T₀, is 0.0583 in. The number of layers, L_L, is established from the relationship:

$$L_L = \frac{T_0}{t_{s, 1}}, \text{ where } t_{s, 1} = \text{thickness of a single layer.}$$

From experimental laboratory work, it has been established that the thickness of a single cured layer of yarn wrapped in a side-by-side pattern is about 0.011 in. Therefore, let

$$L_L = 6$$

$$t_{s, 1} = \frac{T_0}{L_L} = \frac{0.0583}{6} = 0.00972 \text{ in.}$$

given by: (b) Number of Revolutions. The number of revolutions, N_1 , is

$$N_1 = \frac{L_L}{2} = \frac{6}{2} = 3$$

(c) Tape Width and Turns per Revolution. Laboratory experiments were conducted using various combinations of yarns in bundles and winding them onto the 8-in. diameter by 13-in. long liner. Based on this work, it was determined that winding two bundles consisting of six Thornel 50 yarns, each side-by-side, would provide a good tape for vessel winding.

The winding tape width for each bundle, W_L , is given by:

$$W_L = \frac{A_y N_y}{t_{s, 1} P_{vg}}$$

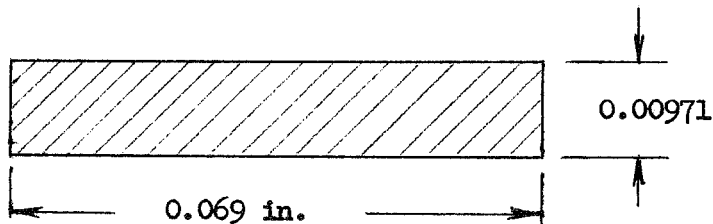
where

N_y = number of yarns/bundle = 6

P_{vg} = vol. fraction filaments in composite = 0.65

$$W_L = \frac{(72.3 \times 10^{-6}) (6)}{(0.00971) (0.65)} = 0.069 \text{ in.}$$

Each 6-yarn bundle has the following idealized cured geometry:



The number of turns per revolution, N_3 , is given by:

$$N_3 = \frac{\pi D_c \cos \alpha}{2 W_L} \text{ where two bundles of width } W_L \text{ are used and}$$

D_c = neutral axis diameter of longitudinal filament-wound composite = 7.824 in.

α = in-plane wrap angle = 13°

$$N_3 = \frac{(\pi) (7.824) (0.974)}{(2) (0.069)} = 174 \text{ turns/revolution}$$

(2) Hoop

(a) Number of Layers. The required hoop-wound composite thickness, T_H , is 0.100 in. This composite was wrapped with a 6-yarn bundle.

The number of layers, L_H , is established:

$$L_H = \frac{T_H}{t_{s,h}} = \frac{0.100}{0.00971} = 10.3 \text{ layers}$$

Experimental winding showed better compaction by using 9 layers. Therefore, use 9 layers and adjust t_s ,

$$t_{s,h} = \frac{T_H}{L_H} = \frac{0.100}{9} = 0.0111 \text{ in.}$$

(b) Tape Width and Turns per Layer. The required tape width is:

$$W_L = \frac{A_y N_y}{t_{s,h} P_{vg}} = \frac{(72.3 \times 10^{-6}) (6)}{(0.011) (0.65)} = 0.061$$

The turns per layer, N_5 , is:

$$N_5 = \frac{L_c}{W_L} = \frac{7.34}{0.061} = 120 \text{ turns in } 7.34 \text{ in.}$$

c. Morganite (Type II) Winding Pattern

(1) Longitudinal

(a) Number of Layers. Let

$$L_L = 6$$

then

$$t_{s,l} = \frac{T_O}{L_L} = \frac{0.0583}{6} = 0.00972 \text{ in.}$$

(b) Number of Revolutions

$$N_1 = \frac{L_L}{2} = \frac{6}{2} = 3 \text{ revolutions}$$

UNCLASSIFIED
NOLTR 69-183

(c) Tape Width and Turns per Revolution. The winding was accomplished using two Morganite II tows. Let

$$t_{s,1} = 0.00972$$

Then

$$W_L = \frac{A_y N_y}{t_{s,1} P_{vg}} = \frac{(774 \times 10^{-6}) (2)}{(0.00972) (0.65)} = 0.245 \text{ in.}$$

$$\begin{aligned} N_3 &= \frac{\pi D_c \cos \alpha}{W_L} \\ &= \frac{\pi (7.824) (0.974)}{0.245} = 98 \text{ turns/revolution} \end{aligned}$$

(2) Hoop

(a) Number of Layers. Let

$$L_H = 10 \text{ layers}$$

$$t_{s,h} = \frac{T_H}{L_H} = \frac{0.100}{10} = 0.010 \text{ in.}$$

(b) Tape Width and Turns per Layer

$$W_L = \frac{A_y N_y}{t_{s,h} P_{vg}} = \frac{(744 \times 10^{-6}) (1)}{(0.010) (0.65)} = 0.119 \text{ in.}$$

$$N_5 = \frac{L_c}{W_L} = \frac{7.34}{0.119} = 61.7 \text{ turns in } 7.34 \text{ in.}$$

TABLE C-1

DESIGN PARAMETERS FOR GRAPHITE FILAMENT-WOUND PRESSURE VESSELS

	<u>Part A</u>					
	<u>Thornel 50</u>		<u>-1 Morganite II</u>		<u>-2 Morganite II</u>	
	<u>Vessel</u>		<u>Vessel^a</u>		<u>Vessel^b</u>	
	<u>in.</u>	<u>cm</u>	<u>in.</u>	<u>cm</u>	<u>in.</u>	<u>cm</u>
Liner Diameter	7.766	19.726	7.766	19.726	7.766	19.726
Vessel Length Between FWL Neutral Axis at Bosses	12.250	31.115	12.250	31.115	12.250	31.115
Polar-Boss Diameter	2.900	7.366	2.900	7.366	2.900	7.366
Metal-Liner Thickness	0.006	0.015	0.006	0.015	0.006	0.015
Longitudinal Filament-Wound Composite Thickness	0.058	0.147	0.058	0.147	0.039	0.099
Hoop Filament-Wound Com- posite Thickness	0.100	0.254	0.100	0.254	0.067	0.170
Design Burst Pressures at 75°F, psig ^a n/m ²	2500 17.24 x 10 ⁶		2500 17.24 x 10 ⁶			

a Three-thirds wall vessel

b Two-thirds wall vessel

UNCLASSIFIED
NOLTR 69-183

TABLE C-1

DESIGN PARAMETERS FOR GRAPHITE FILAMENT-WOUND PRESSURE VESSELS

<u>Properties</u>	<u>Part B</u>		
	<u>Type 304 Stainless Steel Annealed</u>	<u>Graphite Filament-Wound Composite</u>	
		<u>Thornel 50</u>	<u>Morganite II</u>
Density			
lb/in. ³	0.289	0.054	0.056
gm/cm ³	8.000	1.495	1.551
Coefficient of Thermal Expansion			
in./in./°F at +75 to -423°F	6.760 x 10 ⁻⁶	--	--
cm/cm/°C at +22 to -253°C	12.168 x 10 ⁻⁶	--	--
Tensile Yield Strength			
psi	38,000	--	--
n/m ²	262 x 10 ⁶	--	--
Derivative of Yield Strength with Respect to Temperature			
psi/°F	-116.0	--	--
n/m ² /°C	-1.44 x 10 ⁶	--	--
Elastic Modulus			
psi	29.4 x 10 ⁶	50.0 x 10 ⁶ *	35 x 10 ⁶
n/m ²	203 x 10 ⁹	345 x 10 ⁹	241 x 10 ⁹
Derivative of Elastic Modulus with Respect to Temperature			
psi/°F	-8030	-3500	--
n/m ² /°C	-99.7 x 10 ⁶	-43.4 x 10 ⁶	--
Plastic Modulus			
psi	800,000	--	--
n/m ²	5.5 x 10 ⁹	--	--
Derivative of Plastic Modulus with Respect to Temperature			
psi/°F	-0.1	--	--
n/m ² /°C	-1240	--	--
Poisson's Ratio	0.295	--	--
Derivative of Poisson's Ratio with Respect to Temperature			
1/°F	0.1	--	--
1/°C	0.18		

TABLE C-1

DESIGN PARAMETERS FOR GRAPHITE FILAMENT-WOUND PRESSURE VESSELS

Part B (continued)

<u>Properties</u>	Type 304 Stainless Steel <u>Annealed</u>	Graphite Filament-Wound Composite	
		<u>Thornel 50</u>	<u>Morganite II</u>
Volume Fraction of Filament in Composite	--	0.65	0.65
Filament, Design Allowable Stress		<u>Hoop</u>	<u>Longitudinal</u>
10 ³ psi at 75°F		143.0	130.0
n/m ² at 22°C		986 x 10 ⁶	896 x 10 ⁶

* Filament Modulus

UNCLASSIFIED
NOLTR 69-183

TABLE C-2

DIMENSIONAL AND MATERIAL PARAMETERS -
GRAPHITE FILAMENT-WOUND PRESSURE VESSELS^c

<u>Dimensions:</u>	<u>Thornel 50 Vessel</u>		<u>-1 Morganite II Vessel^a</u>		<u>-2 Morganite II Vessel^b</u>	
Outside Cylinder Diameter	8.082	20.528	8.082	20.528	7.977	20.262
Outside Diameter of Metal Cylinder	7.766	19.726	7.766	19.726	7.766	19.726
Inside Diameter of Metal Cylinder	7.754	19.695	7.754	19.695	7.754	19.695
Metal-Liner Thickness	0.006	0.015	0.006	0.015	0.006	0.015
Total Composite Cylinder Wall Thickness	0.158	0.401	0.158	0.401	0.106	0.269
Longitudinal Wound Composite Thickness	0.058	0.147	0.058	0.147	0.039	0.099
Hoop Wound Composite Thickness	0.100	0.254	0.100	0.254	0.067	0.170
Boss-to-Boss Length	13.16	33.43	13.16	33.43	13.16	33.43
Cylinder Length, Tangent to Tangent	7.34	18.64	7.34	18.64	7.34	18.64
Forward Boss Outside Diameter	2.90	7.37	2.90	7.37	2.90	7.37
Aft Boss Outside Diameter	2.90	7.37	2.90	7.37	2.90	7.37

Material Parameters:

Liner and Boss Material	Type 304 Stainless Steel (Annealed)
Filaments Type	Thornel 50 or Morganite (Type II)
Resin Matrix	Epon 828/Empol 1040/DSA/BDMA
Liner-to-Composite Adhesive	Adiprene L-100/Epi-rez 5101/MOCA (80/20/17)

a Three-Thirds Wall Vessel

b Two-Thirds Wall Vessel

c Identification information (continued next page)

TABLE C-2 (continued)

Identification information:

Thornel 50 pressure vessel, Aerojet drawing No. 1269214-1
-1 Morganite II pressure vessel, Aerojet drawing No. 1269228-1
-2 Morganite II pressure vessel, Aerojet drawing No. 1269228-2

Liner for Thornel 50 vessel, Aerojet drawing No. 1269205-1
Liner for -1 Morganite II vessel, Aerojet drawing No. 1269205-1
Liner for -2 Morganite II vessel, Aerojet drawing No. 1269205-1

Internal volume for Thornel 50 vessel - 511.3 cu in.
8379 cu cm

Internal volume for -1 Morganite II vessel - 511.3 cu in.
8379 cu cm

Internal volume for -2 Morganite II vessel - 511.3 cu in.
8379 cu cm

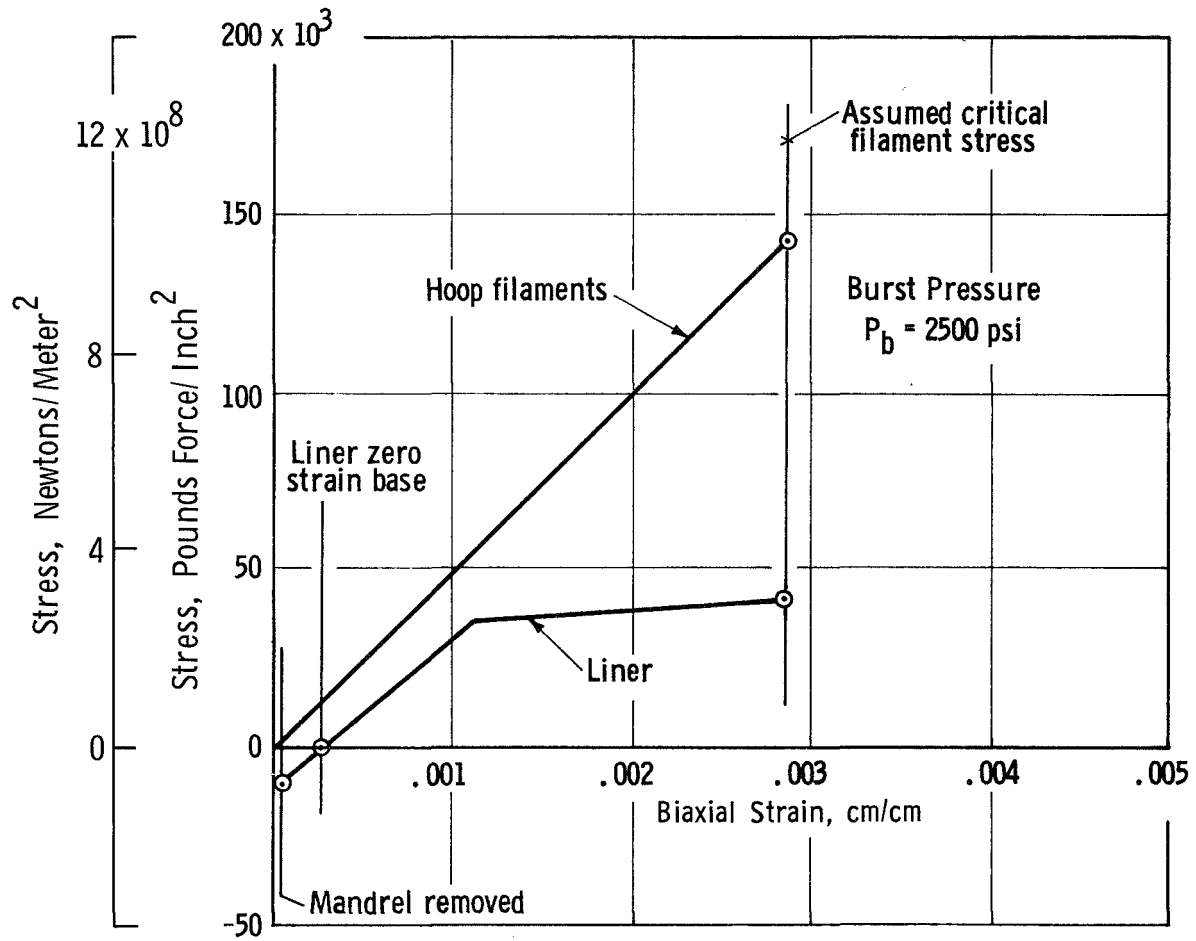


FIG. C-1 THORNEL 50 PRESSURE VESSEL STRESS-STRAIN RELATIONSHIPS
HOOP DIRECTION OF CYLINDER, 22°C (75°F)

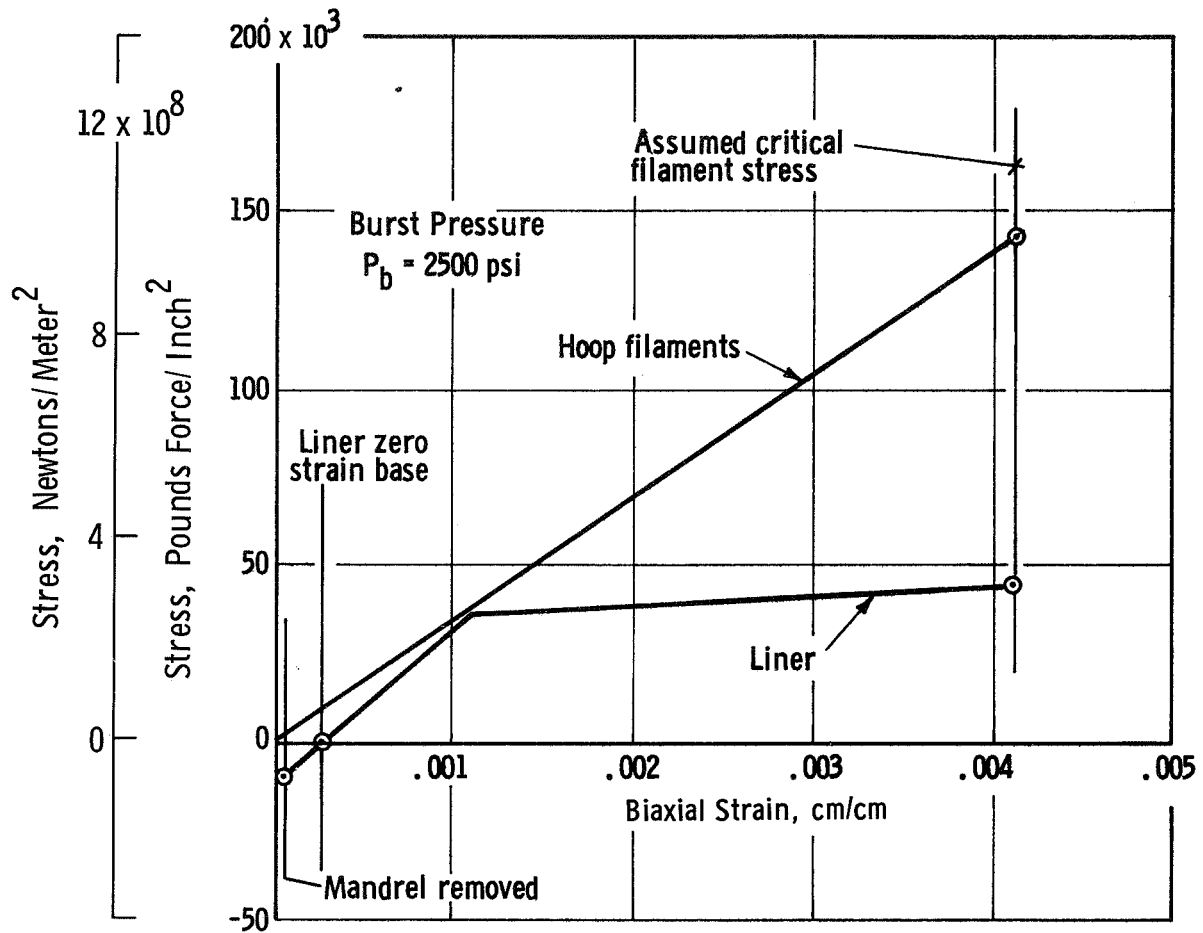


FIG. C-2 MORGANITE (TYPE II) PRESSURE VESSEL STRESS-STRAIN RELATIONSHIPS, HOOP DIRECTION OF CYLINDER, 22°C (75°F) (THREE-THIRDS WALL VESSEL)

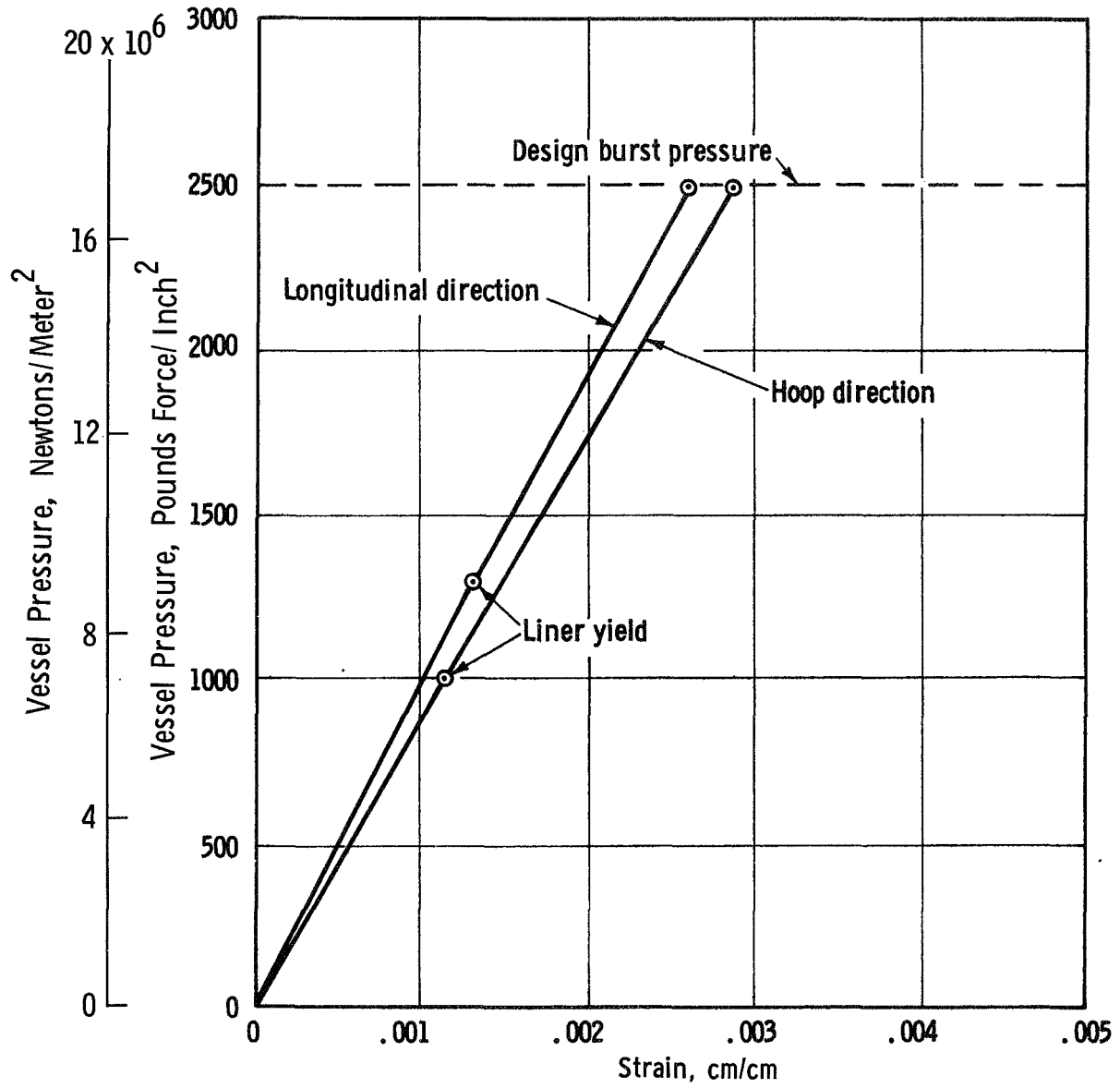


FIG. C-3 THORNEL 50 VESSEL PRESSURE - STRAIN RELATIONSHIPS

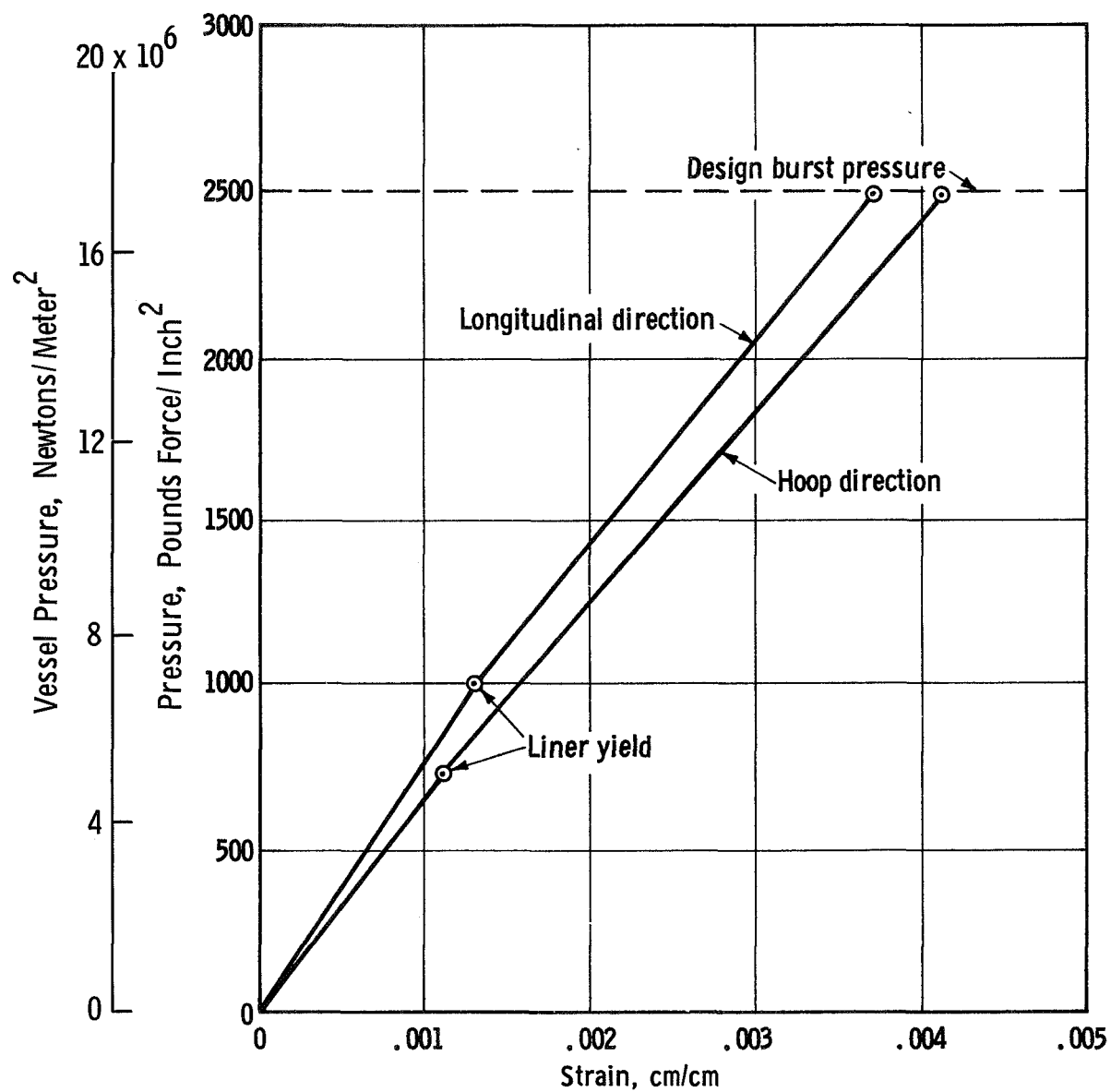


FIG. C-4 MORGANITE (TYPE II) VESSEL PRESSURE-STRAIN RELATIONSHIPS
(THREE-THIRDS WALL VESSEL)

APPENDIX D

FABRICATION OF VESSEL LINERS

The liners were made of SS 304 stainless steel, 0.015 cm (0.006 in.) thick. The liner head sections were formed by sandwiching the liner between steel sheets and forcing the sandwich through a ring using a plug of the proper contour. After heat treatment to relieve stresses introduced in fabrication, the head section was removed from the sandwich and trimmed, and the opening for the polar boss was punched.

The polar bosses were machined from SS 304 bar stock in accordance with Figure 4b in the main text; particular care was taken to maintain the thickness of the flange. Welding doublers used to join the head to the boss were fabricated from 0.020 cm (0.008 in.) thick stainless steel foil. A slight radius was rolled into each doubler to provide close contact between the head section and the boss flange.

The cylindrical section was rolled from 0.015 cm (0.006 in.) thick SS 304 foil and was roll-resistance seam welded to the required diameter.

The liner components were joined by roll-resistance seam welding after being fixed in position by spot welding. The bosses were first welded to the heads. The doubler was used over the head to minimize damage to the thin liner and to assure weld integrity and, thus, prevent leakage. The heads were then joined to the cylinder with the aid of a curved electrode inserted through the boss opening.

Two leak checks were made on each tank liner--the first, a soap solution leak test under an internal pressure of $48 \times 10^3 \text{ n/m}^2$ (7 psi), and, the second, a helium leak check with a mass spectrometer at a pressure differential of $138 \times 10^3 \text{ n/m}^2$ (20 psi). All liners passed the tests.

Following the helium leak check, the liners were cleaned and etched, in accord with Aerojet Process Standard AGC 1221 which requires cleaning in a solution of 63% nitric acid and 0.4% hydrofluoric acid. Each liner was dried and enclosed in a polyethylene bag until it was used for filament winding.

APPENDIX E

VESSEL WINDING PROCEDURE

Appendix E contains a description of the fibers, the vessel winding and curing, and the problems encountered.

1. Graphite Filament

The graphite filament used for the winding of the twelve vessels was supplied by NOL. In-process impregnation of wet resin was required by the contract.

a. Thornel 50. Twelve 450 gm (one-pound) rolls of Thornel 50 were supplied for the winding of the first six vessels. The manufacturer of the yarn (Union Carbide) provided tensile strength and modulus data marked on each roll. These data are shown in Table 1 of the main text.

The cross-sectional area of Thornel yarn is approximately one-sixth that of a 20-end glass filament roving. Longitudinal winding with such a small area yarn can lead to excessive buildup of the composite around the polar bosses of a pressure vessel unless a number of yarns are gathered to form a wider ribbon or tape. A number of combinations of yarn count (simulated by a three-end glass roving representing each Thornel yarn), turns per revolution, and revolutions per vessel were tried for longitudinal winding to minimize the buildup at the boss. A review of the results led to the selection of two yarn bundles, each bundle consisting of six Thornel 50 yarns, for the longitudinal winding. For hoop winding, a single bundle of six yarns was selected. This information was used in the design analysis and winding pattern calculations, Appendix C.

In support of this concept of six-yarn bundles, six rolls of Thornel 50 yarn were collated into a bundle and rewound on a Leesona way-winding machine, stopping after collation of enough material for the winding of one vessel. After the first vessel was successfully wound, the balance of Thornel 50 yarn was collated into six-yarn rolls.

During the collation process, numerous breaks and splices were encountered in the yarn as it paid off from the spool. At times the yarn broke at tensions estimated at less than one-tenth kilogram (one-quarter pound) per yarn. Visual inspection of the rolls showed small surface cuts across the exposed surface of the yarn as received. Also, the broken end of one ply of the yarn* was buried under adjacent winding turns; this was judged to be the cause of some of the breakage. A third source of breakage was the presence of yarn splices in the as-received roll, numbering from five to eight per roll. These splices were found to be wound into the roll, apparently without allowing time for the splicing glue to dry. This tended to make the splice stick to the balance of the roll, causing breakage during offwinding.

* Thornel 50 yarn is composed of two plies of 720 filaments each.

The number of breaks encountered during the re-spooling process varied from two to twenty per roll. It is estimated that the re-spooling tension on the six-yarn bundle was between 0.9 and 1.8 kilograms (two and four pounds) for the bundle. Although the re-spooling caused breaks, it also upgraded the re-spooled material where 1.8 kilograms (four pounds) winding tension could be applied to the bundle during subsequent vessel winding, thus minimizing, though not eliminating, breakage at this point.

b. Morganite II. Five and four-tenths kilograms (twelve pounds) of Morganite II tow were furnished for use on the contract. Shipment was in three lots of 1.8 kilograms (four pounds) each, with a total of sixteen rolls.

The initial shipment sustained extreme handling damage, in spite of the well-designed packaging. The denting of metal cans surrounding the plastic spools was so severe that the cardboard cushions wrapped around the continuous tow were compacted tightly on the surface of the spooled Morganite tow. The supplier's values of tensile strength and modulus were not marked on the roll or container but were provided on a supplementary sheet or were provided to Aerojet by NOL.

The tow, as received, was severely lacking in cross-sectional uniformity and integrity and displayed numerous snarls and spooling effects which contributed to tow breakage during vessel winding. The ragged construction of the tow led to pickup of filaments from one turn by adjacent turns until finally a sufficiently small cross-section remained so that a 1.8 kilogram (four-pound) tension resulted in tow breakage. Tow breakage during winding occurred on the average of one or two times per vessel. The cross-sectional area of Morganite II tow was sufficiently large to allow vessel winding using two tows on the longitudinal mode without encountering severe buildup around the polar bosses.

2. Preparation for Filament Winding

A resin adhesive was applied to the liner before filament winding to better distribute the expansion of the thin metal liner to the graphite composite during pressure testing. The process consisted of cleaning the liner with a paste cleaner, priming it, and applying the adhesive, using a thin nylon scrim cloth over the metal liner to provide a uniform adhesive thickness of approximately 0.008 cm (0.003 in.).

3. Vessel Winding

The tanks were filament wound using a combination longitudinal- and hoop-winding machine.

The winding shaft was installed in the liner, mounted in the winding machine, and the adhesive system applied to the liner. The longitudinal pattern was tried, using 20-end glass roving to confirm the winding pattern. Two to three plies of No. 112 glass cloth fabric were applied to the liner weld areas for fairing-in the lap joints used in roll-resistance seam welding.

An epoxy-resin system consisting of Epon 828, DSA, Empol 1040 and BDMA (resin 2) was used for filament winding, as specified from Task I work. On the

first vessel (Thornel 50 vessel T-1), the resin was brushed on the liner and the composite during winding, with filament tensioning, before impregnation, provided by a hysteresis type of tensioning device. The NOL Program Manager advised that a better "wetting-out" of the filament could be attained on a nontensioned graphite yarn. Accordingly, the resin system was applied on all subsequent vessels (except the last Morganite II vessel) by passing untensioned yarn through a resin pot before applying tension by a Prony brake tensioning device. On the last Morganite II vessel (Tank M-6), the material furnished was in very ragged and fuzzed condition and a brush application of resin was used to minimize damage to the yarn sustained when passing the wet material through subsequent Prony brake and payoff rollers.

One revolution (two layers) of resin-impregnated graphite yarn or tow was wound longitudinally over the liner assembly followed by three layers of hoop windings in the cylindrical section. For Thornel 50 vessels and "three-thirds wall" Morganite II vessels, the sequence of one longitudinal revolution plus three hoop layers was repeated two more times to develop a total composite wall of six layers of longitudinal and nine layers of hoop windings. In the "two-thirds wall" Morganite II vessels, only two revolutions of longitudinal winding (four layers) and six layers of hoop winding were deposited. The winding mandrel was internally pressurized to maintain proper size and shape as the fiber windings were put on. Temperature sensors (copper-constantan thermocouples for ambient and liquid nitrogen temperature testing, and platinum resistance transducers for liquid nitrogen and liquid hydrogen temperature testing) were wrapped into the composite wall, under the last two layers of hoop winding. Extensometer attachment pins were wound under the last hoop layer. Problems encountered in filament winding and curing of the relatively thick graphite filament-wound composite are discussed in a subsequent section.

4. Vessel Curing

The contract originally specified that the vessels were to be vacuum-bagged during curing. Accordingly, a study was performed using flat composite sections and Aerojet's standard small filament-wound test bottles (10.2 cm diameter by 15.2 cm long (4 in. diameter by 6 in. long)) to determine the appropriate time and temperature of the first stage of curing at which vacuum could be applied to the vessel without causing excessive squeeze-out and flow of the resin and subsequent relaxation of winding tension. Although the study yielded a cure process which gave the firm composite structure desired for the 20.3 cm dia. by 33 cm long (8 in. dia. by 13 in. long) vessels covered by this program, difficulty was encountered in the vacuum bag cure of the larger, thicker vessels and the vacuum bag technique was discontinued, with the concurrence of NOL, after the cure of the first two 20.3 cm (8 in.) tanks. Instead, the composite was staged overnight under heat lamps at a temperature of 52 to 66°C (125 to 150°F). The vessel was rotated slowly to eliminate resin runoff. Although the resin content of the composite was higher than desired, due to the wet-winding process, the overnight staging firmed the structure sufficiently so that bleed-out and relaxation during the final oven cure were not experienced to any great degree. The final oven cure cycle was two hours at 93°C (200°F), two hours at 121°C (250°F), and four hours at 149°C (300°F). The step-cure used slow rates of temperature increase in a further attempt to minimize resin flow-out. Internal pressure was maintained in the mandrel throughout the cure

cycle. After cure, the vessel was cooled slowly to room temperature; then the winding shaft removed. The vessel interior was cleaned and dried and its final weight recorded before pressure testing.

5. Winding and Curing Problems

Yarn and ply breakage in the case of Thornel 50 and tow breakage in the case of Morganite II was a serious problem during filament winding. The winding tension attempted when the material was running smoothly was four pounds for the bundle of six Thornel yarns or a single Morganite tow. Good sections of Thornel yarns had a breaking strength of 1.8 to 2.7 kilograms (four to six pounds) and Morganite II tow showed a breaking strength of about 36 kilograms (80 pounds) in the as-received conditions, directly from the roll. The low breaking strength encountered in winding is attributable in part to lack of uniformity in the material, since the breaks occurred many times in both types of material in strands which had not as yet passed through the resin pot, Prony brakes, or pay-off rollers. If the Thornel 50 yarn had not been previously screened by the collation procedure, the incidence of breakage would have been still higher. Passage of the yarns and tows through pots, rollers, and brakes caused further visible damage, even though low tension (0.9 to 1.8 kilograms (two to four pounds)) was maintained and squeegee rollers on the resin pot were padded with soft rubber.

When the low breaking strength during winding is compared to the breaking strength of a cured resin-impregnated strand, a gain in strength of 30 to 100 times is seen. This points out the necessity for shear transfer between the filaments during winding with the wet resin to maintain acceptable winding tension. It is believed that the stress transfer may be obtained by use of a ductile but advanced preimpregnated yarn.

Another problem in the filament winding was the inability to run with a lower resin content, as a result of the requirement for in-process resin pot impregnation. The squeegee rollers were run with light pressure and soft padding to minimize filament damage, and as a result, resin contents by weight were 50 to 60% when checked at the vessel. This gave a tendency towards slippage in the winding, which was complicated on longitudinal winding by a relatively large boss-to-chamber diameter ratio and a 1.5 length-to-diameter ratio. The slippage was counteracted in several ways. First, the winding tension was reduced from 1.8 to 0.9 kilograms (four to two pounds) at the knuckle area. Second, the resin in the impregnation pot was heated to 46°C (115°F) to reduce its viscosity and reduce resin pick-up by the strand. Third, the longitudinal layers were advanced in their cure by exposing to 52°C (125°F) overnight prior to additional winding. When major breakage was encountered, the winding was stopped and a new start was made with an overlap from one to two centimeters (one-half to three-quarters of an inch) wide.

The problems of light tensioning and filament slippage resulted in a "soft" wound structure with high resin content. Thickness was about 0.635 cm (0.25 in.) thickness and, as mentioned previously, difficulty was encountered with vacuum bag curing of the initial 20.3 cm (8 in.) diameter vessels because of fiber wash. This caused buckling or wrinkling of the composite, thus destroying the remaining pretensioning and causing serious stress concentration areas.

UNCLASSIFIED
NOLTR 69-183

A typical vacuum-bagged surface is shown in Figure 5 of the main text. The vacuum-bagging process was therefore discontinued and a prestaging and final oven cure without composite compaction was utilized. The relatively thick graphite filament-wound composite caused by the light tension, filament slippage, and high resin content was a structure which gave visual indications of being less than optimum in strength.

APPENDIX F

VESSEL CRYOGENIC TEST PROCEDURE AND INSTRUMENTATION

1. Cryogenic-Test Facility

Liquid nitrogen (LN_2) was used to pressurize the vessels for the -195°C (-320°F) tests, with the pressurization rate regulated by gas controlled valves. The test fixture consisted of a vacuum chamber with provisions for instrument leads and vacuum-jacketed pressurization lines. The chamber interior and exterior were coated with aluminum paint and a layer of aluminum foil was installed inside to provide additional reflective insulation.

To aid in maintaining minimum test temperatures, the vessels installed in the vacuum chamber were equipped with external cooling coils through which liquid cryogen (nitrogen or hydrogen, as applicable) was flowed at essentially atmospheric pressure. A cylinder of reflective foil insulation was used around the exterior cooling coils. The vacuum chamber was pumped down to 5.3×10^{-2} n/m² (4×10^{-4} mm Hg) to assure maintenance of the required temperatures. The tank temperatures were maintained as low as possible, and thermal equilibrium was obtained before testing was initiated. Thermal equilibrium for liquid nitrogen testing was defined as a vessel flange or skin temperature of -184°C (-300°F), or less, with -190°C (-310°F), or less, at the vessel outlet vent line. For liquid hydrogen testing, the two temperatures were -240°C and -246°C (-400°F and -410°F), respectively.

2. Instrumentation

Temperatures, longitudinal and circumferential strains, and internal pressures of the vessel test specimen were monitored throughout testing. Figure F-1 shows the instrument locations.

The electronic and digital equipment used for these measurements was calibrated periodically, against standards traceable to the National Bureau of Standards, by the Metrology Department of the Aerojet Quality Control and Test Division. The calibration records are on file at Aerojet.

Platinum resistance thermometers and copper-constantan thermocouples were used in the -196°C and -253°C (-320°F and -423°F) tests. The measurements were made on the exterior surface near the tangency at one end of the tank. In addition, the temperatures of the cryogenic fluids inside and outside the tank were recorded.

The Aerojet-developed "bow-tie" extensometer was used to make strain measurements. It consists of a piece of beryllium copper sheet in a configuration that provides two cantilever beams fitted with bonded strain gages. Metal-foil strip, approximately 0.64 cm (0.25 in.) wide, was used to link the beam ends to the gage-length end points. Both the extensometers and the foil strips were positioned against the test vessel surface. The small deflections of the high-modulus graphite-filament-wound tanks required the development of a special bow-tie extensometer configuration that would accurately measure the low strains encountered.

For girth (hoop) strain measurements, a thin metal strip was placed around the cylinder and secured to opposite ends of the extensometer; circumferential deflection resulted in a proportional output of the gages on the cantilever beams. For longitudinal-deflection measurements, metal strips were affixed to instrumentation-pin terminals wound into the tank near the ends of the cylindrical section. The strips were run along the cylinder longitudinally; the cantilever-beam ends were connected to the ends of the strips at the midsection of the tank. A longitudinal deflection produced a proportional strain-gage output.

The accuracy of the strain gages depends on the gage factor, which is extremely sensitive to cryogenic-temperature variations. To provide the required accuracy, the concept of controlled-temperature strain transduction was employed: Heaters were provided to maintain the gage temperatures within their compensation range, and a sensor was added to record the vessel-surface temperature in the vicinity of the extensometer. This sensor was used to verify that the heat input to the extensometer did not warm the tank surface significantly in the region of the transducer. Thermal insulation was used under the heated extensometers to minimize heat transfer to the vessel. The test data showed that no significant vessel warming was produced. Figures F-2 and F-3 show vessel temperatures during test.

Before testing, each extensometer was installed on the vessel and shunt calibrated under ambient conditions throughout its anticipated range of deflection. The gage factors did not vary under cryogenic conditions, because the heaters kept the gages essentially at the ambient temperature. Monitoring during the cryogenic tests revealed that the gages were usually maintained at $24 \pm 11^\circ\text{C}$ ($75 \pm 20^\circ\text{F}$). Because the gage factor varies only 1% per 38°C (100°F) change in the 24°C (75°F) range, there was negligible loss in accuracy.

To calibrate for longitudinal displacements, the distance between the bow-tie attachment points or terminals (L_2) was carefully measured. The instrument and its metal-strip extensions were then stretched to the maximum expected deflection, using accurately determined positions (ΔL_2). The strain was calculated as $\Delta L_2/L_2$ to indicate the total between the two attachment points. To calibrate the girth extensometer, the tank circumference (L_1) was measured and the bow-tie attachment band was moved to produce the maximum expected deflection (ΔL_1). The girth strain was calculated as $\Delta L_1/L_1$. Calibration was performed under ambient conditions, and a shift in the zero point occurred due to thermal contraction when the tank was cooled to cryogenic levels. To correct for this shift, it was only necessary to reset the recorder to zero, because the repeatability under ambient conditions was essentially linear and the heaters maintained ambient temperatures.

Two types of long-wire strain gages* were provided by NASA, Lewis Research Center for evaluation on the test program. The evaluation was desirable because of the extremely low cost of these gages. Two strain gages of each

* The strain gages were Model No. A-9 (cellulose-paper-backed) and Model No. AB-9 (phenolic-glass-backed) manufactured by BLH Electronics, Waltham, Mass., a Division of Baldwin-Lima-Hamilton.

type were installed on each of the six Morganite II vessels. One strain gage of each type was installed in each of the longitudinal and hoop directions using resin 2 (the resin used in the filament-winding of the vessels) as an adhesive. The strain gages were adhered to the cured surface of the vessel and the vessel was cured an additional two hours at 149°C (300°F), adequate for the thin layer of adhesive.

On tests at -195°C and -253°C, the strain gages failed during cool-down of the vessel, as evidenced by a sudden open circuit observed in the strain gage circuits, and thus gave no strain results.

On tests of vessels at ambient temperatures (Serial No. M-1 and M-6) the strain gages functioned well and showed reasonably close agreement with the bow-tie extensometers used as the prime strain measurement instruments. The recorded strain is plotted for comparison on Figures 35 and 40 of the main text. On vessel M-6, both paper-backed strain gages recorded up to the failure level of 0.4 to 0.5% strain, but one phenolic-backed strain gage failed about half-way through the test at a strain of 0.25%, giving erratic readings at that point which were attributed to adhesive failure. The second phenolic-backed gage failed to give representative strain readings at any time during the test, possibly because of a broken wire.

On vessel M-1, three strain gages measured strain all the way to the vessel burst point, a strain of 0.4%. Two of the strain gages were phenolic-backed and one was paper-backed; the second paper-backed gage failed to provide usable readings.

It appears that each of the two types of strain gages are acceptable candidates for further evaluation at ambient temperature but should be used redundantly due to their apparent lack of reliability. Redundant use, however, adds additional testing cost due to the additional number of instrumentation channels required, and there is no saving over bow-tie extensometer strain measurement. Neither of the two types of long-wire strain gages appears feasible for cryogenic testing.

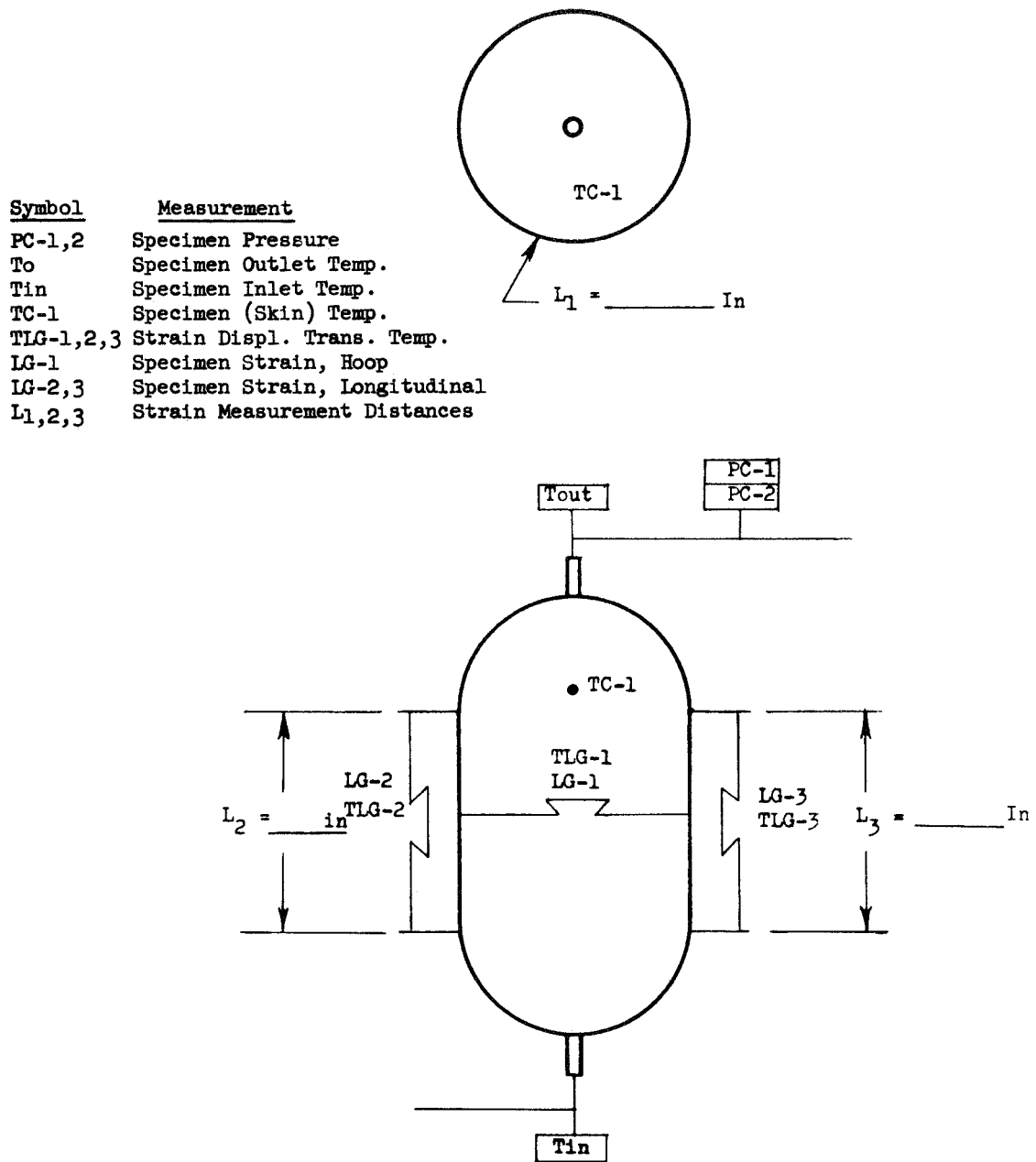


FIG. F-1 LOCATION OF INSTRUMENTATION ON TEST VESSEL

NOLTR 69-183

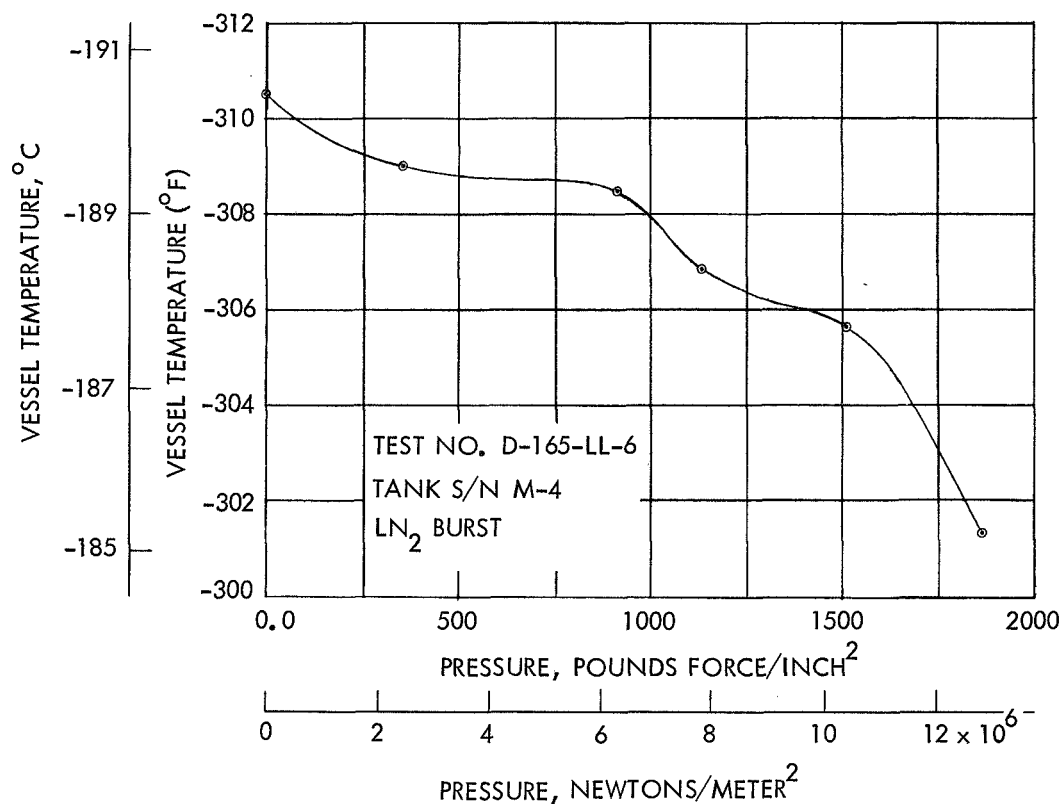


FIG. F-2 PRESSURE VS TEMPERATURE - LIQUID NITROGEN TEST

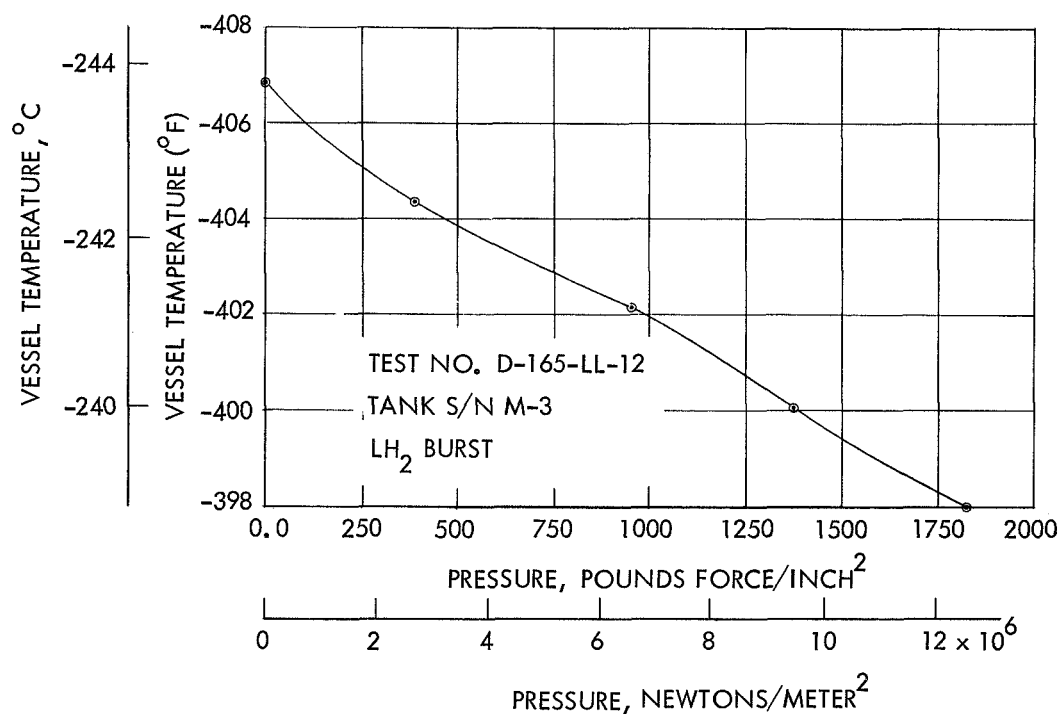


FIG. F-3 PRESSURE VS TEMPERATURE - LIQUID NITROGEN TEST

UNCLASSIFIED
NOLTR 69-183

DISTRIBUTION

Copies

National Aeronautics & Space Administration
Lewis Research Center
21000 Brookpark Road
Cleveland, Ohio 44135

Attn: Contracting Officer, MS 500-313	
Liquid Rocket Technology Branch, MS 500-209	3
Technical Report Control Office, MS 5-5	
Technology Utilization Office, MS 3-16	
AFSC Liaison Office, MS 4-1	2
Library	2
Office of Reliability & Quality Assurance, MS 500-111	
D. L. Nored, Chief, LRTB, MS 500-209	
R. F. Lark, Project Manager, MS 500-209	10
E. W. Conrad, MS 500-204	
R. H. Kemp, MS 49-1	
M. Hanson, MS 49-1	
M. Ault, MS 105-1	

Chief, Liquid Experimental Engineering, RPX
Office of Advanced Research & Technology
NASA Headquarters
Washington, D. C. 20546

Director, Research Division, RR
Office of Advanced Research & Technology
NASA Headquarters
Washington, D. C. 20546

Attn: Library
G. C. Deutsch, Code RR-1
J. J. Gangler, Code RRM

Air Force Material Laboratory
Wright-Patterson Air Force Base, Ohio 45433

Attn: AFML (MAN)
J. D. Ray (MANC)
W. H. Gloor (MANF)
H. S. Schwartz (MAN)

Commanding Officer
Ballistic Research Laboratories
Aberdeen Proving Ground, Maryland 21005
Attn: AMXBR-L

Department of the Army
U. S. Army Material Command
Washington, D. C. 20315
Attn: AMCRD-RC

DISTRIBUTION

Copies

Air Force Material Laboratory
Wright-Patterson Air Force Base, Ohio, 45433
Attn: AFML (MAC)
G. P. Peterson
Wm. J. Schulz
E. Jaffe

Air Force Material Laboratory
Wright-Patterson Air Force Base, Ohio, 45433
Attn: MAT
S. Litvak (MATC)

Air Force Material Laboratory
Wright-Patterson Air Force Base, Ohio, 45433
Attn: MAA
A. Olevitch (MAEE)
T. Reinhart (MAAE)

Department of the Navy
Office of Naval Research
Washington, D. C. 20360
Attn: Library
J. H. Shenk

Department of the Army
U. S. Army Aviation Material Laboratories
Fort Eustis, Virginia 23604
Attn: Library
A. J. Gustafson
R. Berrisford

Department of the Army
U. S. Army Aviation Systems Command
P. O. Box 209
St. Louis, Missouri, 63166
Attn: Library
R. Vollmer, AMSAV-A-UE

Chief, Liquid Propulsion Technology, RPL
Office of Advanced Research & Technology
NASA Headquarters
Washington, D. C. 20546
Attn: F. E. Compitello, Code RPL

Director, Launch Vehicles & Propulsion, SV
Office of Space Science & Applications
NASA Headquarters
Washington, D. C. 20546

DISTRIBUTION

Copies

Chief, Environmental Factors & Aerodynamics
Code RV-1
Office of Advanced Research & Technology
NASA Headquarters
Washington, D.C. 20546

Chief, Space Vehicles Structures
Office of Advanced Research & Technology
NASA Headquarters
Washington, D.C. 20546
Attn: M.G. Rosche, Code RV-2
N.J. Mayer, Code RV-2

Director, Advanced Manned Missions, MT
Office of Manned Space Flight
NASA Headquarters
Washington, D.C. 20546

NASA Scientific & Technical Information Facility
P.O. Box 33
College Park, Maryland, 20740

6

Director, Technology Utilization Division
Office of Technology Utilization
NASA Headquarters
Washington, D.C. 20546

National Aeronautics & Space Administration
Ames Research Center
Moffett Field, California 94035
Attn: Library

National Aeronautics & Space Administration
Flight Research Center
P.O. Box 273
Edwards, California 93523
Attn: Library

National Aeronautics & Space Administration
Goddard Space Flight Center
Greenbelt, Maryland 20771
Attn: Library

National Aeronautics & Space Administration
John F. Kennedy Space Center
Cocoa Beach, Florida, 32931
Attn: Library

NOLTR 69-183

DISTRIBUTION

Copies

National Aeronautics & Space Administration
Langley Research Center
Langley Station
Hampton, Virginia 23365
Attn: Library
R.R. Heldenfels, MS 188
E.E. Mathauser, MS 188A
R.A. Pride, MS 188A

National Aeronautics & Space Administration
Manned Spacecraft Center
Houston, Texas 77001
Attn: Library
L.G. St. Leger, Code ES-4

National Aeronautics & Space Administration
George C. Marshall Space Flight Center
Huntsville, Alabama 35812
Attn: Library
John T. Schell

Jet Propulsion Laboratory
4800 Oak Grove Drive
Pasadena, California 91103
Attn: Library
Henry Burlage, Jr.
Warren Jensen
J. Conger

Office of the Director of Defense
Research & Engineering
Washington, D.C. 20301
Attn: Office of Asst. Dir. (Chem. Technology)

Advanced Research Projects Agency
Room 3D-179-Pentagon
Washington, D.C.
Attn: R.A. Huggins

Advanced Research Projects Agency
Washington, D.C. 20525
Attn: Library

Aeronautical Systems Division
Air Force Systems Command
Wright-Patterson Air Force Base
Attn: Library

Air Force Systems Command
Andrews Air Force Base
Washington, D.C. 20332
Attn: Library

DISTRIBUTION

Copies

Air Force Rocket Propulsion Laboratory
Edwards, California 93523
Attn: Library
J. Branigan

Air Force Office of Scientific Research
Washington, D.C. 20333
Attn: Library
SREP, Dr. J.F. Masi

Space & Missile Systems Organization
Air Force Unit Post Office
Los Angeles, California 90045
Attn: Technical Data Center

Office of Research Analyses (OAR)
Holloman Air Force Base, New Mexico 88330
Attn: Library
RRRD

U. S. Air Force
Washington, D.C.
Attn: Library
Col. C.K. Stambaugh, Code AFRST

Commanding Officer
U.S. Army Research Office (Durham)
Box CM, Duke Station
Durham, North Carolina 27706
Attn: Library

U. S. Army Missile Command
Redstone Scientific Information Center
Redstone Arsenal, Alabama, 35808
Attn: Document Section

Commander
U.S. Naval Missile Center
Point Mugu, California 93041
Attn: Technical Library

Commander
U.S. Naval Weapons Center
China Lake, California 93557
Attn: Library

Commanding Officer
Naval Research Branch Office
1030 E. Green Street
Pasadena, California 91101
Attn: Library

NOLTR 69-183

DISTRIBUTION

Copies

Electronics Division
Aerojet-General Corporation
P.O. Box 296
Azusa, California 91703
Attn: Library
E. Morris
R. Alfring
D.E. Deutsch
I. Petker

Aeronutronic Division of Philco Ford Corp
Ford Road
Newport Beach, California, 92663
Attn: Technical Information Department

ARO, Incorporated
Arnold Engineering Development Center
Arnold AF Station, Tennessee 37389
Attn: Library

Bell Aerosystems, Inc
Box 1
Buffalo, New York, 14205
Attn: Library
D. Hanley

Bell Helicopter Company
P.O. Box 482
Fort Worth, Texas, 76101
Attn: Library
H. Zinberg

Bendix Corporation
401 Bendix Dr.
South Bend, Indiana 46619
Attn: A. Courtney

Case-Western Reserve University
University Circle
Cleveland, Ohio 44106
Attn: T.P. Kicher

Boeing Company
Space Division
P.O. Box 868
Seattle, Washington, 98124
Attn: Library
J.T. Hoggatt
J.L. White

DISTRIBUTION

Copies

The Boeing Company
Vertrol Division
Morton, Pennsylvania 19070
Attn: Library
W.D. Harris
R. Pickney

The Boeing Company
P.O. Box 707
Renton, Washington, 98055
Attn: R. June

Chemical Propulsion Information Agency
Applied Physics Laboratory
8621 Georgia Avenue
Silver Spring, Maryland 20910

Fairchild Hiller Corporation
Republic Aviation Division
Farmingdale, New York 11735
Attn: Library
J. Clark
F. Damasco
W. Fuchs

General Dynamics/Convair
P.O. Box 1128
San Diego, California 92112
Attn: Library
J.L. Christian

Missiles and Space Systems Center
General Electric Company
Valley Forge Space Technology Center
P.O. Box 8555
Philadelphia, Pennsylvania 19101
Attn: Library
L.R. McCreight
K. Hall
W. Postelnek

General Electric Company
Flight Propulsion Lab. Department
Cincinnati, Ohio
Attn: Library

U.S. Polymeric Chemicals, Inc.
700 E. Dyer Rd.
Santa Ana, California 92707
Attn: Library
J. Williamson
W. Condon

NOLTR 69-183

DISTRIBUTION

Copies

Denver Division
Martin-Marietta Corporation
P.O. Box 179
Denver, Colorado 80201
Attn: Library
A. Feldman
W.S. Barrett

McDonnell Douglas Aircraft Corporation
3855 Lakewood Blvd.
Long Beach, California 90810
Attn: Library
H.C. Schjelderup
D.C. Smillie
W.I. Stler

McDonnell Douglas Aircraft Corporation
P.O. Box 516
Lambert Field, Missouri 63166
Attn: Library
J.C. Watson
W. Jakway

North American Rockwell, Inc.
4300 E. Fifth St.
Columbus, Ohio, 43219
Attn: R.L. Foye
R. Freedman
L. Hackman

Northrop Space Laboratories
3401 West Broadway
Hawthorne, California 90250
Attn: Library
D. Stanbarger
B.B. Bowen
E.L. Hormon

General Dynamics
P.O. Box 748
Fort Worth, Texas 76100
Attn: Library
W.S. Hay
T.P. Airhart
W.K. Bailey
B.G. Reed
C. Rogers

DISTRIBUTION

Copies

Radio Corporation of America
Astro-Electronics Products
Princeton, New Jersey 08540
Attn: Library

TRW Systems, Inc.
23555 Euclid Ave.
Euclid, Ohio 44111
Attn: Library
W.E. Winters
P.T. Angell
J. Alexander

United Aircraft Corporation
Corporation Library
400 Main Street
East Hartford, Connecticut 06108

United Aircraft Corporation
Research Laboratories
East Hartford, Connecticut 06108
Attn: Library
K. Kreider

Commanding Officer
Ballistic Research Laboratories
Aberdeen Proving Ground, Maryland 21005
Attn: AMXBR-L

Department of the Army
U.S. Army Material Command
Washington, D.C. 20315
Attn: AMCRD-RC

United Aircraft Corporation
Pratt & Whitney Division
Florida Research & Development Center
P.O. Box 2691
West Palm Beach, Florida 33402
Attn: Library
W.L. Gorton
A. Cox
J. Ashley
J. Price

U. S. Naval Applied Science Laboratory
Brooklyn, New York 11251
Attn: Library

NOLTR 69-183

DISTRIBUTION

Copies

E.I. duPont deNemours & Company
Eastern Laboratory
Gibbstown, New Jersey 08027
Attn: Library

Esso Research & Engineering Company
P.O. Box 45
Linden, New Jersey 07036
Attn: Library
D.J. Angier
M.S. Cohen

Institute for Defense Analyses
400 Army-Navy Drive
Arlington, Virginia 22202
Attn: Classified Library

Whitaker Corporation
3640 Aero Court
San Diego, California 92123
Attn: Library
V. Chase
K.R. Berg
C. Segal
M. Burg

Commanding Officer
U.S. Naval Underwater Ordnance Station
Newport, Rhode Island 02844
Attn: Library

Lockheed/Georgia Corporation
Marietta, Georgia 30060
Attn: Library
W.S. Cremens
W.E. Horvill
J.F. Sutton
W.T. Schuler
J. Gilmer
J.M. Bloom

Sandia Corporation
P.O. Box 969
Livermore, California 94550
Attn: Technical Library
H. Lucas

Marino Engineering Laboratory
NSRDC ANNADIV
Annapolis, Maryland 21402
Attn: Library

DISTRIBUTION

Copies

Brunswick Corporation
Defense Products Division
P.O. Box 4594
43000 Industrial Avenue
Lincoln, Nebraska
Attn: Library
J. Carter

Thiokol Chemical Corporation
Wasatch Division
P.O. Box 524
Brigham City, Utah 84302
Attn: Library Section

General Electric Company
Apollo Support Department
P.O. Box 2500
Daytona Beach, Florida 32015
Attn: Library

FMC Corporation
Chemical Research & Development Center
P.O. Box 8
Princeton, New Jersey 08540
Attn: Security Officer

Department of the Army
Watertown Arsenal
Watertown, Massachusetts 02172
Attn: Library
A. Thomas

Westinghouse Research Laboratories
Buelah Road, Churchill Boro
Pittsburgh, Pennsylvania 15235
Attention: Library

Frankford Arsenal
Philadelphia, Pennsylvania 19137
Attn: 1320, Library

Department of the Army
Watervliet Arsenal
Watervliet, New York 12189
Attn: Library
F.W. Schmiedershoff

NOLTR 69-183

DISTRIBUTION

Copies

Director
Strategic Systems Projects Office
Department of the Navy
Washington, D.C. 20360

Grumman Aircraft Engineering Corporation
Bethpage, Long Island, New York 11714
Attn: Library

Hercules Corporation
Allegheny Ballistics Laboratory
P.O. Box 210
Cumberland, Maryland 21052
Attn: Library
C.E. Jordon
J. Leslie
G. Moody

The Fiberite Corporation
512 W. Fourth St.
Winona, Minnesota 55987
Attn: S.P. Prosen

IIT Research Institute
Technology Center
Chicago, Illinois 60616
Attn: Library

Kidde Aer-Space Division
Walter Kidde & Company, Inc.
567 Main Street
Belleville, New Jersey 07109

Ling-Temco-Vought Corporation
P.O. Box 5003
Dallas, Texas 75222
Attn: Library
M. Pollos
G. A. Starr
E. E. Koltko

Lockheed Missiles & Space Company
P.O. Box 504
Sunnyvale, California 94087
Attn: Library; R. W. Fenn; A. C. Johnson; P. Plank

Lockheed /California Corp.
Burbank, California 91503
Attn: Library
M.G. Childers

DISTRIBUTION

Copies

Lockheed Propulsion Company
P. O. Box 111
Redlands, California 92374
Attn: Library, Thackwell

Marquardt Corporation
16555 Saticoy Street
Van Nuys, California 91406
Attn: J.F. Dolowy

Goodyear Aerospace Corporation
1210 Massillon Road
Akron, Ohio 44315
Attn: Library
L.W. Toth
R.E. Stankard

Union Carbide Corp.
P.O. Box 6116
Cleveland, Ohio 44101
Attn: Library
G.B. Spence
J. Bowman

Hercules, Inc.
Wilmington, Delaware 19899
Attn: G. McHugh

Lawrence Radiation Laboratory
P.O. Box 808
Livermore, California 94550
Attn: Library
T.T. Chiao
W.W. Gerberich

Great Lakes Carbon Company
Elizabethtown, Tennessee 37643
Attn: Library
R. Prescott
W.R. Benn

HITCO
1600 W. 135th Street
Gardena, California 90249
Attn: Library
M.S. Allison
D.J. Maneely

NOLTR 69-183

DISTRIBUTION

Copies

AVCO Corporation
Applied Technology Division
Lowell Industrial Park
Lowell, Massachusetts 01851
Attn: Mr. Allan S. Bufferd

Commander, Naval Air Systems Command
U. S. Navy Department
Washington, D. C. 20360
AIR-5203 (P. Goodwin)
AIR-52032 (P. Stone)
AIR-52032A (C. Bersch)
AIR-52032C (J. Gurtowski)
AIR-52032D (M. Stander)
AIR-320A (T. Kearns)
AIR-604 (Library)

Commander, Naval Ordnance Systems Command
U. S. Navy Department
Washington, D. C. 20360
ORD-033 (B. Drimmer)
ORD-0333 (S. Matesky)
ORD-0333A (M. Kinna)
ORD-9132

Director, Deep Submergence Systems Project
6900 Wisconsin Avenue
Washington, D. C. 20015
Attn: DSSP-221 (H. Bernstein)

Commander, Naval Ship Engineering Center
Center Building
Prince Georges Center
Hyattsville, Maryland 20792
Code 6101E03 (W. Graner)
Code 6101e (J. Alfors)

Director, Naval Research Laboratory
Washington, D. C. 20390
Attn: J. Kies, Code 8430
Dr. W. Zisman, Code 6050
Dr. R. Kagarise, Code 6100
Dr. I. Wolock, Code 8433

Commander, Naval Weapons Center
China Lake, California 93555

Commanding Officer, Picatinny Arsenal
Dover, New Jersey 07801
Attn: Plastics Laboratory

DISTRIBUTION

Copies

Commanding Officer
Army Materials & Mechanics Research Center
Watertown, Massachusetts 02172
Attn: Library

Commander
Natick Laboratories
U. S. Army
Natick, Massachusetts 01762
Attn: T. Ciavarini

Director
Air Force Office of Scientific Research
1400 Wilson Boulevard
Arlington, Virginia 22209
Attn: SIGL

Plastics Technical Evaluation Center
Picatinny Arsenal
Dover, New Jersey 07801

Commanding Officer and Director
Naval Ship Research and Development
Center, Carderock
Washington, D. C. 20007
Attn: M. Krenzke

Commander, Naval Weapons Laboratory
Dahlgren, Virginia 22448
Attn: W. A. Mannschreck, Code EA

Commander, Naval Undersea Warfare Center
3203 E. Foothill Boulevard
Pasadena, California 91107

Commander, Naval Command Control
Communications Laboratory Center
San Diego, California 92152

UNCLASSIFIED

Security Classification

DOCUMENT CONTROL DATA - R & D

(Security classification of title, body of abstract and indexing annotation must be entered when the overall report is classified)

1. ORIGINATING ACTIVITY (Corporate author) U. S. Naval Ordnance Laboratory White Oak Silver Spring, Maryland 20910		2a. REPORT SECURITY CLASSIFICATION Unclassified	
		2b. GROUP	
3. REPORT TITLE Properties of Graphite Fiber Composites at Cryogenic Temperatures			
4. DESCRIPTIVE NOTES (Type of report and inclusive dates)			
5. AUTHOR(S) (First name, middle initial, last name) Robert A. Simon Richard Alfring			
6. REPORT DATE 13 May 1970		7a. TOTAL NO. OF PAGES 111	7b. NO. OF REFS 11
8a. CONTRACT OR GRANT NO. Defense Purchase Request C10360B		9a. ORIGINATOR'S REPORT NUMBER(S) NOLTR 69-183	
b. PROJECT NO.			
c.		9b. OTHER REPORT NO(S) (Any other numbers that may be assigned this report)	
d.		NASA CR-72652	
10. DISTRIBUTION STATEMENT			
11. SUPPLEMENTARY NOTES		12. SPONSORING MILITARY ACTIVITY NASA, Lewis Research Center 21000 Brookpark Road Cleveland, Ohio 44135	
13. ABSTRACT Need for low-weight, cryogenic pressure vessels for spacecraft resulted in NASA, Lewis funding an investigation at NOL to measure graphite fiber composite properties at cryogenic temperatures. The investigation was divided into six tasks; only Tasks I and II are reported herein. Task I was an investigation of mechanical properties of several fibers and resins as composite strands, bars, and NOL rings and showed that composite moduli increased by 0 to 20% at -195°C, and composite tensile strengths decreased by 0 to 30%. Bending fatigue at 50% breaking stress and 1000 cycles deteriorated rings less when cold than when at room temperature. Thermal contraction tests of composites showed the graphite fibers to have a slight negative coefficient. Combined with resins in composites, the resin matrix would experience up to 1.5% strain when cold due to its thermal contraction. Task II was the design, fabrication, and testing of graphite filament wound pressure vessels and was contracted to the Aerojet-General Corporation, Azusa, California. Vessel ultimate strains of 0.2 to 0.5% were found, which are generally compatible with the stainless steel liners used or with other candidate liner materials. The pressure vessel performance factor of PV/W showed the graphite vessels to be competitive with boron and two-thirds as high as fiberglass.			

DD FORM 1 NOV 65 1473 (PAGE 1)

S/N 0101-807-6801

UNCLASSIFIED
Security Classification

UNCLASSIFIED

Security Classification

14. KEY WORDS	LINK A		LINK B		LINK C	
	ROLE	WT	ROLE	WT	ROLE	WT
Graphite Fiber Composites Cryogenic Temperatures Pressure Vessel Low Strain Metal Liner Compatibility						